UNIVERSITY OF CALIFORNIA SAN DIEGO

Using patient-derived induced pluripotent stem cells to investigate the role of TrkA signaling in Bipolar Disorder

A dissertation submitted in partial satisfaction of the requirements for the degree Doctor of Philosophy

in

Biomedical Sciences

by

Alannah Hope Miranda

Committee in charge:

Professor John Kelsoe, Chair
Professor Fred H. Gage
Professor Bruce Hamilton
Professor Alysson Muotri
Professor Nicholas Spitzer
Professor Chengbiao Wu

2021

The Dissertation of Alannah Hope Miranda is approved and it is acceptable in quality and form for publication on microfilm and electronically:

_____

_____

_____

_____

_____

_____
Chair

University of California San Diego

2021

TABLE OF CONTENTS

LIST OF ABBREVIATIONS

Bipolar Disorder (BD)

Neural stem cells (NSCs)

Tropomyosin-related kinase A (TrkA)

Nerve growth factor (NGF)

SHC-transforming protein 1 (SHC)

Fibroblast growth factor receptor substrate 2 (Frs2)

Mitogen-activated protein kinase (MAPK) or Extracellular signal-related kinase (ERK)

Acetylcholine (ACh)

Choline acetyl transferase (ChAT)

Single Nucleotide Polymorphisms (SNPs)

Autosomal dominant tubulo-interstitial kidney disease (ADTKD)

Induced pluripotent stem cells (iPSCs)

Basal forebrain cholinergic neurons (BFCNs)

LIST OF FIGURES

LIST OF TABLES

ACKNOWLEDGEMENTS

I would like to acknowledge Dr. John Kelsoe for his support as the chair of my committee. His endless enthusiasm and support for my ventures, both in and out of lab, has been a source of encouragement and motivation, even throughout the depths of western blot and R torture.

I would also like to acknowledge the previous and current members of the Kelsoe lab, in particular Tanya Shekhtman, Dr. Yabin Wei and Dr. Nathaniel Miller, who all played an essential role in helping me become the independent and resourceful scientist that I am today.

I would also like to thank the family on whom this work is based on, for their participation and commitment to helping others. Without their contribution, our contribution to science could not have occurred.

I would also like to acknowledge that this work was supported by grants to Dr. John Kelsoe from the NIMH (MH094483) and Dr .Bruce Hamilton from the UCSD Genetics Training Grant (T32 GM008666). Special thank you to Dr. Hamilton, for your guidance throughout the training program, and continuously inspiring me to question everything, but respectfully.

Chapter 2.1, in part, is a reprint of the material as it appears in Study of 45 candidate genes in identifies CACNG2 and NRG1 as associated with lithium response in Bipolar Disorder in *Journal of Affective Disorders* 2019. Miranda, A., Shekhtman, T., McCarthy, M., DeModena, A., Leckband, S., & Kelsoe, J. The dissertation author was the primary investigator and author of this paper.

Chapters 2.2 and 3 in part, are reprints of the material as it appears in *Ntrk1* mutation co-segregating with bipolar disorder and inherited kidney disease in a multiplex family causes defects in neuronal growth and depression-like behavior in mice in *Translational Psychiatry*, 2020 K. Nakajima, A. Miranda, D.W. Craig, T. Shekhtman, S.Kmoch, A. Bleyer, S. Szelinger, T. Kato and J. Kelsoe The dissertation author was a primary investigator and author of this material.

Chapters 4 and 5 in part, are currently being prepared for submission for publication of the material. Miranda, Alannah; Kelsoe, John. The dissertation author was the primary investigator and author of this material.

VITA

2014 Bachelor of Science, California State University, San Marcos

2021 Doctor of Philosophy, University of California San Diego

PUBLICATIONS

Miranda, A., Shekhtman, T., McCarthy, M., DeModena, A., Leckband, S. G., & Kelsoe, J. R. (2019). Study of 45 candidate genes suggests CACNG2 may be associated with lithium response in bipolar disorder. *Journal of affective disorders*, *248*, 175-179.

Nakajima, Kazuo, et al. "Ntrk1 mutation co-segregating with bipolar disorder and inherited kidney disease in a multiplex family causes defects in neuronal growth and depression-like behavior in mice." Translational psychiatry 10.1 (2020): 1-13.

FIELDS OF STUDY

Major Field: Biochemistry

Professors Matthew Escobar, Jose Mendoza, Denise Garcia and Suzanne Hizer

ABSTRACT OF THE DISSERTATION

Using patient-derived induced pluripotent stem cells to investigate the role of TrkA signaling in Bipolar Disorder

by

Alannah Hope Miranda

Doctor of Philosophy in Biomedical Sciences

University of California San Diego, 2021

Professor John Kelsoe, Chair

Bipolar disorder (BD) is a neuropsychiatric disorder that is characterized by a fluctuation between depressive and manic phases. In previous studies of a multi-generational family with bipolar disorder, a variant was identified in *NTRK1* which codes for TrkA. The variant, rs144901788, causes an amino acid change from glutamate to

lysine at position 492. This is located in close proximity to the SHC/Frs2 binding site at tyrosine 490, through which TrkA is known to play a role in cell survival and neurite growth. iPSCs have been generated from lymphoblast cell lines taken from members of the family, both with and without the mutation. These are further differentiated into neural stem cells (NSCs). NSCs derived from the affected patients exhibited differences in gene expression and neurite outgrowth. Downstream signaling of TrkA binding was also evaluated. *NTRK1* appeared to be downregulated in the affected neural stem cells. Additionally, *NTRK1*, as well as it's ligand nerve growth factor (NGF), have been found to be associated with bipolar disorder in genome wide association studies. Understanding the role of *NTRK1* in bipolar disorder may allow for establishing distinct sub-forms of illness that operate through different pathways, yet ultimately culminating in a final disease presentation.

Chapter 1

Bipolar disorder and the cholinergic system

Bipolar disorder (BD) is a neuropsychiatric disorder that is characterized by shifts in mood between manic and depressive phases. A recent estimate for the global 12-month prevalence of bipolar disorder is 1.5% of the adult population.(1) However the 12-month estimated prevalence in the U.S. in the past year was found to be as high as 2.9%, as estimated by the NCS-R. In addition to the great number of individuals affected by mood disorders such as BD, the impact on the health care system and economic burden is great. According to one study, in 2015 the total costs attributed to just BD Type I amounted to $202.1 billion, or $81, 559 per person on average, in the United States.(2) This included not only direct health care costs, but also indirect costs, such as productivity, unemployment and caregiving. Another study analyzed the direct healthcare costs in the United States from 2007-2017 associated with mood disorders. This study found that the annual direct health care costs amounted to $172 billion. This demonstrates that there is a profound impact of mood disorders on not only the vast number of affected individuals, but also to the population as a whole.

A 12-month global prevalence of bipolar disorder at 1.5% shows that there is clearly a large number of affected persons, however the diagnoses of neuropsychiatric disorders such as BD is a complex process, indicating that there are likely many more affected, yet still undiagnosed, individuals. Diagnoses are based on the DSM-V, which consists of various behavioral patterns associated with each psychiatric disorder. There is a vast amount of heterogeneity in the presentation of BD, as well as overlap with many other mental illnesses. This also contributes to a high rate of misdiagnosis, as high as 69% according to one study, which further hinders individuals from getting accurate diagnoses and treatments.(3)

Additionally, BD can be sub-categorized into 4 main classifications; bipolar type 1 (BD I), bipolar type 2 (BD II), cyclothymia and atypical forms which do not fit into any of the previous classifications. Some of the symptoms that BD patients in manic phases suffer from include decreased need for sleep, racing thoughts and poor decision making, and in depressive phases individuals suffer from contrasting symptoms, such as low mood, hypersomnia, inability to think or concentrate, anhedonia, and suicidality. While the predominant feature of all types of BD are debilitating shifts between the described manic and depressive symptoms, there is great variation in the mood changes, as well as many other symptoms and comorbidities. For example, patients diagnosed with BD I experience at least one episode of mania, whereas BD II patients are characterized as having at least one hypomanic episode and one major depressive episode. Hypomania includes the same symptoms as BDI mania, but is milder and without impairment. Those affected with any type of BD may also be comorbid with anxiety disorders, personality disorders, psychosis or substance abuse disorders.(1) The suicide rate of BD patients is also alarming high, with approximately 1/3 of patients attempting suicide at least once. If treated 5% of those patients will complete those attempts, however if left untreated the percentage jumps to 15-20% of those attempts being completed.(1)

There is clearly a great need to understand the etiology of BD in order to more effectively treat its causes and eliminate the suffering these individuals endure. However, in addition to the difficulties in diagnosing neuropsychiatric disorders, researching their cellular pathologies is also problematic. These disorders are difficult to replicate in animals, as the behavioral cues may not be directly related to those

presented in humans. Additionally, due to its origin in the brain, biological differences in psychiatric disorders are difficult to directly observe in patients, apart from post-mortem studies and imaging. Regardless, there has still been great progress in elucidating the putative mechanisms behind bipolar disorder.

Mood disorders such as BD have been found to be highly heritable, with SNP heritability explaining up to 30% of risk for developing BD(4). Family studies have shown that the prevalence of BD in individuals with a first-degree relative with BD is 10-15%, compared to 1-3% in the general population. Monozygotic twins have a concordance rate of roughly 80% compared to20-30% in dizygotic twins(4). A 2013 genome wide association study (GWAS) discovered a significant genetic overlap between five mental health disorders; autism, ADHD, bipolar disorder, major depression and schizophrenia.(5)

This data combined indicates that bipolar disorder, along with many other mental health disorders, have a strong genetic component. Following these GWAS, has been a movement to understand how any genes that are identified as associated with BD are affecting BD neuropathology and thus contributing to behavioral symptoms that are observed.

1.1 The cholinergic hypothesis of bipolar disorder

Prior to GWAS studies, neuropharmacological and neuroimaging studies have supported a cholinergic-adrenergic hypothesis as a cause for BD. This hypothesis was drawn from the idea that there is a tendency towards a natural homeostasis between the two primary branches of the autonomic nervous system; the sympathetic system, regulated by adrenergic neurotransmitters, and the parasympathetic system, regulated

by cholinergic neurotransmitters. This hypothesis states that a high level of cholinergic activity, compared to a low level of adrenergic activity, causes the depressive state of bipolar disorder, while mania resulted from the opposite.(6,7)

One key piece of evidence for the cholinergic hypothesis of BD was the use of cholinomimetic and anticholinergic drugs, particularly physostigmine, an acetylcholinesterase inhibitor, in patients with mood and affective disorders. Cholinesterase inhibitors such as physostigmine, will bind to acetylcholinesterase and block acetylcholine (ACh) degradation. This leads to an accumulation of ACh within the synaptic cleft. It was found that when administered, symptoms of depression were induced in patients that had a history of major depression disorder or BD more robustly than in unaffected control patients, and biological markers of depression were found to be altered in individuals with mood disorders after physostigmine administration. (8–10)

The muscarinic agonist, arecoline has also been shown to induce depression symptoms in individuals affected by major depressive disorder and BD.(11,12) These studies reinforce the idea that the cholinergic system plays a role in mood regulation. Another study investigating the disrupted sleep pattern of depressed patients also appears to be consistent with the cholinergic-adrenergic hypothesis. Induction of REM sleep can be a biomarker for depression. In this study, the administration of arecoline was found to induce REM-sleep more quickly in patients with an affective disorder (major depression and bipolar disorder), as compared to administration of a control treatment, as well as compared to psychiatrically healthy controls. This hypersensitivity to REM sleep induction indicates that the muscarinic receptors may somehow be

upregulated or hypersensitive to cholinergic signaling, in patients with a history of depression.(13)

Neuroimaging studies have further supported the cholinergic-adrenergic hypothesis. PET imaging has revealed that patients with BD have significantly reduced muscarinic (M2) receptor binding. The binding of a radioligand was reduced due to competition for M2 receptor binding with endogenous ACh.(14) Post-mortem studies found there was no difference in M2 or M4 receptor population between BD and control subjects, suggesting that the difference in M2 and M4 binding was due to a high level of endogenous ACh, rather than a difference in receptor density.(15)

Existing cholinergic agonists primarily target muscarinic receptors, indicating that mood may be principally regulated by muscarinic receptors. However, nicotine is a well characterized nicotine receptor agonist, often studied in the context of smoking and smoking cessation. It has been shown that nicotine withdrawal during smoking cessation can induce depression, especially in individuals with a history of past depression.(16,17) One study demonstrated that there was a lower availability of β2 nicotinic receptors observed in patients with major depressive disorder, and then later confirmed in BD patients.(18,19) However, after ACh was removed, the differences between affected patients and controls disappeared.(18)

Pharmacological studies of the cholinergic system have heavily relied on 3 categories of drug; AChE inhibitors, muscarinic and nicotinic agonists. These categories encompass the drugs described in the previously mentioned studies; physostigmine, arecoline and nicotine, respectively. These studies of muscarinic and nicotinic receptors suggest that the depressive state of BD can be attributed to a hypercholinergic state,

altering both muscarinic and nicotinic ACh receptor binding.(10) While the pharmacological literature described here supports the hypothesis that the cholinergic system significantly impacts mood, the mechanisms by which this may occur is incredibly complex.

Both muscarinic and nicotinic receptors bind ACh, leading to a variety of downstream activities, which varies significantly based on the receptor localization within the brain. For instance, cholinergic synapses in the hippocampus and cortex are comprised of both muscarinic (mAChRs) and nicotinic(nAChRs) receptors. However mAChRs are localized at both pre-synaptic positions and post- synaptic positions, whereas nAChRs appear to be predominantly localized at pre-synaptic positions.(20) The complexity of interactions between nAChRs and mAChRs in response to ACh stimulation can also be observed when evaluating effects of the AChE inhibitors such as physotigmine. Physostigmine increases levels of intracellular ACh by blocking the degradation of it, however this increase in intracellular ACh can lead to excessive stimulation of muscarinic receptors.(21) In another example, an mAChR agonist such as arecoline, will inhibit post-synaptic mAChR stimulation. However mAChR agonists such as arecoline are non-selective, which results in the pre-synaptic mAChRs being inhibited as well, again leading to an increase in ACh release. This can in turn lead to a high level of intracellular ACh stimulating extracellular nAChRs.(21)

Neurotrophins, particularly NGF, are proposed to play an integral role in regulation of the cholinergic system. NGF is the high affinity ligand to TrkA, a cell surface receptor found on cholinergic neurons. NGF/TrkA signaling is of particular interest due to its role in altering ACh release in basal forebrain neurons. Basal

forebrain cholinergic neurons that are treated with NGF display an increase in ACh release and choline acetyltransferase (ChAT) activity. Additionally, this was found to be dependent on TrkA. After treatment with K252a, an inhibitor of TrkA kinase activity, NGF-induced ACh release was blocked.(22) Removal of *NTRK1* in mice has been shown to disrupt the cholinergic circuitry. While TrkA does not appear to be necessary for cell survival, it has been shown to regulate basal forebrain cholinergic neuron innervation and when removed, reduces ERK activation and ChAT expression.(23) There is also evidence that TrkA plays a role in the upregulation of ChAT and vesicular acetylcholine transporter (VAChT), two enzymes responsible for synthesis and storage of ACh. In one study, the mouse cholinergic cell line SN56 was transfected to express TrkA. mRNA transcript levels of ChAT and VAChT were found to be increased in response to NGF treatment in the TrkA-transfected cell lines.(24)

NGF-TrkA signaling has also been observed to provide neuroprotective properties in neural stem cells via the PI3K and ERK pathways. For example, NSCs exposed to the neurotoxin staurosporine, resulted in cell apoptosis in mouse neural stem cells, however this apoptosis was prevented in cells that were pre-treated with NGF.(25) This effect was diminished when TrkA was inhibited. Combined, these data suggest that NGF-TrkA signaling may directly affect ACh release, and also alter the pathways of basal forebrain cholinergic neurons development, differentiation and survival.

1.2 Downstream activity of NGF-TrkA

NGF-TrkA signaling is a complex process that involves a large number of adaptor and effector proteins, resulting in many different cellular effects. While the

previous chapter section largely focused on those cellular effects within the context of the cholinergic system, this section will focus on the downstream factors involved in the NGF-TrkA signaling cascade. NGF-TrkA signaling occurs through several main pathways, many of which appear to interact and complement each other. However, it is also apparent that the different NGF-TrkA signaling cascades also result in opposing cellular actions, for example regulation of apoptosis and cellular proliferation can both occur downstream of NGF-TrkA. Here we will explore these different pathways, the known factors involved in each, and how they may interact.

TrkA dimerizes and binds NGF, which then causes the autophosphorylation of several tyrosines. The autophosphorylation of Y490 allows for the binding of SHC and Frs2, as well as a potential transmembrane interaction with the protein ankyrin repeat-rich membrane spanning (ARMS). Interactions with all three of these proteins is associated with the activation of MAPK, however, this occurs through different mechanisms. Additionally, the PI3K-Akt pathway can also be activated through the Y490 autophosporylation site. Both of these pathways play crucial roles in cell survival, neural differentiation and neurite outgrowth.(26,27)

Signaling through SHC results in transient activation of the Ras-ERK and PI3K pathways, which typically is associated with a cell proliferation response, however it has also been seen to induce neurite growth.(28) In contrast, signaling through Frs2 leads to the formation of NGF-TrkA signaling endosomes and prolonged ERK signaling. Prolonged, or sustained, ERK signaling is associated with a cell differentiation response.(26,28) Prolonged and transient ERK signaling through NGF-TrkA signaling is

directly involved in the regulation of both cell proliferation and cell differentiation in neural cells, and may act as a switch between the two cellular activities.

Y490 binding of SHC is perhaps the most well established interaction in initial NGF-TrkA signaling. Once SHC is bound to TrkA, it allows for the recruitment of Grb2, which then forms a complex with SOS, thereby activating Ras via GTP. Raf-1 and B-Raf are then activated, which go on to activate ERK1/2. Activation of ERK1/2 leads to the phosphorylation of CREB, which induces the expression of genes related to neuronal survival and differentiation.(29) This activation of the MAPK pathway is transient and occurs rapidly, with activation of MAPK lasting for less than 5 minutes. The SHC-Grb2 complex can also lead to the activation of the PI3K pathway. Grb2 recruits Gab1, which has been shown to be associated with PI3K. The PI3K-Gab1 complex appears to be associated with enhanced neuronal survival. This pathway can be activated both through Y490 and the SHC-Grb2 complex, as well as a through a secondary TrkA phosphorylation site at Y751.(29) As briefly described in the previous section, NGF induced neuroprotection against a neurotoxin, staurosporine, appears to occur through the PI3K pathway, however the exact mechanism through which this occurs is not clear.(25) However, there is also evidence that activation of PI3K can induce the expression of genes as well, which may in turn lead to neuronal survival. Other studies have shown that PI3K plays an integral role in mediating the expression of cholinergic genes such as ChAT and VAChT, as well as TrkA through the activation of Lhx8, which binds to the TrkA gene enhancer region after stimulation with NGF.(30,31)

Prolonged MAPK activation, where MAPK remains activated for several hours, occurs after binding through Frs2 or a transmembrane interaction with ARMS. In order

for prolonged MAPK activation to occur, the NGF-TrkA complex forms a signaling endosome by either clathrin-mediated endocytosis or pincher-mediated micropinocytosis.(32) Frs2 binding likely occurs prior to TrkA-NGF endocytosis, however it binds competitively to Y490 with SHC, and at a much slower rate.(33) Once Frs2 binds to TrkA, it is phosphorylated, which allows it to recruit Grb2 and Crk. Crk then activates C3G which activates Rap1, eventually leading to the phosphorylation of MAPK. Crk is also recruited to TrkA by ARMS.(26) ARMS is closely associated with TrkA at the plasma membrane, and has been shown to rapidly phosphorylate following NGF stimulation. Phosphorylation of ARMS allows for the docking of the CrkL-C3G complex, resulting in prolonged activation of MAPK through Rap1.(34) Prolonged MAPK activation is typically associated with neuronal survival and neuronal differentiation.

Many of these downstream pathways overlap, resulting in similar cellular outcomes. For example, both transient activation of MAPK through SHC and prolonged activation of MAPK through Frs2 or ARMS can result in the expression of genes associated with neuronal survival. However the mechanisms through which neuronal survival is initiated by these pathways are very different. When MAPK is activated via the SHC pathway, Erk1/2 activates Rsk kinases that phosphorylates CREB, which induces the transcription of genes that control neuronal survival, such as the pro-survival gene, bcl-2.(35) Interestingly, bcl-2 levels have also been associated with bipolar disorder manic symptoms, as well as lithium response.(36,37) When MAPK is activated by the Frs2-Crk or ARMS-CrkL pathways, ERK5 is activated, which then activates the MADS box transcription enhancer factor 2 polypeptide D (MEFD2). This induces the transcription of antiapoptotic genes, such as bcl-w, thereby leading to

neuron survival.(29) In another study, the authors posit that the activation of ERK1/2 or ERK5 both result in neuronal survival, however the location at which NGF is received by the neuron, results in different cellular mechanisms by which CREB is phosphorylated. When NGF binds to TrkA at distal axons, the activated TrkA is endocytosed and retrogradely transported to the cell body where the ERK5 pathway is activated leading to CREB activation in the nucleus. Conversely, when NGF binds to TrkA directly at the cell body, ERK1/2 and ERK5 pathways are both induced.(38)

Localization of TrkA also plays a key role in how differentiation is regulated by NGF-TrkA signaling. Studies in PC12 cells have demonstrated that transient MAPK signaling induced by NGF alone is sufficient to produce neurite growth.(34),(39) However, the mechanisms behind and relationship between neurite growth and axon formation as it relates to TrkA signaling is an ongoing research question. NGF stimulation appears to not only trigger the retrograde transport of NGF but also can lead to an accumulation of activated TrkA in the distal axon.(40) Accumulation of the activated TrkA at the distal axon has been observed as a key step in the formation of axons. Activated TrkA is then endocytosed, resulting in prolonged MAPK activation. Following the endocytosis of NGF-TrkA and retrograde transport to the nucleus, MAPK activation through ERK5 induces neuronal differentiation.(41) Activated TrkA has also been demonstrated to play a role in spatial organization of other factors to a single dendritic tip, such as PI3K and Rac1. The recruitment of these factors may lead to the depolymerization of actin at the dendritic tip allowing for rapid, favorable outgrowth of a particular dendritic tip and thus formation of the axon.(42) Both transient and prolonged activation of MAPK have been shown to result in similar neuronal differentiation

responses, suggesting that both contribute to different aspects of neuronal differentiation and work synergistically in development of neuronal populations.

Figure 1 details the primary players in the NGF-TrkA system downstream of Y490, however it is evident that NGF-TrkA signaling is an intricate process, with much still to be understood and investigated. While NGF-TrkA is purported to play a particularly key role in the cholinergic system, it also appears to play a crucial role in general neuronal development processes. The studies and mechanisms described in this chapter suggests that defects in TrkA could be an significant effector in the risk and development of psychiatric disorders, especially in depression related disorders such as bipolar disorder.

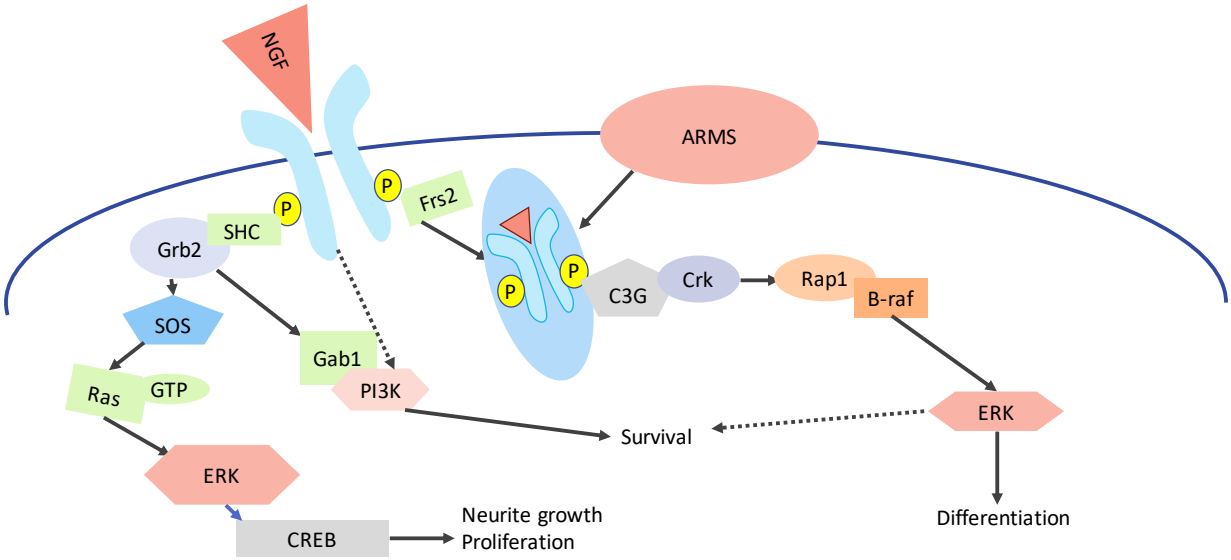

Figure 1: Schematic of the main factors involved in downstream NGF-TrkA signaling.

Chapter 2

Association of *NTRK1* with bipolar disorder and lithium response

NTRK1 as a main target in understanding bipolar disorder has been further investigated as a part of several genome wide association studies. A BD sample was collected and genotyped as a part of the Genetic Association Information Network Initiative (GAIN). The GAIN dataset was also analyzed as a part of the Bipolar Genome Study (BiGS). (43) The BiGS dataset consisted of case samples collected in 5 waves. Waves 1-4 included 2,936 subjects from multiplex families and sib-pair families and the fifth wave consisted largely of individual, unrelated cases. Controls were from 4,586 individuals across the U.S. that donated a blood sample and completed a medical questionnaire.

The Translation Genomics Research Institute (TGEN) performed an exon deep sequencing analysis on an early subset of the GAIN data set and identified 5 non-synonymous *NTRK1* and *NGF* SNPs in the cases that were not present in controls, 3 of which were novel SNPs, as well as several SNPs present in cases and controls. (Table 1) The complete BIGS data set was also later analyzed using Targeted Deep Sequencing of four neurotrophic genes *NGF*, *NTRK2*, *NTRK1*, and *BDNF*.

More recently, a DEPICT analysis (Data-driven Expression-Prioritized Integration for Complex Traits) was performed on the world's largest cohort of bipolar genomic data. This analysis identified the NGF signaling via TrkA from the plasma membrane as one of the top significant pathways implicated in bipolar disorder.(44)

Table 1: List of NTRK1/NGF non-synonymous variants identified in GAIN dataset.

Position	rs ID	Cases (C) or Case and Control(C/C)	Gene	Frequency
155110237	novel	C	NTRK1	n/a
155110312	novel	C	NTRK1	n/a
115630905	novel	C	NGF	n/a
155112912	rs121964866	C	NTRK1	0.000034
155100793	rs13914006	C	NTRK1	n/a
155097366	novel	C/C	NTRK1	n/a
155110063	rs137979116	C/C	NTRK1	0.000918
155118006	rs35669708	C/C	NTRK1	0.003655
155097529	novel	C/C	NTRK1	n/a
115630701	rs11466111	C/C	NGF	0.010786
155097403	rs1007211	C/C	NTRK1	0.00483
155110079	novel	C/C	NTRK1	n/a
115630836	rs6330	C/C	NGF	0.365572
155115776	novel	C/C	NTRK1	n/a
155112055	rs144901788	C/C	NTRK1	0.000520

2.1 NTRK1 association with lithium response in a candidate gene study

As evidenced above*, NTRK1* has repeatedly been observed as a top hit in genome wide association studies of BD. Therefore *NTRK1*, as well as *BDNF*, *NTRK2* and *NTRK3* were included in a candidate gene study to evaluate lithium response in BD patients. This study aimed to identify genetic markers associated with a positive response to lithium in BD patients. In addition to these neurotrophin and neurotrophin-related genes, 41 other genes were selected for analysis as well. Genes were selected for the candidate study based on whether 1) they had previously been reported as to be associated with lithium response, 2) they were found to be involved in lithium's purported mechanisms of action and 3) genes were associated with risk for bipolar disorder. 684 SNPs were selected within these genes due to either to optimally tag the gene or had a known functional effect. A list of genes and number of SNPs can be found in Table 2.

Table 2: : Genes and # of SNPs selected for analysis in the retrospective study. Genes and SNPs were selected based on prior association with lithium pathways or bipolar disorder.

Gene	SNP count	Gene	SNP count
ADCY1	21	*MAPK1*	7
AKT1	5	*MAPK3*	1
AKT3	24	*MARCKS*	5
BAD	8	*NRG1*	51
BCL2	17	*NTRK1*	49
BDNF	9	*NTRK2*	32
CACNG2	41	*NTRK3*	49
CLOCK	10	*P2RX7*	17
CREB1	2	*PDE11A*	34
CREM	10	*PDE4B*	34
CSNK1E	4	*PER3*	13
CTNNB1	20	*PIK3C2A*	6
DAOA	9	*PIK3C2B*	9
DGKH	37	*PIK3CA*	8
FAIM	5	*PIK3CB*	3
FKBP5	6	*PIK3CG*	32
GSK3A	3	*PLCG1*	5
GSK3B	5	*PPP1R1B*	2
HTR2A	21	*SLC10A5*	1
IMPA1	5	*SOS1*	11
IMPA2	14	*SOS2*	15
INPP1	7	*YWHAG*	4
KCNMB3	13		
Total: 684			

Methods

Subjects

All subjects provided written informed consent according to the Institutional Review Board (IRB) approved protocol. Subjects came from two independent studies of lithium response, one with retrospective assessment of lithium response, the other was a prospective trial with a relapse prevention design. Subjects in the retrospective sample were ascertained as part of a family based linkage study or a case control study of bipolar disorder genetics. From each family only the proband was included. Each subject underwent diagnostic assessment using the Diagnostic Interview for Genetic Studies (DIGS). (45) Only subjects with a Bipolar Disorder Type I (BDI) diagnosis were included. Demographic information on both the retrospective and prospective cohorts can be found in Table 3. The cohorts were not significantly different in terms of age, lithium response (good or poor), or family history. The two cohorts were significantly different in gender. This is largely due to the prospective cohort being recruited from the veteran population (largely males within the VA).

Table 3: Demographics for subjects in both cohorts. Retrospective study (n=286) and prospective (n=68) study, including Caucasian subjects only.

	Retrospective	Prospective	p-value
Gender (M/F)	148 / 138	60 / 8	<0.0001
Mean Age (Range)	44.8 (15-76)	45.75 (23-70)	.611
Lithium Response (Good/Poor)	135 / 151	40 / 28	0.085
Family History (Positive/Negative)	152 / 134	43/ 25	.133

Assessment of Lithium Response

Retrospective sample

As part of the assessment, subjects were queried regarding all their past medication trials. Subjects were included if they had a past history of lithium treatment. Patients who had taken lithium, were then queried on whether the lithium reduced their symptoms by 50% or more. All clinical information, including the DIGS interview, review of medical history, medical records and family informants was reviewed by a panel of experienced clinicians who were blind to genotype. The subject's response over their lifetime was assessed. Those who were rated as positive lithium responders (>50% reduction in symptoms) were classified as good responders, and those with a self-reported negative lithium response (<50% reduction in symptoms) were classified as non, or poor, responders. We have validated this retrospective assessment method, by comparing blind retrospective scoring of prospective subjects to their prospective outcome. (Appendix Figure 1 and Table 1)

Prospective sample

In the prospective study, patients with BDI were placed on lithium monotherapy and their progress was noted over the course of 2 years. This study consisted of 3 phases, the first stage being stabilization, during which patients were tapered off other medications and titrated up to a therapeutic lithium level. They were then judged to either be stabilized and a responder or a non-responder. Stabilization phase lasted for 4 months, and was followed by the observation phase, where subjects were observed on lithium monotherapy for 1 month in order to document response. Subjects then entered

the maintenance phase which lasted over 2 years. During this time, they were monitored every 2 months for relapse. The physician rated Clinical Global Impression Scale (CGI) was used as the primary measure of response. Subjects rated as having only mild symptoms were considered responders and allowed to advance to maintenance. Subjects were also assessed with the Hamilton Rating Scale for Depression, the Young Mania Rating Scale, the Internal State Scale and the Beck Depression Inventory. Two different outcome measures were used: 1) for acute response. Patients were classified as either responders or non-responders based on their ability to stabilize on lithium monotherapy and enter maintenance; 2) for survival analysis, time to event was used as a measure, where the event is either failure to remit or relapse once remitted. The prospective study was designed for replication of results in the retrospective study. It is the gold standard for assessing response, but allowed only a small sample size.

Genotyping

SNPs were directly genotyped in the retrospective study, using either the SNPlex multiplex method or Taqman genotyping (Life Technologies, San Diego) as previously described and according to the manufacturer's directions. (46) In the prospective study, genotyping data from the prospective study was completed on the PsychArray Chip (Illumina, San Diego).

Statistical Analysis

Phenotype and demographic differences between the retrospective and prospective cohorts, as well as between responders and non-responders within each cohort, were tested in SPSS using either the independent T-test or Chi-square test. P-

values for these analyses, as well as other phenotype information can be found in Table 3.

Association analyses were completed using logistic regression in PLINK version 1.9. Principal components were computed in plink using the population stratification functions in PLINK version 1.9. For both the retrospective and prospective study, principal components were calculated based on pairwise identity by state (IBS) clustering. Principal components were calculated for the Caucasian population of each study, and as well the entire subject population.

In the retrospective study, the analysis was completed on 684 directly genotyped SNPs within the 45 selected genes (Table 2). This analysis included Caucasian subjects only, comparing lithium responders to non-responders, using age, sex and 3 principal components (within the Caucasian subject population) as covariates in the logistic regression.

For the prospective analysis, again only Caucasian subjects were analyzed in a single SNP association analysis, using age, sex and 3 principal components (within the Caucasian subject population). Analyses were conducted using the acute response (entered maintenance) with covariates in PLINK.

In order to increase statistical power, a gene-based set analysis was also performed in PLINK. SNPs and subjects were similarly filtered in both cohorts for minor allele frequency, missingness and genotyping rate, as described for the SNP by SNP analysis. Only Caucasian subjects were analyzed for both cohorts, again similar to the SNP by SNP analysis. The number of permutations for this analysis is set to 10,000 and the empirical p-value result is the number of times the permuted test statistic exceeds

the original test statistic. This p-value has been corrected for the multiple SNPs within a set.

Results

Retrospective analysis

Of the 45 selected candidate genes, 9 contained SNPs that showed nominal significance (p>0.05) in a Caucasian only (n=286), retrospective analysis. After accounting for SNPs in LD, a total of 174 distinct clusters of SNPs was determined. Using this to correct for multiple comparisons, no SNPs were found to be significant. The SNP with the highest significance was found in the CACNG2 gene (rs140040; p=0.002632, OR=1.728). (Table 4)

Table 4: SNPs and genes associated with a positive response to lithium in the retrospective analysis; (p<0.05) after LD clumping (*N*=number of SNPs in LD with index SNP, $r^2 = 0.1$)

SNP	OR	P	N	Gene
rs140040	1.728	0.00263	9	*CACNG2*
rs2975498	0.516	0.00532	7	*NRG1*
rs11208844	2.019	0.00557	3	*PDE4B*
rs10908523	3.509	0.00693	2	*NTRK1*
rs42154	1.661	0.0132	1	*PIK3CG*
rs7585543	1.801	0.0157	12	*PDE11A*
rs1211166	1.784	0.0201	13	*NTRK2*
rs9638987	1.68	0.0244	5	*ADCY1*
rs11208816	0.6781	0.027	5	*PDE4B*
rs2466061	1.976	0.029	4	*NRG1*
rs17664708	1.897	0.036	6	*NRG1*
rs2150906	0.4587	0.0396	7	*NTRK1*
rs10149742	1.811	0.046	2	*SOS2*
rs868362	0.5793	0.0462	1	*ADCY1*

A gene-based set analysis in PLINK showed that 10 genes had at least one SNP which had a p-value <0.05. The top hit in the retrospective gene based analysis was

CACNG2 (p=0.07249). The empirical p-values for all 10 genes are reported in the Table 5. No gene was nominally significant in this analysis.

Table 5: Gene-based set test results using PLINK in the retrospective cohort. Genes and empirical p-values for gene sets in which at least one SNP in a given set had a p-value of <0.05.

Gene	P-value
CACNG2	0.07249
MAPK1	0.08114
PIK3CG	0.09279
SOS2	0.1653
NRG1	0.2002
NTRK2	0.2093
PDE4B	0.2835
ADCY1	0.2869
PDE11A	0.3074
NTRK1	0.3309

Prospective analysis

11 genes showed nominal significance in the single SNP association analysis of the Caucasian prospective subjects (n=68). After accounting for LD, there were a total of 146 distinct clusters of SNPs. In using this number to correct for multiple comparisons, no SNPs reached significance. The most highly associated SNP in the prospective study (rs1347441; p=0.00993, OR=3.417) was found to be in PDE11A. Another SNP in *CACNG2* was also found to be nominally significant (rs2283967; p=0.0136, OR=.2596). Upon further examination of the clumping groups for the retrospective and prospective studies, the SNPs, rs140040 and rs2283967, were found to be clumped together in both the retrospective and prospective studies. LD calculations done in PLINK using the retrospective dataset, report an r^2 of 0.194451 and a D' of 0.678938 for these SNPs. The most significant SNP in PDE11A from the

retrospective analysis (rs7585543; p=0.0157, OR=1.801) and the most significant SNP in PDE11A in the prospective study (rs1347441; p=0.00993, OR=3.417) were not clumped together by PLINK. (Table 6)

Table 6: SNPs and genes associated with a positive response to lithium in the prospective analysis; (p<0.05) after LD clumping (*N*=number of SNPs in LD with index SNP, $r^2 = 0.1$), using directly genotyped SNPs.

SNP	OR	P	N	Gene
rs1347441	3.417	0.00993	11	*PDE11A*
rs1491851	0.2705	0.01306	2	*BDNF*
rs2283967	0.2596	0.0136	8	*CACNG2*
rs2076148	3.398	0.01371	5	*PLCG1*
rs12741937	0.1863	0.01661	6	*PER3*
rs5755694	0.3556	0.01742	7	*MAPK1*
rs484698	2.877	0.01911	6	*FAIM*
rs13329385	0.2859	0.02618	14	*NTRK3*
rs16879922	3.579	0.02901	8	*NRG1*
rs13003683	3.842	0.03077	8	*PDE11A*
rs6339	0.2184	0.04543	4	*NTRK1*
rs2070062	2.856	0.04883	8	*CLOCK*

In a secondary analysis only the nominally significant SNPs from the retrospective analysis were tested in the prospective cohort, in order to reduce the number of comparisons necessary to reach significance. However, this strategy resulted in no SNPs reaching even nominal significance. Additionally, the most significant SNP from the retrospective analysis was excluded in this secondary analysis due to a missingness rate higher than 10%

A gene-based set analysis in PLINK showed that 8 genes had at least one SNP which had a p-value <0.05. The top hit in the retrospective gene based analysis was CACNG2 (p=0.008799). The empirical p-values for all 8 genes are reported in the Table 7. CACNG2 was also the top hit in this analysis and was nominally significant, however it was short of reaching significance after multiple comparisons. The analysis was

repeated using only the 10 genes which returned an empirical p-value in the retrospective analysis. These results can be found in Table 8. CACNG2 was the top hit once again, and nominally significant (p=0.008199). However, it failed to pass the multiple comparisons threshold (p=0.005).

Table 7: Gene-based set test results using PLINK in the prospective cohort. Genes and empirical p-values for gene sets in which at least one SNP in a given set had a p-value of <0.05.

Gene	P-value
CACNG2	0.008799
MAPK1	0.06434
PLCG1	0.06779
FAIM	0.08814
PER3	0.1012
PDE11A	0.1027
NTRK3	0.4034
NRG1	0.6571

Table 8: Gene-based set test results using PLINK in the prospective cohort, and only genes from Table 7. Genes and empirical p-values for gene sets in which at least one SNP in a given set had a p-value of <0.05.

Gene	P-value
CACNG2	0.008199
MAPK1	0.06139
PDE11A	0.1007
NRG1	0.6556

After determining that the gene with the highest significance in both the retrospective and prospective studies appeared to be in *CACNG2*, the top SNP from the Silberberg study, rs2284017, was directly genotyped in the prospective cohort. This study previously found that *CACNG2* was significantly associated with lithium response in two cohorts(47). However, a Kaplan-Meier survival analysis showed no significant difference in genotype between the responders and non-responders. (Figure 2) A meta-

analysis using the program METAL did not result in any statistically significant SNPs when looking at the combined prospective and retrospective studies. (Table 9) (48)

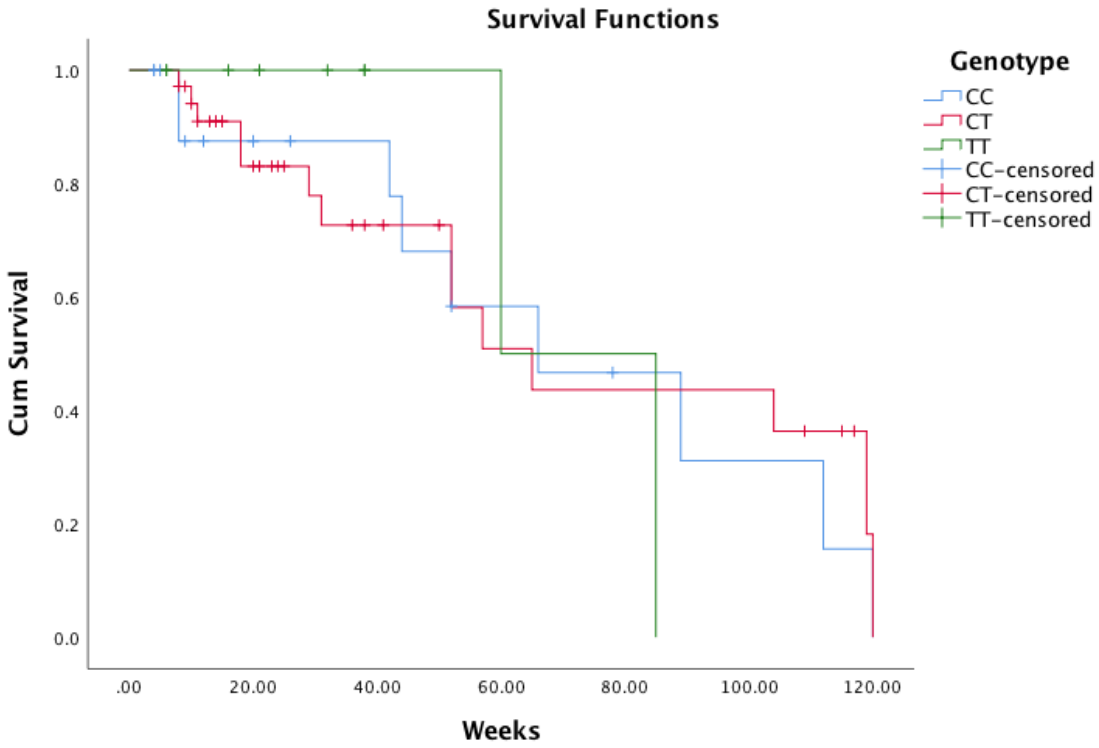

Figure 2: Kaplan-Meier survival analysis for rs2284017 in the prospective cohort. (p=.958)

Table 9: Nominally significant P-values and Z-scores of combined meta-analysis of the retrospective and prospective p-values, using the program METAL.

SNP	Zscore	P-value	Direction
rs11208844	3.033	0.002422	++
rs140040	3.008	0.002632	?+
rs764059	2.704	0.006858	++
rs10908523	2.7	0.006933	?+
rs1491851	2.698	0.006981	++
rs2975498	2.636	0.008394	++
rs2076148	2.615	0.008911	++
rs2228703	2.588	0.009644	++
rs6336	2.541	0.01106	++
rs6750869	2.508	0.01214	+?
rs4821503	2.505	0.01224	?+
rs42154	2.479	0.01316	?+
rs5755694	2.468	0.01357	++
rs12624863	2.381	0.01727	++
rs11208816	2.364	0.01807	++
rs1718134	2.354	0.01855	++
rs7585543	2.353	0.01862	++
rs868362	2.339	0.01935	++
rs11121029	2.303	0.02128	++
rs4733126	2.25	0.02447	++
rs4820239	2.199	0.02788	+?
rs2466061	2.183	0.02902	?+
rs11932595	2.144	0.03207	++
rs5749998	2.139	0.03242	++
rs12649507	2.138	0.03253	++
rs12741937	2.129	0.03322	++
rs9639924	2.049	0.04048	++
rs13081085	2.047	0.04067	++
rs13329385	2.028	0.04261	++
rs12731764	2.022	0.04314	?+
rs1435575	2.013	0.04416	++
rs6339	2.001	0.04543	+?
rs4820242	2	0.04555	++
rs7305883	1.999	0.04556	++
rs1128994	1.994	0.0461	++
rs10503927	1.985	0.04714	++
rs1801260	1.97	0.04883	+?

The study did not yield any significant SNPs that met the multiple comparisons threshold, and additional analyses also failed to reach significance after multiple comparisons. However, this study was limited in sample size, in particular the prospective study. Additionally there can be errors in assessing lithium response, for example, due to variations prescription history in the prospective response or variations in patient recollections in the retrospective response.

However, despite the limitations and lack of SNPs meeting the multiple comparisons threshold, there were many nominally significant SNPs that may be linked with positive lithium response. The top nominally significant SNPs in the retrospective and prospective cohorts can be seen in Tables 4 and 6. In particular, many SNPs in *CACNG2* were found to be nominally associated with lithium response, which is confirmatory of findings in a previous study identifying *CACNG2* as associated with lithium response in bipolar disorder.(47) Additionally, the most significant SNP in the retrospective study was found to be in *CACNG2* and the third more significant SNP in the prospective study was also in *CACNG2*. When using PLINK clumping, both *CACNG2* SNPs, rs2283967and rs140040, were found to be clumped together using PLINK LD clumping. Both are located in an intronic region of *CACNG2*, and while there is no report in the literature that suggests how either SNP may effect lithium efficacy, in a pharmacogenetics study of antipsychotic response, rs2283967 was shown to be a top hit associated with discontinuation of risperidone due to inefficacy. However it also failed to meet the multiple comparisons threshold in that study.(49)

Previous studies have also reported genome-wide significant linkage to *CACNG2* in a set of 20 families and 164 subjects using 443 microsatellite markers. The highest

LOD score 3.8 was found to be at chromosome 22q12, near *CACNG2*.(50) Further analysis of the region identified significant association in a region near *CACNG2*.(46)

Other notable nominally significant SNPs in the retrospective and prospective studies included *NTRK1*, *NTRK2*, *NTRK3*, *MAPK* and *BDNF*. This helps to bolster the hypothesis that neurotrophin-pathway related genes, including *NTRK1*, may play a role in BD mechanisms and treatments.

2.2 Family 6807 and identification of NTRK1 mutation

Previous studies in the lab identified a large pedigree, in which bipolar disorder co-segregated with autosomal dominant tubulo-interstitial kidney disease (ADTKD).(51) ADTKD is a rare autosomal dominant disorder characterized by tubulointerstitial fibrosis, with chronic kidney disease progressing variably to end-stage kidney disease between 20 and 80 years. The responsible gene for ADTKD in this family, was identified as *MUC1* at 1q22 encoding Mucin 1, a protein that forms protective mucous barriers on the surfaces of epithelial cells and is involved in cell signaling.(52) The function of *MUC1* and its lack of expression in the brain suggest that the gene for BD is likely linked to *MUC1*. Figure 3 is a pedigree of Family 6807, demonstrating which members are affected by both ADTKD and mood disorders. Detailed phenotype information can be found in Appendix Table 2.

Figure 3: The pedigree of family 6807

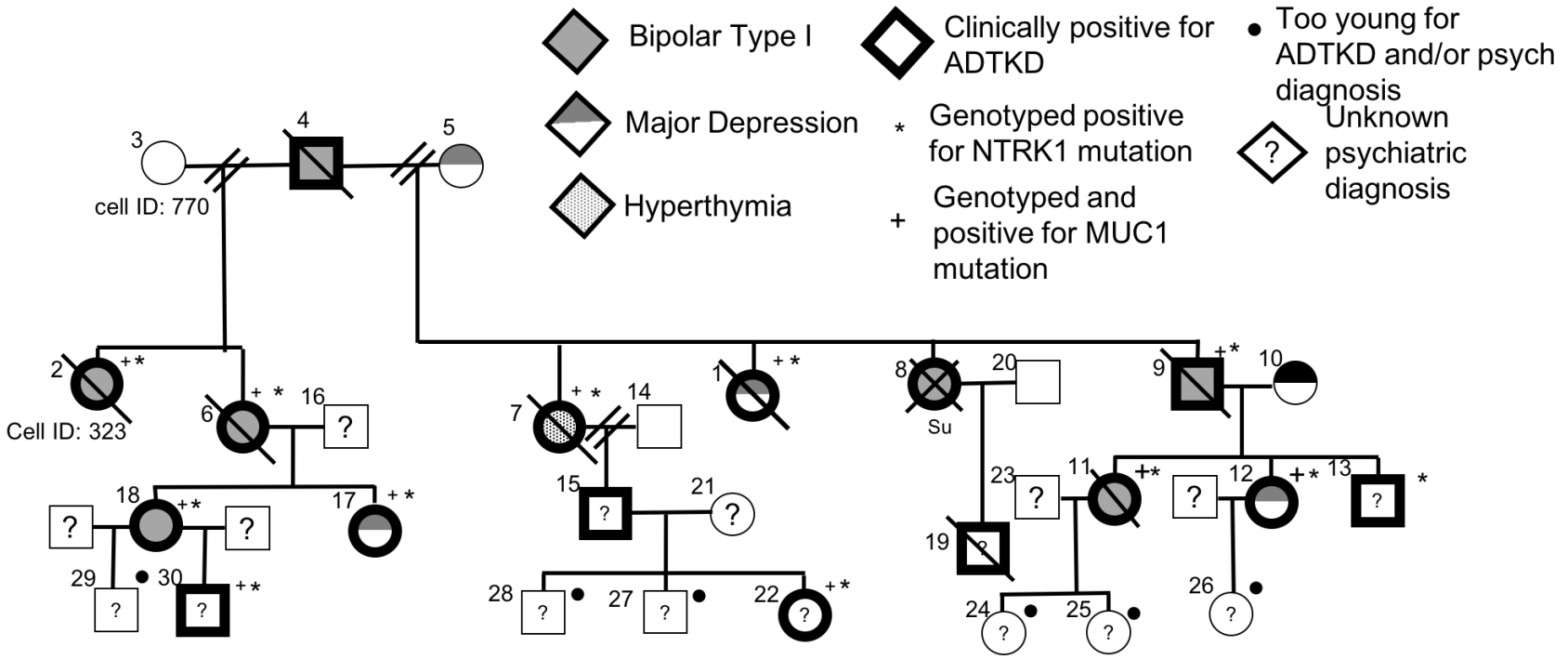
Bipolar Type I
Major Depression
Hyperthymia
Clinically positive for ADTKD
Genotyped positive for NTRK1 mutation
Genotyped and positive for MUC1 mutation
Too young for ADTKD and/or psych diagnosis
Unknown psychiatric diagnosis
cell ID: 770
Cell ID: 323
Su

Filter Method	SNP Type	Genome	Exome
First Pass: all SNPs	Total	3,333,079	108,976
	TiTv Ratio (All)	2.05	2.21
	TiTV Ratio (novel)	1.73	1.61
	Ti Tv Ratio (dbSNP)	2.10	2.29
	No. in dbSNP 129 (%)	2,909,250 (87)	97,914 (90)
	Concordance with dbSNP (%)	99.87	99.79
	No. not in dbSNP	423,829	11,062
	No. not in 1000 Genomes	242,057	7,116
	No. not in 12 exomes	241,918	6,960
Second Pass: all Coding SNPs	All Coding Variants (CDS)	22,304	20,244
	TiTv Ratio (All)	2.82	2.86
	TiTV Ratio (novel)	1.80	1.72
	Ti Tv Ratio (dbSNP)	2.98	3.03
	Homozygote	8,910	8,232
	Heterozygote	13,330	12,008
	Synonymous	10,959	10,245
	Missense	11,281	9,995
	Nonsense	141	103
	Splice Site	310	267
Third pass: all Novel SNPs	Novel Coding Varinats (CDS)	2,087	1,767
	TiTv Ratio (novel)	1.87	1.52
	No. not in 1000 Genomes	1,001	1,000
	No. not in 12 exomes	932	860
	Synonymous	291	280
	Missense	639	580
	Missense in CCDS	393	431
	Homozygote or Compound Heterozygote	298	371
	Homozygote	8	12
	Heterozygote	289	359
	Nonsense	5	14
	Splice Site	6	8
	Linked to Disease (HGMD)	75	92
Fourth Pass: Linkage Region	Novel, Missense under linkage peaks	43	49
	Homozygote	0	0
	Heterozygote	43	49
	Linked to diesase (HGMD)	9	15
	Associated with Neurological condition	1	2
	Associated with Kidney Condidtion	2	3
	Complex Disease	4	7
	Mendelian Disease	3	3

Figure 4: Sequencing and SNP filtering Summary Sequencing was performed over a number of platforms including Illumina Genome Analyzer I, Genome Analyzer II, and a HiSeq 2000. Multiple pass, hypothesis driven SNP filtering method was applied where all available databases was used to filter out common variants. We used dbSNP129, 1000 Genomes Project and common variants deposited to the public domain from 12 human exomes. Quality analysis indicated that the transition/transversion ratio of novel coding variants were under the 3.0 expected ratio, indicating challenges in calling variants correctly without false positive call inflation.

In order to determine genes likely to contribute to the BD in this pedigree, blood was initially drawn from 13 members, spanning 3 generations, including both affected and non-affected members. DNA was prepared from lymphoblastoid cell lines by phenol/chloroform extraction. Genotyping for linkage analysis was performed as described in a previous paper and linkage analysis was performed in Merlin using a non-parametric exponential model.(53) Whole genome sequencing was then completed at TGen using Illumina Genome Analyzer I, Genome Analyzer II and HiSeq 2000 platforms. Exome sequencing of the proband was completed to expand coding regions. Alignment, quality control and variant calling was completed using pipeline developed for the 1000 Genomes Project. Quality control was completed using the Genome Analysis Toolkit (GATK). FASTQ alignments were aligned with BWA to Build 36 using a paired-gapped alignment. Duplicate pairs were marked using Picard. SNPs were called using the GATK toolkit and post-filtering processing was completed to eliminate any false positives. Linkage-disequilibrium based calling was completed using Beagle or MACH. A detailed table for the filtering parameters can be found in Figure 4.

Linkage analysis using blood drawn from the initial 13 members and approximately 400 microsatellite markers found suggestive peaks with LOD scores between 1-2 on chromosomes 1, 12, 13, 19 and 22. (Figure 5) The linkage peak on 1q21 was of immediate interest due to its close proximity to the *MUC1* gene. Stretches of homozygosity on each of these chromosomes was shared by all members of the 2nd generation. Additionally, subsequent analysis of the 3rd generation revealed that nearly all 3rd generation members had also received the same haplotype on chromosome 1.

a

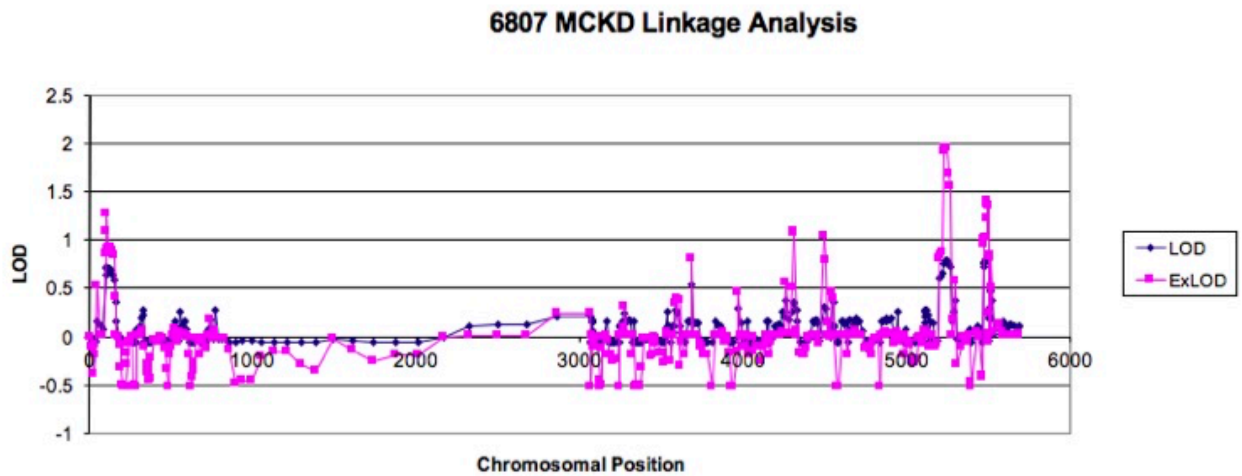

b

2nd | 3rd

Microsat FAMILY 6807 [Most Likely]Chr1

<table>
<tr><th></th><th>3(F)</th><th>4 (F)</th><th>5 (F)</th><th>10 (F)</th><th>14(F)</th><th>16(F)</th><th>2(3,4)</th><th>6(3,4)</th><th>1(5,4)</th><th>9(5,4)</th><th>7(5,4)</th><th>15(7,14)</th><th>12(10,9)</th><th>13(10,9)</th><th>17(6,16)</th><th>18(6,16)</th></tr>
<tr><td>D1S1665</td><td>2 : 2</td><td>? : 4</td><td>2 : 3</td><td>2 : 1</td><td>2 : ?</td><td>2 : ?</td><td>2 | 4</td><td>2 | 4</td><td>3 | 4</td><td>2 / 4</td><td>2 \ 4</td><td>2 | 2</td><td>2 | 4</td><td>2 + 4</td><td>4 | 2</td><td>4 | 2</td></tr>
<tr><td>D1S500</td><td>1 : 2</td><td>? : 3</td><td>3 : 3</td><td>1 : ?</td><td>3 : ?</td><td>3 : ?</td><td>2 | 3</td><td>1 | 3</td><td>3 / 3</td><td>3 | 3</td><td>3 | 3</td><td>3 | 3</td><td>1 | 3</td><td>1 | 3</td><td>3 | 3</td><td>3 | 3</td></tr>
<tr><td>D1S551</td><td>3 : 3</td><td>? : 4</td><td>4 : 3</td><td>2 : 3</td><td>3 : ?</td><td>1 : ?</td><td>3 | 4</td><td>3 | 4</td><td>4 | 4</td><td>4 | 4</td><td>4 | 4</td><td>4 | 3</td><td>2 | 4</td><td>2 | 4</td><td>4 | 1</td><td>4 | 1</td></tr>
<tr><td>D1S1588</td><td>2 : 2</td><td>? : 2</td><td>2 : 1</td><td>3 : 1</td><td>1 : ?</td><td>2 : ?</td><td>2 | 2</td><td>2 | 2</td><td>2 | 2</td><td>1 / 2</td><td>2 | 2</td><td>2 | 1</td><td>3 | 2</td><td>3 | 2</td><td>2 | 2</td><td>2 | 2</td></tr>
<tr><td>D1S1631</td><td>4 : 1</td><td>? : 4</td><td>4 : 5</td><td>3 : 2</td><td>1 : ?</td><td>5 : ?</td><td>1 | 4</td><td>4 | 4</td><td>5 / 4</td><td>5 | 4</td><td>4 | 4</td><td>4 | 1</td><td>3 | 4</td><td>3 | 4</td><td>4 | 5</td><td>4 | 5</td></tr>
<tr><td>D1S3723</td><td>3 : 4</td><td>? : 1</td><td>2 : 3</td><td>1 : 1</td><td>3 : ?</td><td>3 : ?</td><td>4 | 1</td><td>3 | 1</td><td>3 | 1</td><td>3 | 1</td><td>2 | 1</td><td>2 | 3</td><td>1 | 1</td><td>1 | 1</td><td>1 | 3</td><td>1 | 3</td></tr>
<tr><td>D1S1675</td><td>2 : 3</td><td>? : 2</td><td>3 : 2</td><td>1 : 1</td><td>1 : ?</td><td>2 : ?</td><td>3 | 2</td><td>2 | 2</td><td>2 | 2</td><td>2 | 2</td><td>3 | 2</td><td>3 | 1</td><td>1 | 2</td><td>1 | 2</td><td>2 | 2</td><td>2 | 2</td></tr>
<tr><td>D1S534</td><td>3 : 3</td><td>? : 3</td><td>3 : 3</td><td>4 : 4</td><td>1 : ?</td><td>2 : ?</td><td>3 | 3</td><td>3 | 3</td><td>3 | 3</td><td>3 | 3</td><td>3 | 3</td><td>3 | 1</td><td>4 | 3</td><td>4 | 3</td><td>3 | 2</td><td>3 | 2</td></tr>
<tr><td>D1S1595</td><td>1 : 2</td><td>? : 2</td><td>3 : 2</td><td>1 : 3</td><td>4 : ?</td><td>1 : ?</td><td>1 / 2</td><td>1 | 2</td><td>2 | 2</td><td>2 | 2</td><td>3 | 2</td><td>2 / 4</td><td>1 | 2</td><td>1 | 2</td><td>2 | 1</td><td>2 | 1</td></tr>
<tr><td>D1S1679</td><td>4 : 1</td><td>3 : 3</td><td>1 : 6</td><td>5 : 2</td><td>3 : ?</td><td>5 : ?</td><td>4 | 3</td><td>4 | 3</td><td>6 | 3</td><td>6 \ 3</td><td>1 | 3</td><td>3 | 3</td><td>5 | 3</td><td>5 | 3</td><td>3 | 5</td><td>3 | 5</td></tr>
</table>

Figure 5: Identification of loci of interest on chromosome 1 a) Linkage analysis of Family 6807, showing peaks at chromosomal positions associated with chromosomes 1, 12, 13, 19 and 22. b) Microsatellite markers for chromosome 1, including *NTRK1* region. Haplotypes for available members of the family (orange indicates 2nd generation, green indicates 3rd generation) and inferred haplotype for 1st generation father. Yellow columns indicate regions of homozygosity and blue regions indicate recombination events.

Whole genome sequencing of the proband (member 323) identified a total of 11,407 nonsynonymous coding sequence SNPs. Of these SNPs, 386 were found to be novel. These variants were then filtered and mapped to within 5 linkage regions identified in the previously described linkage analysis, resulting in 52 possible variants. These remaining SNPs were then filtered for genes expressed either in the brain, kidney or both and then further filtered for those predicted to be damaging by SIFT or

Pholyphen2. A *NTRK1* mutation found in this family was a single nucleotide G to A variant (Chromosome 1: 156,875,639 [hg38]), causing substitution of glutamate to lysine at the 492 residue of TrkA protein (*NTRK1* E492K), and was predicted to be damaging by Polyphen2 with a probability score of 0.99.

Sanger sequencing or genotyping confirmed the mutation in all affected members of the family, where samples were available for testing, including members up to the 4th generation. A linkage analysis of chromosome 1 for the SNP had a LOD score of 1.6, though not statistically significant or the largest in the genome scan, is noteworthy when considering the small sample size of a single family, the high degree of segregation with the two disease phenotypes and the proximity to an ADTKD gene.

The small sample size of this family study presents a limitation to presenting this mutation as associated with BD. In this case, the mutation (Chromosome 1: 156,875,639 [hg38]) is registered in the gnomAD database (1- 156845431-G-A; rs144901788) and found in 124 of 282262 alleles (0.043%). Assuming an odds ratio of 10, which is still less than the known major genetic risk factors of psychiatric disorders such as 22q11.2 deletion for schizophrenia (odds ratio = 67.7)(54) and loss of function mutations of SETD1A (Odds ratio = 20.0 calculated from SCHEMA browser) and given the statistical power to detect the association is 0.79, it may be possible to determine association of the SNP in a reasonably sized case-control study. However, given the limitation of low frequency of this SNP, family studies, such as the one presented here, are the preferred method to study the mutation in the context of mood disorders. In this particular situation, perfect co-segregation of this mutation with ADTKD comorbid with

mood disorders in this family provides a reasonable support for the role of this mutation in mood disorders in this family.

This mutation was also examined in case-control data from a previous study (Ament et al, 2015), of 3,014 cases and 1,717 controls, however rs144901788 was not identified in any sample. We did observe this mutation in one case and one control, in the TGEN targeted exome sequencing data set of 992 cases and 480 controls (Table 1). Though the statistical power to detect the association in this sample size with the same assumption is too small to draw a conclusion (0.47), the presence of this mutation in one affected individual, unrelated to the pedigree presented within this manuscript, might provide further evidence for this rare variant to play a possible role in bipolar disorder. While the presence of the SNP in a control sample appears to be contradictory, research suggests a polygenic nature of BD.(55) Therefore it is possible that the SNP may work in concert with other variants to produce the bipolar symptoms, of which the identified case may not also possess. The family presented in this study has numerous other abnormalities in their genome which may amplify the effect of this SNP. Alternatively, the case presented here may have variants which confer protection, as protective genotypes have been identified in other studies.(56,57)

Although this mutation is listed in the genome database, psychiatric health information is not available on these individuals, therefore it is impossible to determine whether or not those individuals also carry a mood phenotype. The mutation has also been reported in the literature as linked to a patient with congenital insensitivity to pain with anhidrosis (CIPA).(58) This patient experienced symptoms including developmental delay, sensory neuropathy and deafness, and family members were unavailable for

segregation analysis. The primary symptom of CIPA is insensitivity to pain, which has not been noted in any of the patients in the 6807 pedigree, however the reported CIPA patient was homozygous for the mutation, whereas patients in this pedigree are heterozygous. Additionally, there is a vast heterogeneity of clinical features in CIPA, including mood related symptoms, frequently described as hyperactive, irritable and emotionally instable.(59,60)

While there are many limitations in using a small family study to associate the *NTRK1* mutation with BD, much of the existing literature still supports the hypothesis that this *NTRK1* mutation may contribute to mood regulation. Despite the suggestion that the homozygous form of this mutation may be associated with CIPA, and no members of the family report insensitivity to pain symptoms, evidence also suggests those afflicted with CIPA may also exhibit mood symptoms. Additionally, the strong co-segregation of the mutation through 4 generations of affected family members, as well as the close proximity of the mutation to the ADTKD gene, which appears to be similarly highly penetrative, still supports for the role of this mutation in mood disorders in this family.

Chapter 2.1, in part, is a reprint of the material as it appears in Study of 45 candidate genes in identifies CACNG2 and NRG1 as associated with lithium response in Bipolar Disorder in *Journal of Affective Disorders* 2019. Miranda, A., Shekhtman, T., McCarthy, M., DeModena, A., Leckband, S., & Kelsoe, J. The dissertation author was the primary investigator and author of this paper.

Chapter 2.2, in part, is a reprint of the material as it appears in *Ntrk1* mutation co-segregating with bipolar disorder and inherited kidney disease in a multiplex family causes defects in neuronal growth and depression-like behavior in mice in Translational Psychiatry, 2020 K. Nakajima, A. Miranda, D.W. Craig, T. Shekhtman, S.Kmoch, A. Bleyer, S. Szelinger, T. Kato and J. Kelsoe The dissertation author was a primary investigator and author of this material.

Chapter 3

Neuronal defects caused by *NTRK1* mutation in NSCs and mice

Stem cells have become an invaluable tool in understanding many mood and developmental disorders. Induced pluripotent stem cells (iPSCs) have been used to study neuropsychiatric disorders in a manner that allows scientists to directly relate an individual patient's behavioral history to biological and genetic changes with changes in their own cells, in a disease relevant cell type. For instance, in one study of schizophrenia, skin fibroblasts were taken from patients and subsequently reprogrammed into iPSCs. These iPSCs were then differentiated in neurons and neural progenitor cells. Neuronal phenotypes were observed, including gene expression, synaptic density and electrophysiology and compared to iPSCs derived from healthy controls.(61) This non-invasive and patient specific model has quickly become a premiere tool used to investigate the neurobiological pathways of mental health disorders.

There have been numerous efforts to develop protocols to generate region-specific iPSC-derived neurons in order to study specific neuronal disease states and disorders affecting particular subtypes of neurons as well. For example, several studies of Alzheimer's disorder have developed protocols to differentiate human embryonic stem cells into basal forebrain cholinergic neurons (BFCNs)(62–64), in order to better understand the cholinergic system.

In the following study, iPSC technology is utilized to identify functional defects caused by the *NTRK1* mutation observed in this pedigree (Figure 3), in addition to a mouse model of the *NTRK1* mutation developed in collaboration with the Kato Lab at the RIKEN Center for Brain Science in Japan. Combined, these methods are used to determine neuronal defects associated with these mutations.

Methods

Reprogramming of Lymphoblast cell lines

Lymphoblastoid cell lines (LCL) were cultured in a standard PBLC media using RPMI 1640, 10% fetal bovine serum and 1% anti-biotic/anti-mycotic. LCLs were cultured in T-25 culture flasks until confluent, then reprogrammed using the Epi5 Episomal iPSC Reprogramming kit (Invitrogen). Cells were transfected as described in the provided protocol, and plated into Matrigel-coated 6 well plates. Reprogrammed LCLs were cultured in TeSR-E7 reprogramming media (StemCell Tech) for 2 weeks, replacing half the media daily, then transitioned into mTeSR1 iPSC culture media (StemCell Tech). iPSC colonies are expanded by daily complete media changes, then manually picked via pipette and replated into a new Matrigel coated plate.
iPSCs are expanded in mTeSR1 media and treated with ROCK inhibitor (Y-27632, StemRD) for the first day in culture. Media is then changed daily until cells reach 80-90% confluence. Cells are passaged using ReLeSR (StemCell Technologies) as a dissociation reagent. Cells are then frozen in mTeSR1 + 10% DMSO, or passaged and replated onto Matrigel.

Neural Induction and characterization

Neural Induction is completed using the dual SMAD inhibition neural induction kit (StemCell Tech). High quality iPSCs are selected and passaged using ReLeSR and centrifuged to pellet. Cells are then resuspended into a single cell suspension in STEMdiff Neural Induction Medium (StemCell Tech) + 10 μM Y-27632. Cells are replated onto matrigel coated plates at a density of about approximately $1x10^6$ cells/mL

in a 6 well plate. Media is replaced the following day, without the addition of Y-27632, and is replaced every day until cells are confluent, approximately 6-9 days later. The NSCs are then dissociated again using Accutase (StemCell Tech) as a cell dissociation reagent, and replated in STEMdiff Neural Induction Medium + 10 μM Y-27632. Cells are cultured as described above until at least passage 3. Cells can then be characterized, cryopreserved, or further expanded.

Immunocytochemistry staining for Nestin and Sox2 has been used to confirm NSC identity. These are well established markers for human NSCs. Evaluated cell lines are >90% Nestin positive, therefore are primarily NSCs and thus suitable for downstream analysis.

Cell proliferation Assay

Cells were plated in a 96 well plate at 10,000 cells/well, with 3 replicates per cell line per day. Proliferation was measured every day for 5 days using the MTT Cell Proliferation Assay (ThermoFisher) using the Quick Protocol Option. Cells were changed to phenol red free Neurobasal media immediately before being incubated and labeled with MTT for 2 hours. Formazan is produced upon reaction with live cells and is then solubilized using DMSO. Absorbance was measured using the Tecan Infinite 200 Pro.

Neurite Growth assay

Cells were plated at a density of 10,000 cells/well and cultured for two days. Each cell line was plated in 8 wells of a 24 well plate. On day 2 of culture, 2 wells/cell line were treated with 100 ng/mL Nerve Growth Factors (NGF) and incubated overnight. Images were taken in two randomly selected spots per well. Using ImageJ32, the total

number of cells per image were counted, followed by the number of cells with at least one neurite growth.

qPCR

Neural Stem Cell RNA was extracted using the Zymo Quick-PCR Mini-Prep Kit. cDNA was generated using the Superscript III (ThermoFisher) protocol. qPCR was performed using the Taqman Gene Expression Assay for *NTRK1* on the CFX ConnectTM Real Time PCR system and analyzed using the accompanying software, Bio-Rad CFX Manager TM. *HPRT1* was used as the reference gene.

Generation of the Ntrk1 conditional knock-in mice

To establish *NTRK1* E495K conditional KI mice, we employed a flip-excision (FLEx) switch to flip the mutant exon 12 and excise the wild-type exon 12 in conjunction with expression of Cre recombinase. To construct the targeting vector, homology arms were obtained from a BAC clone (RP23-452A12, BACPAC Resources Center) containing genomic DNA for mouse *NTRK1*. FLEX switch (#18925, Addgene) with loxP and lox2272 sequences was utilized. Mutant exon 12 was generated by site directed mutagenesis with PCR. Positive (pgk-neo-polyA) and negative (Diphteria toxin A fragment, DT- A) selections were carried out as described.(65) The targeting vector was linearized and electroporated into the mouse embryonic stem (ES) cell line CMTI- 2 (C57BL/6-derived) with standard gene targeting procedure. Screening of the correctly targeted ES cell clones was performed with Southern blotting using P^{32}- radiolabeled DNA fragments as a probe. Twenty-five out of 400 clones screened were correctly targeted ES cell clones. The ES cell clones were microinjected into mouse blastocysts (Balb/c-derived) to obtain chimeric mice. By crossing the chimeric mice with C57BL/6J

mice, F1 heterozygous flox/+ mice were obtained. Germline transmission was confirmed by PCR using the tail DNAs. After obtaining flox/+ allele, the mice were mated with Nestin-Cre transgenic mice to introduce the FLEx recombination specifically into the brain, or mated with CAG-Cre transgenic mice(66) to obtain the conventional KI mice. Ntrk1 conventional heterozygous knockout mice were produced via CRISPR/Cas9 technology(67), and homozygotes were obtained by inter-crossing of the heterozygotes. Nestin-Cre transgenic mouse line (B6.Cg$^{Tg(Nes\text{-}cre)1Kln/J}$) was obtained from Jackson laboratory. All animal experiments were approved by the Wako Animal Experiment Committee, RIKEN, and were carried out in accordance with the approved guidelines and regulations. All other experimental procedures were approved by the RIKEN Wako Safety Center and were performed in accordance with the approved guidelines. All behavioral analyses were carried out with male mice (3 months old).

Tail suspension test

Thirty minutes before the tail suspension tests, mice were intraperitoneally injected with saline or physostigmine (0.2mg/kg, Tokyo Chemical Industry, Tokyo, Japan). Tail suspension test was performed using an infrared ray sensor system (Taiyo Electric Co. Ltd., Osaka, Japan) which showed activity counts but did not provide immobility time.(68) We performed TST with another system by analyzing images captured with CCD camera (O'Hara & Co., Tokyo, Japan), which provided immobility time as well as activity counts.(69)

ChAT staining and analysis

Mice were anesthetized, transcardially perfused and fixed with 4% paraformaldehyde (PFA). Whole brains were dissected and embedded in paraffine

blocks. Five μm coronal sections were prepared in the basal forebrain (including Medial septum, Diagonal band of Broca, Nucleus basalis). Immunohistochemical (IHC) staining was performed using an anti-cholineacetyltransferase (ChAT) antibody (AB144P, Millipore). The number of ChAT positive cells were counted and the diameter of the major axis of the intense ChAT signals in the cell bodies were measured with Neurolucida software (MBF Bioscience).

Western blotting

Mouse brain tissues (male, 3-6 months) were homogenized with a Potter-type homogenizer in ice-cold buffer (25 mM Tris-HCl, 150 mM NaCl, 1% NP-40, 1% Sodium deoxycholate, 0.1% Sodium dodecyl sulfate) containing protease inhibitors and phosphatase inhibitors. After centrifugation supernatants were recovered and quantified. Proteins were separated by SDS-PAGE, transferred to PVDF membranes, and subjected to western blotting with antibodies for NTRK1 (#06-574, Millipore), Choline acetyltransferase (ChAT; AB144P, Millipore), ERK and phosphorylated-ERK (pERK) (#9101 and #9102 respectively, CST), and beta-actin (A5441, Sigma-Aldrich). As for the fluorescence western blot of pERK/ERK, 30 minutes after physostigmine or saline injection, mice (male and female, 3 months) were sacrificed with cervical translocation. Whole brain tissues were quickly removed, and hippocampi were dissected out from the brain on ice, frozen with liquid nitrogen, and kept at -80°C until use. After thawing on ice, the hippocampi were homogenized in the buffer with a Potter-type homogenizer and centrifuged at 4°C for 15 min. Supernatants were recovered, and protein amounts were quantified by BCA kit. Equal amounts of proteins were loaded onto an SDS-PAGE gel and subjected to western blotting with antibodies for pERK

(#9102, CST) and ERK (#9101 and #9107, CST) antibodies, and for fluorescence western blot, Cy5 or Alexa488 conjugated anti-rabbit or anti-mouse IgG antibodies (CST), respectively. The images were obtained and analyzed by FX fluorescence imager (Bio-Rad).

Analysis of the dendrite morphology

Primary hippocampal neurons were prepared from embryos (embryonic day 16.5) of each genotype.(70) The primary neurons were plated into the 4 well slide chamber with a density of 20,000 cells/well and cultured at 37°C in 5% CO_2 in the minimum essential medium (MEM, Invitrogen) supplemented with B27 (ThermoFisher). After grown for 2 weeks, cells were fixed with 4% paraformaldehyde, permeabilized with 0.1% Triton X-100 and stained with anti-MAP2 antibodies (ab5392, Abcam) to visualize the dendrite morphology. Image acquisition was carried out with a confocal microscope (Olympus, Tokyo, Japan). Sholl analysis was performed with Neurolucida software.

Statistical analysis

Statistical power was calculated by G*Power 3.1.9.2. Statistical analysis for the cell proliferation and neurite growth assays were completed using SPSS

Results

3.1 E492 effect on neural stem cells

3.1.2 E492K neural stem cells have reduced neurite growth

We generated lymphoblastoid cell lines from one member of the pedigree with bipolar disorder and ADTKD as well as a healthy relative. Using the lymphoblastoid cells, we generated induced pluripotent cell lines (iPSCs). Neural induction of the iPSCs into neural stem cells (NSCs) was completed using dual SMAD inhibition. NSC line 323

is derived from the proband who carries the E492K mutation in TrkA. NSC line 770 is an unaffected relative and control. Immunocytochemistry staining for Nestin and Dapi confirmed NSC identify of differentiated iPSCs (Figure 6). During the NSC expansion, the E492K NSC line, 323, appeared to grow more slowly than the control line 770 and seemed to produce less neurites (Figure 7a).

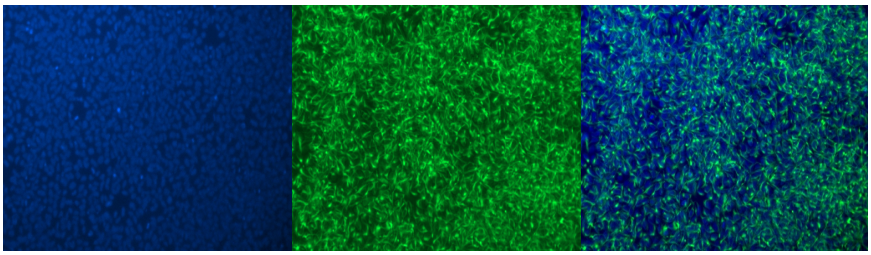

Figure 6: Representative ICC neural stem cell staining; Using DAPI(blue) and Nestin(Green).

In order to verify both of the observed phenotypes, NSCs were plated in equivalent densities in triplicate in 96 well or 24 well plates and a MTT cell proliferation assay was performed. NSC lines were plated in triplicate in 96 well plates and then measured for cell proliferation over the course of 5 days. There was a non-significant trend for reduced growth in the 323 line carrying the mutation. (Figure 7b)
NSC lines plated in 24 well plates were incubated overnight either with or without 100ng/uL of nerve growth factor (NGF) in order to stimulate neurite growth. Each well was imaged twice, in randomly selected areas. The total number of cells were counted per image, as well as the total number of cells with at least one neurite growth. The E492K NSCs with NGF treatment had a significantly reduced proportion of cells with neurite growth when compared to the NGF-treated control cell line. (Figure 7c)

3.1.3 E492K neural stem cells show a reduction in NTRK1 gene expression

In order to test the effect of the E492K mutation on *NTRK1* expression, RNA was extracted from each line for qPCR analysis. qPCR analysis revealed that the control cell line 770 appeared to express *NTRK1*, however the E492K NSC line appeared to have low or ablated *NTRK1* gene expression levels. The analysis was repeated, confirming the previous results, that *NTRK1* expression is reduced in the E492K mutant NSC lines (Figure 7d).

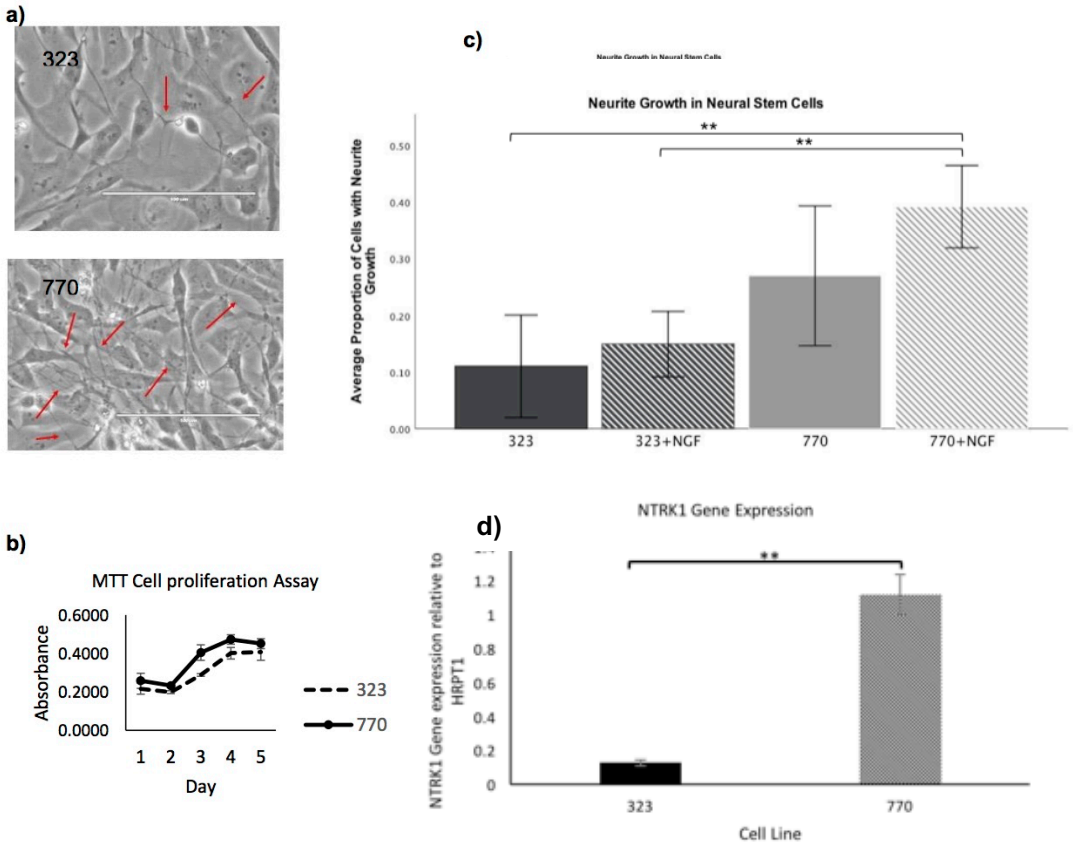

Figure 7: Functional analysis using neural stem cells
a) NSC line morphology of E492K mutant line (323) and control line (770) with red arrows indicating neurite growth. NSC line 770 also appears to have denser growth of cells and more neurite outgrowth b) Cell proliferation measured by absorbance of formazan in NSC lines. (n=3). c) Proportion of neural stem cells in a given field with at least one neurite outgrowth with or without NGF treatment. Control cell line (770) has a significantly higher (One Way ANOVA; n=12, **p<0.01) proportion of cells with neurite outgrowth when treated with NGF. d) *NTRK1* expression of NSCs. *NTRK1* expression of the control cell line, 770, is significantly different (Independent T-test; **p<0.01) when compared to the mutant cell line, 323.

3.2 E492K effect on depressive behavior in mice

In addition to the experiments conducted in NSCs, a collaboration with the Kato Lab at the RIKEN Center for Brain Science in Japan, resulted in the generation of a mouse model with a E495K brain-specific knock-in, which corresponds to the human E492K mutation. These mice exhibited no differences in weight or TrkA protein

expression in the basal forebrain cholinergic neurons (BFCNs) of the mutant mice when compared to the control mice. The mutant mice also did not experience any changes in pain sensation, as *NTRK1* has also been implicated in pain response of peripheral nerves. (Figure 8)

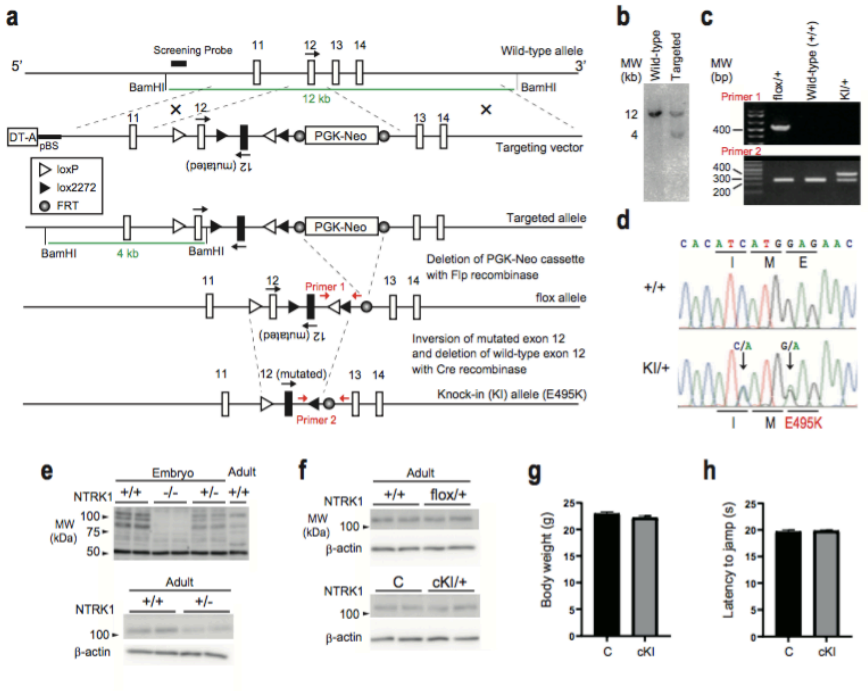

Figure 8: Generation of the brain-specific NTRK1 E495K knock-in (cKI) mice a) Gene targeting strategy. b) Southern blot of the targeted ES cells. c) PCR genotyping of the Ntrk1 recombined alleles. d) Genomic DNA sequencing of the wild-type and KI alleles. e) Validation of the anti-NTRK1 antibody specificity by western blots. Whole brain tissues (embryonic day 18) were used for knockouts. Cerebral cortices were used for the adult mouse samples. f) Expression levels of the NTRK1 protein among genotypes. C, Control. g) Body weight. N=13 for each genotype. h) Hot plate test to assess the pain sensitivity. N=13 for each genotype. Error bars, mean ± s.e.m

As described previously, physostigmine induces depressive phenotypes in bipolar and major depression disorders. E495K mice also exhibited a depression-like phenotype in a tail suspension test after administration of physostigmine. No difference was initially observed between genotypes prior to treatment. However, upon administration of physostigmine there was a rapid decrease in the activity of all

genotypes, and at the 1 minute time point, E495K mice were significantly less active than the controls (Figure 9; p=0.038; t-test, two-tailed). These results were reproduced in another experimental apparatus, which found that E495K mice were significantly less active that controls at the 2 and 3 minute time points. (Figure 9)

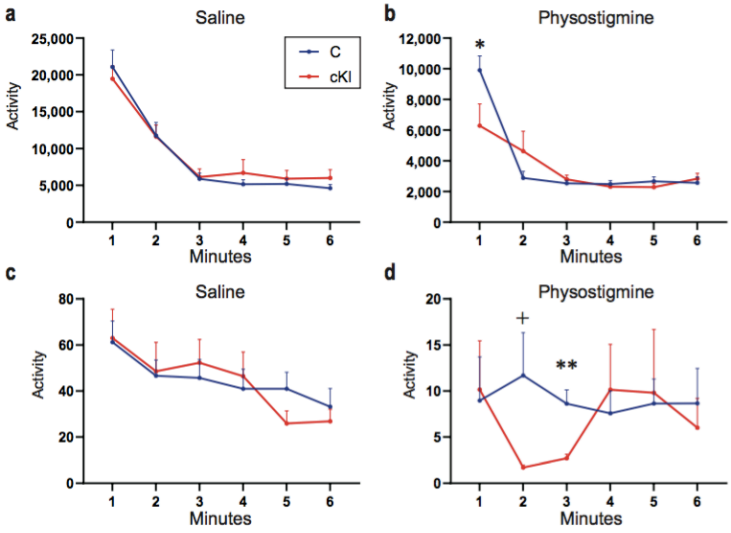

Figure 9: Depression like behavior under physostigmine administration in the Ntrk1 cKI mice
a) Tail suspension test at the drug free state (saline). Control, N=13; cKI, N=13. b) Tail suspension test after the physostigmine injection. Control, N=13; cKI, N=8. (Some cKI mice were lost because of toxicity of Physostigmine.)c) Drug free state (saline) in an independent test. Control, N=8; cKI, N=8. d) Increased depression-like behavior of the cKI mice with physostigmine was reproducibly observed in an independent test. Control, N=8; cKI, N=8. * $p<0.05$, + $p=0.05$, ** $p<0.005$ (t-test, two-tailed); Error bars, mean ± s.e.m.

While there was no change in cell size or morphology between the BFCNs between E495K mice and control mice, there was a difference at the post-synaptic hippocampal target neurons. Phosphorylated ERK (pERK) in the BFCNs was no significantly different, however there was an increase in pERK in the hippocampus. In primary hippocampal neurons from embryonic brain, E495K mice also exhibited a lower degree of dendritic branching. Dendritic branching was quantified using Neurolucida

360 and Scholl analysis. While the length of the dendrites did not differ between genotypes, the number of intersections in dendrites was significantly smaller in the KI/KI neurons, compared to the KI/+ or +/+ neurons. (Figure 10)

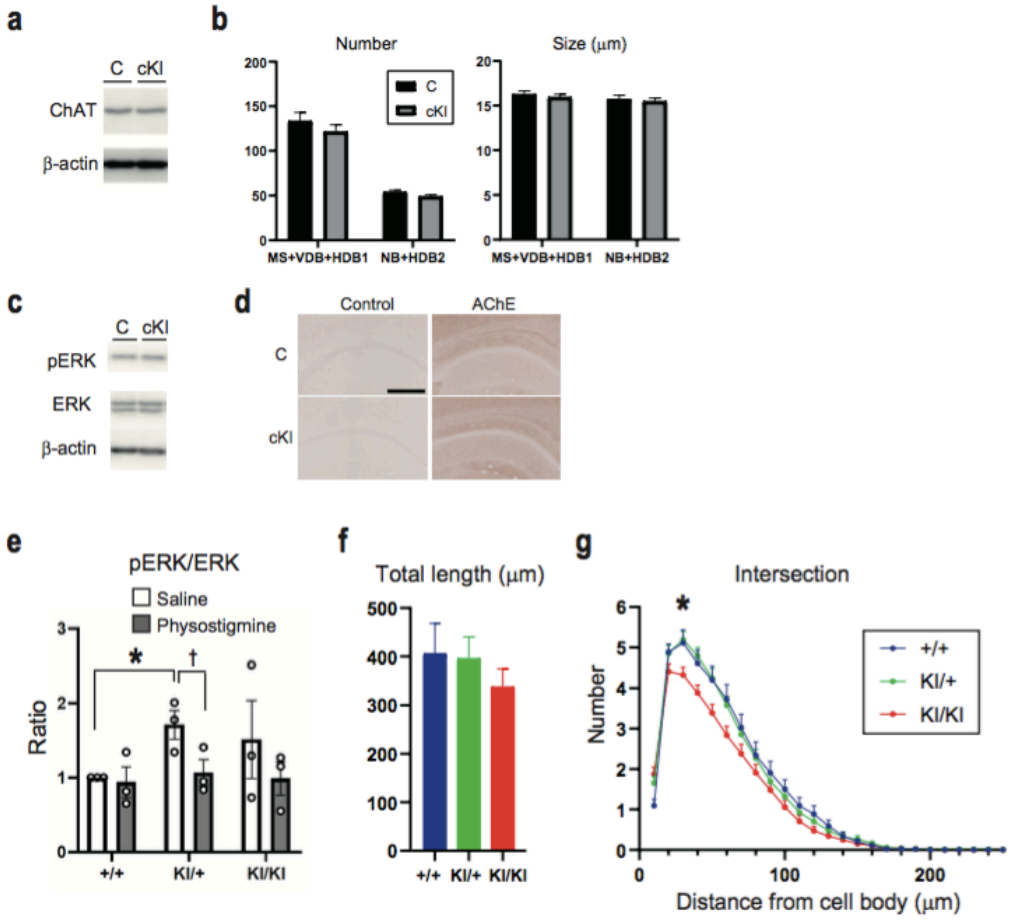

Figure 10: Development and maintenance of the basal forebrain cholinergic neurons were similar among genotypes; but postsynaptic defects were observed in the hippocampal neurons of the Ntrk1 KI mice. a) Western blots of the ChAT protein using the basal forebrain tissue homogenates. N=3 for each genotype, representative blots were shown. b) Numbers and sizes of the basal forebrain cholinergic neurons, N=3 pairs. MS, medial septum; VDB, ventral limb of the diagonal band of Broca; HDB, horizontal limb of the diagonal band of Broca; NB, nucleus of basalis. c) Western blots of the pERK and ERK proteins using the basal forebrain tissue homogenates. N=3 pairs, representative blots were shown. d) Acetylcholine esterase immunohistochemistry in the hippocampal CA1 region. Bar, 250 μm. d) Acetylcholine esterase (AChE) immunohistochemistry in the hippocampal CA1 region. Anti-AChE antibodies (HPA019704, Sigma-Aldrich) were used. Bar, 250 μm. e) pERK/ERK ratios of the hippocampus by fluorescence western blots using the tissue homogenates under saline or physostigmine administration. N=3 pairs. * $p<0.05$; † $p=0.070$ (t-test, two-tailed); Error bars, mean ± s.e.m. f) Total length of the dendrites in the primary hippocampal neurons. g) Number of intersections in the dendrites of the primary hippocampal neurons. (f, g) +/+, N=44; KI/+, N=84; KI/KI, N=85 neurons were counted. * $p<0.05$ (One-way ANOVA followed by Fisher's PLSD post-hoc test); Error bars, mean ± s.e.m.

3.3 E492K putative effects on the cholinergic system

Given the data above, it is reasonable to conclude that this specific mutation may play a role in impairing the cholinergic system. In *NTRK1* NSCs derived from affected patients, there was found to be a decrease in both *NTRK1* expression and neurite growth. TrkA-NGF signaling has been established to lead to the activation of several downstream pathways involving both neuronal differentiation and neuronal proliferation. Both neurite growth and gene expression have been identified as being triggered by the autophosphorylation of Y490 through TrkA and NGF binding. Due to the close proximity of the E492K mutation to this integral binding site, it is likely that the mutation may be interfering with the ability of these downstream activities to occur.

However, in the E495K mice, there was no difference in the cholinergic cells. TrkA expression, pERK expression, cell size and cell morphology were no different in the BFCNs of the E495K mice. Rather, the hippocampal neurons, which are a key target innervation site of BFCNs, were different in the E495K mice. Hippocampal neurons derived from embryonic brain of the E495K mice showed an upregulation of pERK, as well as alterations in dendritic branching. Additionally, the E495K mice demonstrated a greater sensitivity to physostigmine, an acetylcholine esterase inhibitor. The E495K mice were far less active in the Tail Suspension Test, indicative of depressive behavior, in response to the enhanced cholinergic neurotransmission caused by physostigmine stimulation. Together, this suggests that the E495K mice have an altered cholinergic sensitivity in neurons innervated by BFCNs.

It is presumed that the close proximity of the E492K mutation to the SHC and Frs2 binding site, would result in an impairment of TrkA function. This study has

demonstrated that some expected downstream activity of TrkA, such as *NTRK1* expression and neurite growth, is indeed impaired in NSCs. One putative explanation for the observed reduction in gene expression, is that *NTRK1* expression may be regulated in a positive feedback loop. One potential feedback loop is described in another study which found that NGF and TrkA binding led to the activation of the PI3K pathway then the subsequent binding of transcription factor Lhx8 to a TrkA enhancer region, which then led to increased *NTRK1* expression.(31) The study also showed that the MAPK/ERK pathway was also implicated in *NTRK1* expression, however the mechanism through which this occurs is still unknown. However, TrkA expression in cholinergic neurons was not found to be altered in the E495K mice. Instead, cholinergic target neurons were instead found to be altered. This may be suggestive of a compensatory mechanism in vivo leading to a post synaptic sensitivity in the target hippocampal neurons.

The role of NGF-TrkA signaling must still be extensively studied especially in the adult brain. Identification of the *NTRK1* mutation linked with bipolar disorder sheds light on the new role of NGF-TrkA signaling and its relevance to mood disorders. Considering that upregulation of another Trk receptor and ligand, BDNF-TrkB, has been implicated in antidepressant treatment, further studies on the role of NGF- TrkA are warranted which may lead to a new treatment principle.(71)

Chapter 3, in part, is a reprint of the material as it appears in *Ntrk1* mutation co-segregating with bipolar disorder and inherited kidney disease in a multiplex family causes defects in neuronal growth and depression-like behavior in mice in *Translational Psychiatry*, 2020 K. Nakajima*, A. Miranda*, D.W. Craig, T. Shekhtman, S.Kmoch, A. Bleyer, S. Szelinger, T. Kato and J. Kelsoe (These authors are equal contributors) The dissertation author was a primary investigator and author of this material.

Chapter 4

NTRK1 mutation in TrkA-transfected HEK 293 cells and NSCs

The previous chapters have provided an in depth discussion about both the identification of the *NTRK1* mutation, rs144901788, and the functional effects of the mutation in vivo. It is clear that the juxtaposition of the mutation to the key Y490 binding site has the propensity to cause highly damaging effects to cellular function. To summarize, the Y490 binding site has been shown to regulate neuronal survival, proliferation, differentiation and apoptosis. In NSCs derived from patients with the mutation, there is a reduction in neurite growth and *NTRK1* gene expression, when compared to NSCs derived from unaffected relatives. In mice with the mutation, there also appears to be a defect in neurite growth, as well as a distinct depressive phenotype when stimulated with a cholinergic agonist.

The phenotypes observed in NSCs and mice are representative of cellular actions that likely occur as a result of sustained MAPK signaling through TrkA and NGF. Therefore it is reasonable to hypothesize that the mutation may affect the Frs-2 or ARMS interaction with TrkA at Y490, as depicted in Figure 1. However, there are somewhat conflicting results observed between the mouse and NSC models which necessitates further investigation into the downstream activity of NGF-TrkA signaling in the context of the E492K mutation. While human mutant NSCs demonstrate a reduction in *NTRK1* gene expression, there is no difference in BFCNs of mice with the mutation, when compared to controls. Given that NTRK1 appears to play a key role in cholinergic development, it is surprising that no defects in BFCNs is observed in affected mice. Additionally, there appears to be an increase in MAPK signaling in the hippocampal neurons of E495K mice, and no difference in MAPK signaling in BFCNs. However, the difference of MAPK signaling that was observed, showed a increase in basal MAPK in

the mutant hippocampal neurons. Additionally, both mice and NSCs represent widely genetically heterogenous populations, as well as different stages of development, both of which present several issues in comparing phenotype and downstream signaling.

In the study presented in this chapter, MAPK signaling will be investigated in further depth, using HEK 293 cells transfected with either mutant or wild type TrkA tagged with HaloTag® as a visual marker, when bound to a fluorescent ligand, Oregon Green. Although CRISPR gene editing has emerged as a powerful tool in generating isogenic cell lines, there were no existing Cas9 proteins which targeted a PAM sequence in the appropriate proximity of this mutation. While isogenic neural stem cell lines would be an ideal method to observe the phenotypic differences due to the mutation alone, transfected HEK cells still provide a robust model for studying downstream protein effects in a similarly genetically homogenous environment.

As MAPK signaling in the previous chapter and study was not observed in a manner that would distinguish changes in sustained versus transient MAPK activity, the following experiments will explore that system. In addition to investigating changes in downstream protein activity, the following study also aims to identify changes in gene expression in NSCs, other than *NTRK1*, to discern what other pathways may be alternatively expressed as a result of the E492K mutation.

There is considerable cross talk between the Trk receptor pathways that may work in feedback loops to compensate for deficiencies in other pathways. One potential pathway is the BDNF-TrkB pathway, which activates MAPK signaling in hippocampal neurons, and is frequently implicated in mood disorders as well.(71,72) NGF, the primary ligand for TrkA, is also synthesized in hippocampal neurons first, then

retrogradely transported to cholinergic cells.(73) Additionally, *BDNF* is a regulatory target of CREB, which has been shown to be regulated through MAPK signaling through TrkA and NGF.(35)

Trk receptors and their respective neurotrophins share many signaling mechanisms and complementary effects regarding the survival and maintenance of neurons. Therefore one may expect that the TrkA-NGF and TrkB-BDNF pathways interact in as of yet undetermined processes. A TrkA-NGF deficiency early in development, as observed in these NSCs, may lead to a compensatory up-regulation of other pathways in other regions, such as the hippocampus, resulting in an overall impaired cholinergic signaling system. In this chapter, we will identify proteins and genes downstream of TrkA-NGF signaling that are affected by the E492K mutation, as well as begin to elucidate some of the cellular mechanisms through which some of the observed phenotypes may be occurring.

Methods

Transfection of WT and Mutant TrkA into HEK293 cells

In order to test the effects of the E492K mutation in a more genetically homogenous cell type, the mutant and WT TrkA were transfected into HEK-293T cells. The construct used to transfect HEK-293T cells was developed by a former graduate student, using a pHTC HaloTag® CMV-neo (pHTC) vector, with the HaloTag® on the C-terminus of the TrkA protein, therefore enabling the transfected TrkA protein to function without interference by the HaloTag®.(74) Transfection was observed using the Oregon Green ® ligand. The ligand binds to HaloTag®, allowing for the visualization of TrkA. Transfection of both mutant and WT TrkA into HEK293T was initially completed using

Lipofectamine® 3000. However, in order to generate a stable cell line of TrkA-transfected HEK-293T cells, a lentivirus was generated by isolating DNA fragments from the original plasmid construct, then cloned into an HIV1 backbone plasmid by the UCSD Vector Core Laboratory.

HEK-293T cells were cultured in DMEM (ThermoFisher Scientific) supplemented with 15% fetal bovine serum (ThermoFisher Scientific) and 1% antibiotic-antimycotic (ThermoFisher Scientific). Cells were dissociated with 0.25% Trypsin/EDTA one day prior to transfection with the HIV1-(mut or WT) NTRK1-HaloTag® constructs. On the day of transfection, medium was reduced to 0.5 mL and supplemented with polybrene (4μg/mL) with 20 uL of the virus solution. Cells were then incubated with the virus for 3 hours, after which the medium was replaced and cells were allowed to culture until confluence.

When compared to the initial lipid-based transfection, viral transfection of the WT and mutant constructs was considerably lower and resulted in a greater degree of cell death. In order to increase number of transfected cells, the transfection procedure was repeated three more times in a serial transfection.

Western Blotting

HEK293 cells were lysed using RIPA buffer containing protease inhibitors and phosphatase inhibitors. Supernatants were recovered and quantified after centrifugation. Proteins were separated using SDS-PAGE in 4-15% Mini-PROTEAN® TGX™ Gels and transferred to PVDF membranes. Membranes were blocked using 2.5% BSA and incubated overnight in primary antibodies: TrkA(# 2505S, Cell Signaling Technology), ERK (9102S, Cell Signaling Technology), phospho-ERK (9101S, Cell

Signaling Technology), beta-actin (#8227, Abcam) as a loading control. Membranes were then washed with 2.5% BSA up to 3 times, followed by incubation in the secondary antibody (#31460, Invitrogen) for 1 hours at room temperature. Membranes were washed again with 2.5% BSA up to 3 times, then treated with Pierce™ ECL-plus (ThermoScientific) for 1 minute. Membranes were visualized on autoradiography film using X-ray imaging equipment (Konica SRX-101A). Band intensity was then analyzed using ImageJ.

RNA -sequencing

To analyze gene expression in response to NGF, neural stem cells either with (cell line 323) or without (cell line 770) the E492K mutation were treated with NGF (100 ng/uL) or vehicle, for 3 hours. Each cell line + condition was completed in triplicate, for a total of 12 samples. Neural stem cell RNA was extracted using the Zymo Quick-PCR Mini-Prep Kit and RNA concentration was estimated via nanodrop.

High quality RNA was then submitted to the UCSD Institute of Genomic Medicine, Genomics Center, for library prep and RNA sequencing. A more thorough quality control check of sample integrity and concentration was determined using the Agilent Tapestation instrument. Sequencing was conducted using and mRNA library, on the NovaSeq S4, read configuration PE100 and at a 25M read depth.

RNA-sequencing analysis

Data pre-processing and transformation was completed using the San Diego Super Computer Center. Sequencing quality of the reads generated from the NovaSeqS4 was completed using FastQC, under the default program settings. Genome index build and read alignment was performed using STAR. The STAR genome index

was built using chromosome fasta files downloaded from UCSC (September 2020) and the most current gencode release (release 36, GRCh38.p13).

Counts were read into Rstudio (Version 1.3.1093) to perform differential expression analysis. Reads to counts was performed using the *featureCounts* program in the *Rsubread* package. (75) Differential expression analysis was performed using the *limma* and *edgeR* packages.(76,77) Reads were filtered using *edgeR filterByExpr* function default settings, where genes with less than 10 counts in a given sample group were filtered out from the analysis. Samples were normalized using the trimmed mean of M-values method in *edgeR*. Multi-dimensional scaling plots were generated by individual sample and sample group using *limma*. To test which genes were differentially expressed, contrasts were evaluated by the following cell type and treatment groups, in a global contrast method; WT TrkA NPCs vs NGF-stimulated WT TrkA NPCs, mutant TrkA NPCs vs NGF-stimulated Mutant TrkA NPCs, WT vs Mutant TrkA NPCs and which genes respond differently to NGF in mutant NPCs compared to WT NPCs (Interaction effect).(78) Gene names were annotated using the biomaRt package.(79) Gene set analysis was completed using the *camera* method with the Molecular Signatures Database (MSigDB) C2 curated gene set(80–84).

Statistical Analysis

Additional statistical analyses for western blots were conducted using SPSS. Raw p-values generated in the differential expression analysis were corrected for multiple comparisons using the Benjamini and Hochberg method.

Results

4.1 Alterations in downstream signals due to E492K in HEK 293 cells

After lipofectamine transfection, HEK293 cells showed a high transfection efficiency after live imaging with Oregon Green, resulting in up to 80% transfection. After a serial viral transfection of the TrkA-HaloTag construct, transfection efficiency of 85-90% cells was achieved for both wild type and mutant TrkA (Figure 11a). Transfected cells were then treated with NGF (100ng/mL) for 0, 5 or 60 minutes and protein was extracted using RIPA lysis buffer and Halt phosphatase/protease inhibitor protocol. Western blot analysis of transfected HEK-293T cells shows similar transfection of TrkA across all samples. No significant difference in TrkA was detected, regardless of NGF stimulation or length of NGF stimulation. (Figure 11b; n=3; One-way ANOVA, $p>0.1$)

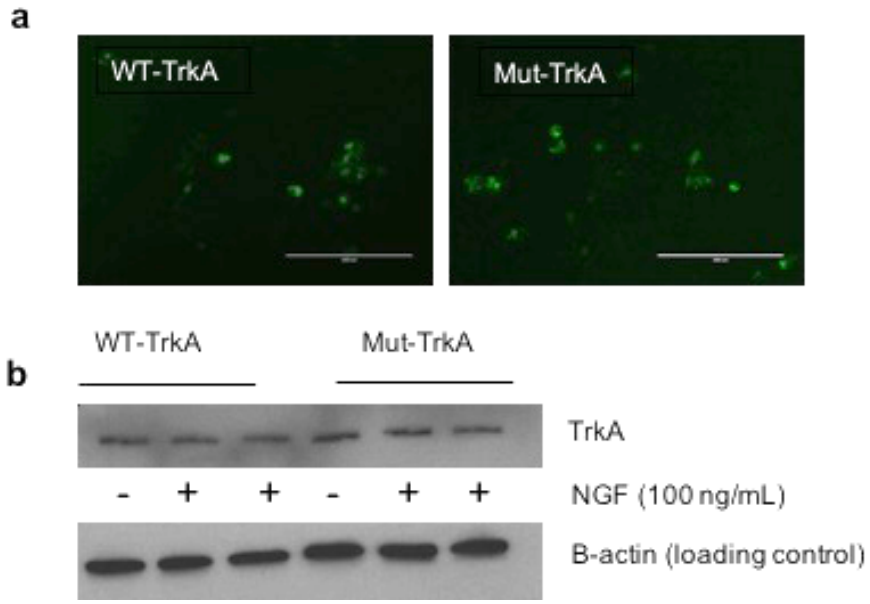

Figure 11: Visualization of mutant and WT TrkA in HEK-293T cells. a) TrkA is visualized via Oregon Green ® ligand and HaloTag® binding. HIV1-CMV-eGFP is shown as a transfection control. b) Representative western blot of transfected WT and mutant TrkA, with or without NGF stimulation, with b-actin as the loading control.

In order to analyze downstream NGF-TrkA signaling, cells were treated with either NGF (100 ng/uL) for 0 min, 1 min, 5 min, 10 min, 30 min and 60 min. pERK signaling after 10 minutes is considered sustained signaling, whereas before 5 minutes, pERK signaling is considered transient. Protein was extracted in triplicate, at each time point for WT and E492K-TrkA HEK cells, and analyzed via western blot, probing for pERK and ERK.

WT TrkA appeared to have the expected response to NGF stimulation over time, with a robust initial transient pERK signaling (1- 5 minutes), with a continued sustained signaling (10-60 min) that slowly returned to baseline. Mutant TrkA cells appeared to have a more robust transient response to NGF (1 minute NGF stimulation). When the overall course of NGF stimulation over time was compared between WT and mutant TrkA-transfected cells, there was a significant effect of cell type on pERK/ERK ratio (Figure 12 a; n=3, $p=0.002$; Two-way ANOVA with repeated measures). In examining the effects at specific time points, NGF stimulation of the mutant TrkA cells had a significantly higher level of pERK signaling at 1, 10 and 30 minutes following NGF stimulation, suggesting both transient and sustained signaling is affected in the mutant TrkA cells. (Figure 12a, * $p<0.05$; Independent T-test)

a

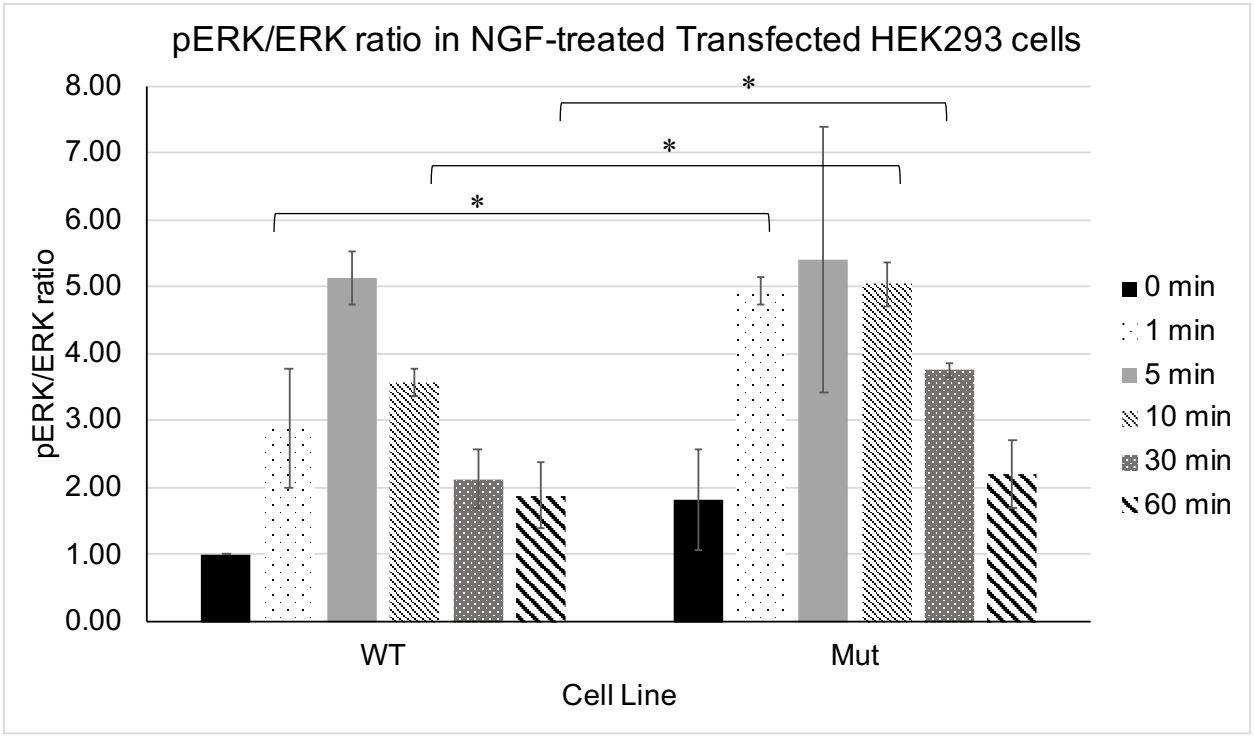

b

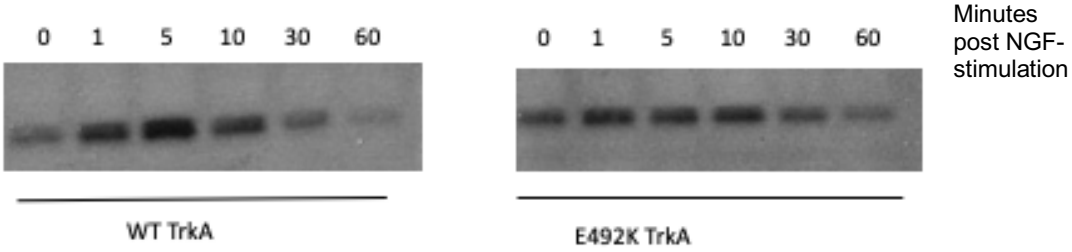

Figure 12: pERK signaling inTrkA-transfected HEK cells. a) pERK/ERK ratios of the transfected HEK cells at 0, 1, 5, 10, 30 and 60 minutes of NGF stimulation. N=3, P=0.002 (ANOVA with repeated measures; * Independent T-test, $p<0.05$); Error bars, mean ± std) b) Representative western blot for pERK, of transfected WT and mutant TrkA, with or without NGF stimulation.

4.2 Changes in gene expression due to E492K in NSCs

The difference in pERK signaling in the mutant TrkA transfected HEK cells in comparison to the wild-type transfected TrkA HEK cells supports the findings that signaling events downstream of the Y490 autophosphorylation site are effected by the mutation. In order to identify other pathways that may be differentially affected by the mutation, RNA sequencing was conducted on wildtype and mutant NSC lines evaluated in the previous neurite growth experiment.

RNA was extracted from wildtype and mutant NSC lines both untreated and treated with NGF after 3 hours. Growth factors play a key role in inducing gene expression to induce a number of cellular actions, vital for cellular proliferation, differentiation and survival. Transcription induced by growth factors can take place over a wide range of time, from a single minute to over the course of several days.(85) In particular, BDNF stimulation has been found to stimulate expression of genes related to neural plasticity in as little as 20 minutes, and up to 3 hrs.(86) There are several studies evaluating the effect of NGF-deprivation on gene expression, or the effect of continuous neuronal culture with NGF on gene expression(87,88). However, NGF stimulation after only 12 hours was enough to generate a clear neurite phenotypic difference in the wildtype and mutant TrkA NSCs. In an effort to capture early gene expression changes, the two NSC lines were treated with NGF for 3 hours, after which RNA was extracted for sequencing in treated and untreated lines.

Both wildtype and mutant treated and untreated NSC lines were cultured and extracted in triplicate, for a total of 12 samples. All samples passed quality control assessment for integrity and concentration. Sequencing quality was also analyzed and

found to be sufficient across all samples. Gene counts were filtered for genes with at least 10 read counts combined in each condition. Figure 13 demonstrates the effect of filtering out genes that are lowly expressed. Filtered counts were also normalized via the TMM method before further analysis.(77) Multi-dimensional scaling plots were used to monitor clustering of samples over two dimensions. When evaluating condition groups, samples appear to cluster appropriately, with the exception of WT replicate #1. All WT and mutant samples cluster separately along the first dimension, however diverge along the second dimension.(Figure 13C) Due to the separation of the single WT replicate from the expected clustering, this sample was dropped from the differential gene expression analysis. (Figure 13D)

Differential expression analysis was performed as 2X2 factorial design, with the goal of determining the following; genes that are differentially expressed in response to NGF stimulation in wildtype TrkA NSCs, genes that are differentially expressed in response to NGF stimulation in mutant TrkA NSCs, genes that respond differently in the mutant TrkA NSCs compared to the wildtype TrkA NSCs, and as a baseline, genes that are differentially expressed between the two cell lines. The comparison with the largest total amount of differentially expressed genes was between the wildtype and mutant cell lines, with a total of 11,632 genes found to be differentially expressed. Of those 5,147 were downregulated and 6,485 were upregulated in the wildtype line when compared to the mutant cell line. It may be expected that two distinct cell lines would have a higher level of differentially expressed genes in comparison to any other group, particularly in this comparison, where there are large regions of homozygosity throughout of the genome of the mutant cell line. However the a large proportion of the genome

consisting of differentially expressed genes in cell lines of the same type is still questionable. This raises questions about the level of development in each NSC line, which is further discussed in Chapter 5, section 3.

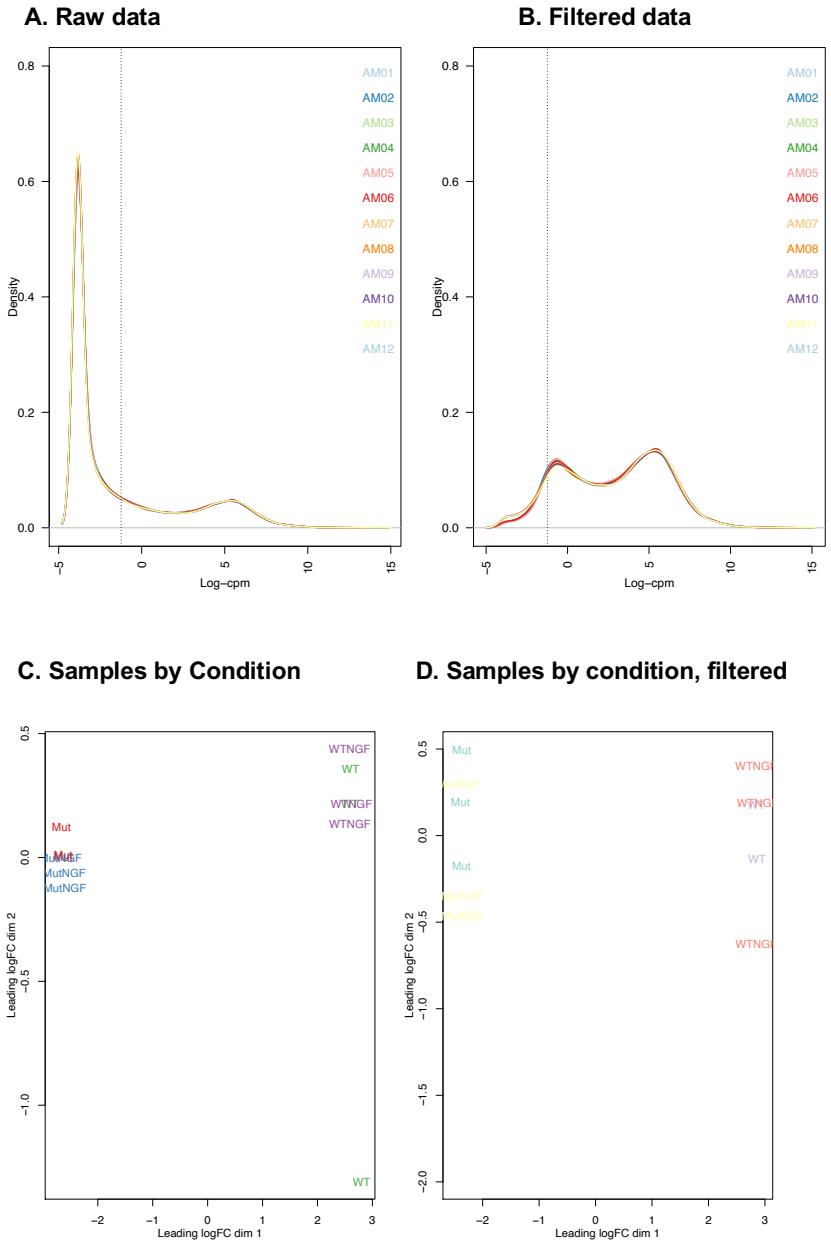

Figure 13: Filtering and quality control assessment of counts and sample groups. a) Density of log-cpm values for raw data and b) data filtered for lowly expressed genes Dotted line indicates logCPM threshold used to filter genes. c) MDS plot by condition groups of all samples. D. MDS plot by condition groups after dropping outlier sample.

In response to NGF, 31 genes were found to be down-regulated in the wildtype cell line and 18 were found to be upregulated. In the mutant cell line, 224 genes were found to be down-regulated and 49 were found to be upregulated. 49 total genes were found to respond differently in the mutant compared to the wildtype, when exposed to NGF. Of those 23 were down-regulated genes and 26 were upregulated genes, however given the large number of genes differentially expressed between cell types, it is unclear whether this interaction effect is still appropriate. (Table 10) A complete list of differentially expressed genes for WT vs WT+NGF, Mut vs Mut+NGF and Differential response to NGF in Mut compared to wildtype NSCs, can be found in Appendix tables 3-5. Differentially expressed genes in each condition group can also be visualized in the mean-difference plots, where red dots indicate upregulated genes and blue dots indicate down regulated genes. (Figure 14A-D)

Table 10: Summary of differentially expressed genes across each comparison group. (FDR $\leq$ 0.05)

	WT vs WT+NGF	Mut vs Mut+NGF	WT vs Mut	Differential response to NGF in Mut vs WT
Down	31	224	5147	23
Up	18	49	6485	26
Total	49	273	11632	49

Interestingly, there does not appear to be any significantly differentially expressed genes due to NGF stimulation between the wildtype and mutant cell lines. (Figure 15B). Visualization of the top 50 differentially expressed genes in each comparison, shows a distinct difference between the two untreated cell lines (Figure

15A). The top 50 genes that respond to NGF in the wildtype and mutant cell lines are distinctly different, however heatmaps of both comparisons shows that those upregulated in wildtype NSCs appear to be generally downregulated in mutant NSCs, and vice versa (Figure 15C-D). This trend holds true when evaluating the top 50 genes differentially expressed in both cell lines in response to NGF. (15E)

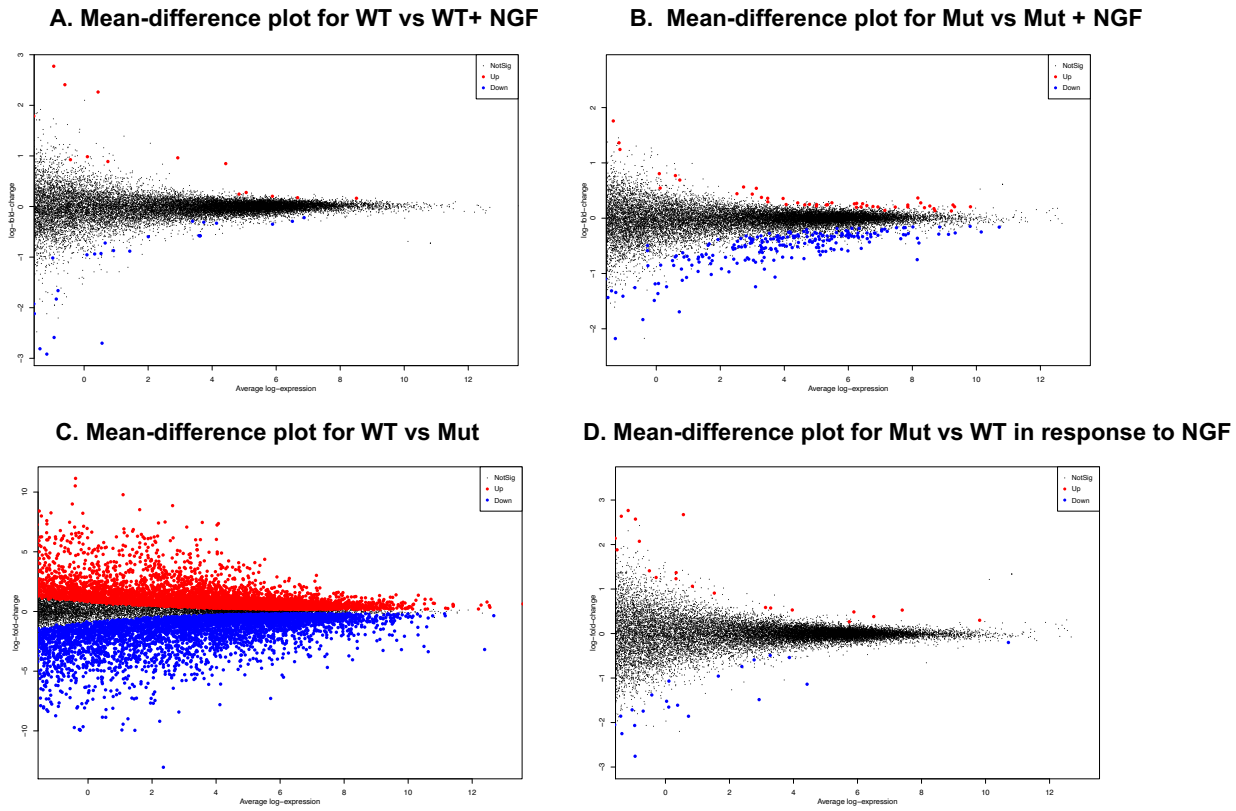

Figure 14: Differentially expressed genes in WT TrkA NSCs and Mut TrkA NSCs in response to NGF stimulation. Mean-difference plots of average log-Fc vs average log-CPM for each condition, upregulated genes in red, downregulated genes in blue for a) WT NSCs vs NGF stimulated WT NSCs b) Mutant NSCs vs NGF stimulated Mutant NSCs c) WT NSCs vs Mutant NSCs d) Mutant NSCs vs WT NSCs differentially expressed due to NGF stimulation.

Figure 15: Top Differentially expressed genes within each group. a) Venn diagram of total significantly differentially expressed genes in wildtype and mutant NSC in response to NGF b) Heatmap of top 50 differentially expressed genes in untreated wildtype and mutant NSCs. c) Heat map of top 50 differentially expressed genes in wildtype and mutant NSCs in response to NGF. d) Top 50 differentially expressed genes in mutant NSCs in response to NGF. e) Heatmap of top 50 differentially expressed genes in wildtype NSCs in response to NGF. **(**FDR $\leq$ 0.05)

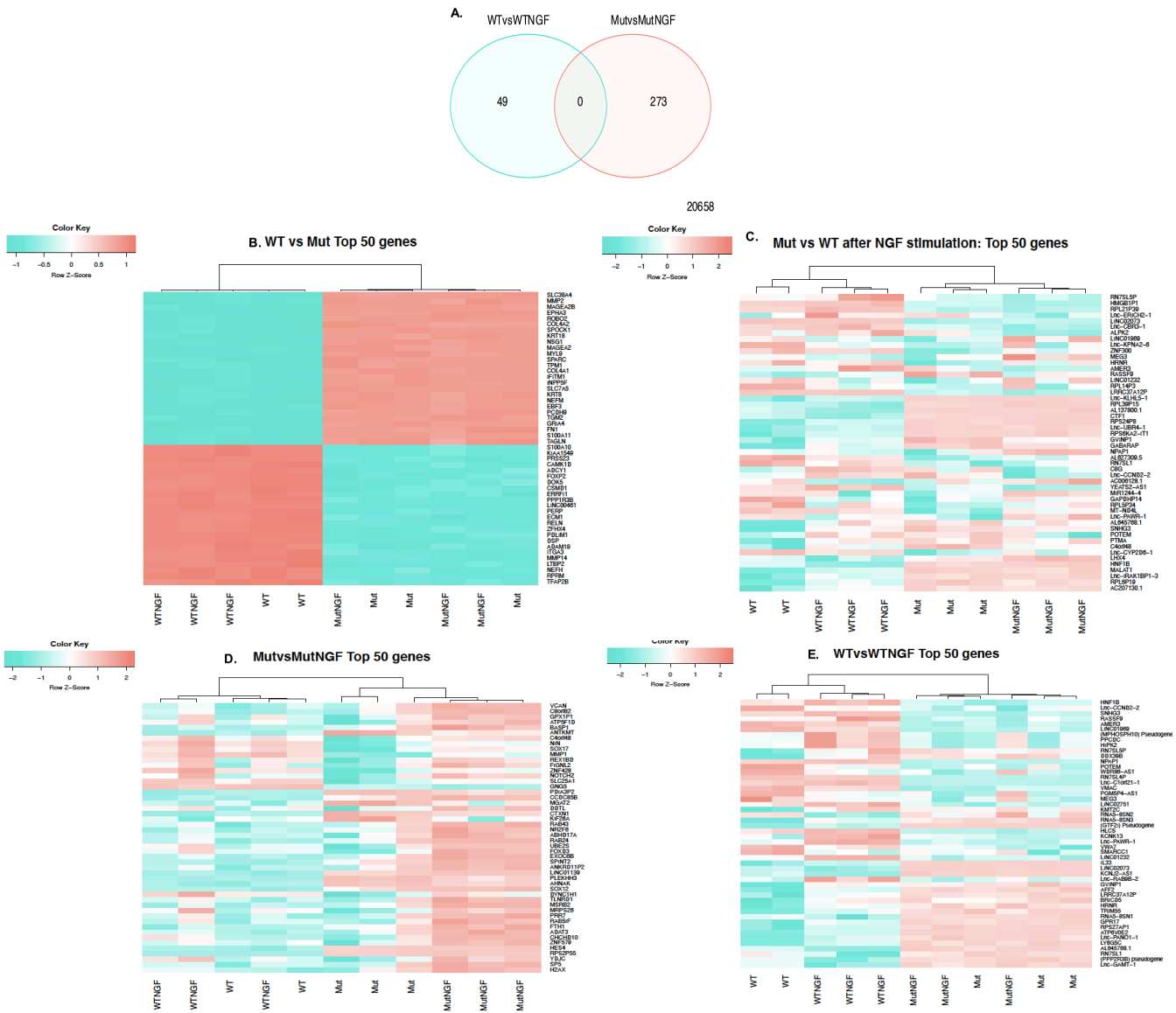
A.
WTvsWTNGF
MutvsMutNGF
49
0
273
20658
B. WT vs Mut Top 50 genes
Color Key
Row Z-Score
WTNGF
WTNGF
WTNGF
WT
WT
MutNGF
Mut
Mut
MutNGF
MutNGF
Mut
C.
Mut vs WT after NGF stimulation: Top 50 genes
D.
MutvsMutNGF Top 50 genes
E.
WTvsWTNGF Top 50 genes

In order to better understand the overall function of the identified differentially expressed genes for each group, a gene set analysis was conducted using the CAMERA method to the C5 GO gene set. There were 1451 GO pathways that passed surpassed the multiple comparisons threshold **(**FDR $\leq$ 0.05) in the baseline wildtype vs mutant NSC comparison. However given the large number of differentially expressed genes in this comparison, this is an expected result.

Fewer pathways passed the multiple comparison threshold in the other comparisons. However, evaluation of the top pathways revealed some interesting trends. As might be expected, in response to NGF stimulation many of the most highly enriched pathways in the wildtype NSCs were associated with neuronal cellular actions. The only two GO pathways that were significantly upregulated in response to NGF were “neuron migration” and “neuron recognition”. Additional, pathways that were of note, included “forebrain development”, and “CNS neuron axonogenesis” which were also both upregulated. This is in line with the reported role of NGF-TrkA signaling in the development of forebrain neurons and neurite outgrowth (Table 11).

Table 11: Top 25 significantly different gene sets using C5 gene ontology sets in wildtype NSCs in response to NGF.

GO gene sets	Genes (n)	Direction	P-Value	FDR
Neuron migration	94	Up	9.90E-06	0.03837408
Neuron recognition	32	Up	1.25E-05	0.03837408
Regulation of synapse organization	93	Up	7.69E-05	0.15792143
Regulation of synapse assembly	62	Up	0.00010673	0.16446638
Histone demethylase activity	24	Up	0.0001646	0.20291595
Transmembrane receptor protein kinase activity	68	Up	0.00027997	0.22767853
Transmembrane receptor protein serine threonine kinase activity	16	Up	0.0003344	0.22767853
Axonal fasciculation	19	Up	0.00034481	0.22767853
Filopodium	86	Up	0.00034592	0.22767853
Structural constituent of ribosome	187	Down	0.00051265	0.22767853
Hippo signaling	20	Up	0.00057898	0.22767853
Transcription factor activity rna polymerase ii core promoter sequence specific	14	Up	0.00058666	0.22767853
Brain morphogenesis	25	Up	0.00058681	0.22767853
Central nervous system neuron axonogenesis	25	Up	0.00076286	0.22767853
Mitochondrial respiratory chain complex i biogenesis	49	Down	0.00077368	0.22767853
Mitochondrial respiratory chain complex i assembly	49	Down	0.00077368	0.22767853
Nadh dehydrogenase complex assembly	49	Down	0.00077368	0.22767853
Coreceptor activity	29	Up	0.00078122	0.22767853
Forebrain development	303	Up	0.00079644	0.22767853
Mitochondrial respiratory chain complex assembly	69	Down	0.00083293	0.22767853
Response to cocaine	39	Up	0.00087632	0.22767853
Ensheathment of neurons	78	Up	0.00094036	0.22767853
Axon ensheathment	78	Up	0.00094036	0.22767853
Platelet derived growth factor receptor signaling pathway	32	Up	0.00097164	0.22767853
Nadh dehydrogenase complex	36	Down	0.00101707	0.22767853

14 gene sets passed the multiple comparison threshold in the mutant NSCs in response to NGF group. However, there were no significantly different gene sets associated with neural activity. Instead, most of the top gene sets were associated with down regulation of ribosome functions (Table 12). This could indicate that there is a cellular change occurring in response to NGF, however based on the significant gene sets it is unclear what the exact change may be leading to. This is a connection to be further researched, however there is some evidence that ribosomal machinery is downregulated as the forebrain develops.(89) Another point of interest is that genes associated with acetylcholine signaling tend to be downregulated at a nominally significant level. T-statistics for genes related to acetylcholine response ranked from low to high, show a downward trend, with most genes having a lower value, with some significantly down regulated and none upregulated. (Figure 16)

Table 12: Top 25 significantly different gene sets using C5 gene ontology sets in mutant NSCs in response to NGF.

GO gene sets	Genes(n)	Direction	PValue	FDR
Cytosolic ribosome	99	Down	3.16E-09	1.95E-05
Ribosomal subunit	147	Down	1.74E-08	5.37E-05
Large ribosomal subunit	87	Down	5.20E-08	0.00010674
Establishment of protein localization to endoplasmic reticulum	96	Down	1.95E-07	0.00030047
Cytosolic large ribosomal subunit	53	Down	3.90E-07	0.00048049
Structural constituent of ribosome	187	Down	5.33E-07	0.00054774
Ribosome	202	Down	1.66E-06	0.00146042
Nuclear transcribed mrna catabolic process nonsense mediated decay	110	Down	3.01E-06	0.00232164
Protein localization to endoplasmic reticulum	111	Down	6.83E-06	0.00467893
Cytosolic small ribosomal subunit	39	Down	1.86E-05	0.01146215
Oxidative phosphorylation	74	Down	2.39E-05	0.01342008
Protein targeting to membrane	141	Down	2.75E-05	0.01414451
Translational initiation	127	Down	6.19E-05	0.02934741
Multi organism metabolic process	130	Down	9.48E-05	0.04172468
Small ribosomal subunit	60	Down	0.00012227	0.050246
Inner mitochondrial membrane protein complex	91	Down	0.00018742	0.07220339
Ventricular septum morphogenesis	25	Down	0.00025808	0.09357634
Organellar large ribosomal subunit	32	Down	0.00036473	0.11918175
Retrograde transport vesicle recycling within golgi	22	Up	0.00038427	0.11918175
Organellar ribosome	66	Down	0.0003867	0.11918175
Mitochondrial electron transport nadh to ubiquinone	35	Down	0.00042097	0.12356489
Cytosolic part	186	Down	0.00048522	0.13595111
Cochlea morphogenesis	18	Down	0.00054195	0.14524239
Hops complex	13	Up	0.00059657	0.15321895
Electron transport chain	82	Down	0.00063061	0.15548261

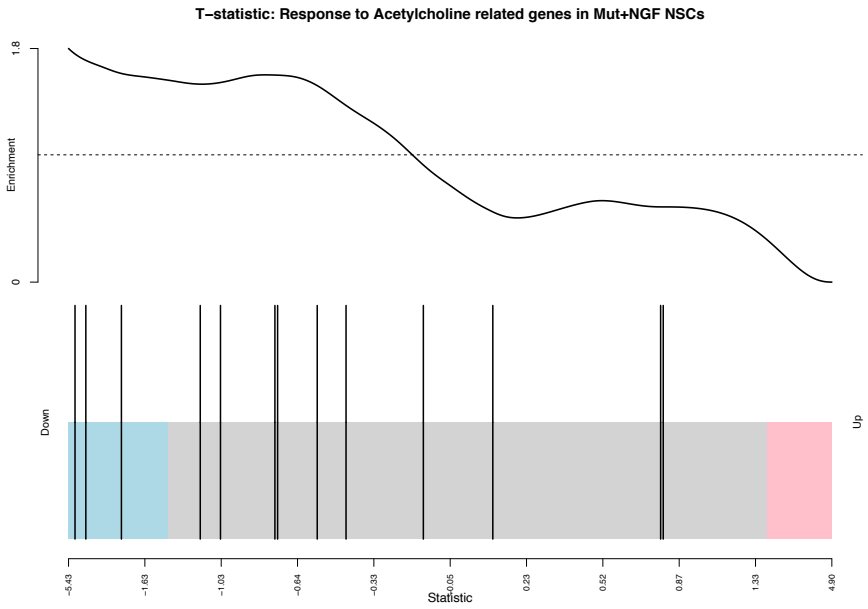

Figure 16: Barcode plot showing t-statistics for GO gene set "Response to Acetylcholine" in the mutant NSCs vs NGF-treated mutant NSCs group.

No gene set passed the multiple comparisons threshold in the group comparing differential gene expression in response to NGF between the mutant and the wildtype

NSCs. However, this is not entirely surprising, given the low number of differentially expressed genes in this comparison group. Additionally the high degree of difference between the cell lines without NGF stimulation indicates that a direct comparison of NGF response in these cells may no longer be appropriate. Regardless, over 300 gene sets reached nominal significance and analysis of the top gene sets suggests interesting further lines of investigation. Of particular interest, are up regulated gene sets in the “negative regulation of neuron differentiation”, “post-synaptic membrane organization” and “regulation of neurotransmitter receptor activity”. (Table 13)

Table 13: Top 25 significantly different gene sets using C5 gene ontology sets in mutant NSCs compared to wildtype NSCs in response to NGF stimulation.

GO gene sets	Genes (n)	Direction	PValue	FDR
Nitric oxide mediated signal transduction	12	Up	0.00023623	0.65025712
Establishment of protein localization to endoplasmic reticulum	96	Up	0.00047774	0.65025712
Protein targeting to membrane	141	Up	0.00048033	0.65025712
Cytosolic ribosome	99	Up	0.00048488	0.65025712
Autonomic nervous system development	34	Up	0.00052746	0.65025712
Nuclear transcribed mrna catabolic process nonsense mediated decay	110	Up	0.00069455	0.68409693
Nucleosomal dna binding	27	Up	0.00077688	0.68409693
Enhancer binding	77	Up	0.00094691	0.72959243
Ventricular septum morphogenesis	25	Up	0.00117366	0.80382336
Nucleosome binding	42	Up	0.00157508	0.82223072
Regulation of alpha amino 3 hydroxy 5 methyl 4 isoxazole propionate selective glutamate receptor activity	15	Up	0.00176958	0.82223072
Skeletal muscle cell differentiation	44	Up	0.00178383	0.82223072
Endoplasmic reticulum to cytosol transport	21	Down	0.00189385	0.82223072
Ventral spinal cord interneuron differentiation	11	Up	0.00205331	0.82223072
Postsynaptic membrane organization	23	Up	0.00209976	0.82223072
Regulation of prostaglandin secretion	8	Down	0.00239918	0.82223072
Ligase activity forming carbon oxygen bonds	44	Down	0.00248059	0.82223072
Cytosolic small ribosomal subunit	39	Up	0.0031116	0.82223072
Chromatin dna binding	64	Up	0.00338707	0.82223072
Regulation of icosanoid secretion	12	Down	0.0035181	0.82223072
Regulation of neurotransmitter receptor activity	24	Up	0.00367174	0.82223072
Stem cell division	27	Up	0.00381526	0.82223072
Transcription factor activity rna polymerase ii core promoter sequence specific	14	Up	0.00383654	0.82223072
Canonical wnt signaling pathway	86	Up	0.00392057	0.82223072
Negative regulation of neuron differentiation	162	Up	0.00395441	0.82223072

RNA sequencing analysis of NGF stimulation in neural stem cells, with and without the NTRK1 mutation is a powerful exploratory experiment. In many instances it has confirmed some of the cellular results that have been discovered over the course of this study. In particular, the gene sets upregulated in response to NGF in the wild type

NSCs confirms that NGF plays a key role in neuronal activity. Even after a relatively short period of stimulation, genes appeared to be upregulated in response, likely triggering the neurite outgrowth phenotypes observed in the study described in the previous chapter. The significant upregulation in these gene sets were not observed in the mutant NSCs. However, in addition to supporting many of the hypotheses posed in previous studies, the observed changes in both downstream pERK signaling and gene expression has opened a large number of avenues for further investigation. In particular, the large number of differentially expressed genes between the wildtype and mutant NSCs raises several questions on the developmental state of the cells, further discussed in the following chapter.

Chapter 4 in part, is currently being prepared for submission for publication of the material. Miranda, Alannah; Kelsoe, John. The dissertation author was the primary investigator and author of this material.

Chapter 5
Conclusions and Future Directions

5.1 Summary of key results

NTRK1 has been shown to play a particularly important role in the development and maintenance of cholinergic neurons. Cholinergic signaling appears to regulate mood and has been shown to effect biomarkers of depression. Therefore, several sequencing and association studies have been used to investigate the association of *NTRK1* and bipolar disorder. Thus far, *NTRK1* has been validated as a putative bipolar associated gene. Another aspect that has been studied in regards to bipolar disorder and *NTRK1* is lithium response. Neurotrophins, in particular BDNF, have been implicated in positive lithium response in bipolar patients. (90) Therefore we first sought to determine whether *NTRK1* and other neurotrophin and neurotrophin receptors could be associated with lithium response in a candidate gene study. While no gene or SNP was significantly associated with lithium response after correcting for multiple comparisons, *NTRK1* was still found to be nominally significant in association with lithium response.

While there have been no studies that have identified *NTRK1* to be associated with bipolar disorder after correcting for multiple comparisons, there have been several rare variants that have been identified in previous sequencing studies to be further investigated. The primary focus of this study has been focused on one of these mutations which was identified in a large pedigree in which mood disorders co-segregate with a mutation in *NTRK1.* The mutation, E492K, spanned across 4 generations and was predicted to be likely damaging due its close proximity to a key autophosphorylation site on TrkA, Y490. This study aimed to understand the function of the mutation and how it may affect neuronal function in a variety of models.

As detailed in Chapter 1, NGF-TrkA signaling is an exceedingly complex process, resulting in a large number of cellular outcomes. Downstream signaling primarily occurs through activation of PI3K, MAPK, and PLCγ. Due to the proximity of the E492K to the SHC and Frs-2 binding site, a significant focus of this study was to investigate what impact the mutation may have on events downstream of this binding site. One of the first goals of this study was to establish a phenotype between neural cells harboring the TrkA mutation and wildtype control cells. It was initially hypothesized that a damaging mutation in a key cholinergic development gene may have negative impacts on the basal forebrain cholinergic neurons. In fact, E492K neural stem cells derived from members of the pedigree, there appeared to be a decrease in NTRK1 gene expression.

However in evaluating mice harboring the analogous mutation, E495K, no changes in morphology, number, ChAT or TrkA expression was found in the basal forebrain cholinergic neurons. Another route of inquiry is neurite growth. It has been well established that neurite growth is induced in PC12 cells through TrkA signaling after stimulation with NGF. Analysis of E492K neural stem cells, generated from affected members of this pedigree, revealed a reduction in neurite outgrowth when compared to wildtype neural stem cells. This finding was later corroborated in primary hippocampal neurons from E495K mouse embryos. Dendritic branching was found to be reduced in the KI/KI mice. Additionally there was a non-significant trend in dendrite length, which appeared to be decreased in the KI/KI mice when compared to wild-type mice.

Despite no apparent changes in cholinergic neurons themselves, there was a distinct cellular response to the cholinergic receptor agonist, physostigmine. Basal

pERK signaling was found to be increased in E495K mice compared to wildtype mice, and decreased after physostigmine treatment in the E95K mice to levels observed in the control mice. Hippocampal cells are one of the primary target neurons innervated by basal forebrain cholinergic neurons, so this suggests that target neurons with the mutation may have an alteration in sensitivity to cholinergic stimulation. This sensitivity to cholinergic stimulation was also observed on a behavioral level, where E495K mice exhibited a longer periods of immobility in a tail suspension test after administration to physostigmine, which was not observed in wildtype mice or mice treated with vehicle. In this experiment, increased immobility is a marker for depressive behavior in mice.

Next, the mutation was generated in more homogenous cell type in order to evaluate the effects of downstream signaling specifically due to *NTRK1*. Given the alterations observed in pERK signaling in the mouse hippocampal neurons, pERK signaling was studied in HEK293 cells which were transfected with both mutant and wildtype TrkA. The TrkA construct used to transfect the HEK293 cells also contained a HaloTag® which bound to the OregonGreen ligand, to allow for visualization of transfected TrkA. Similar to TrkA expression in the mouse model, TrkA was equivalently expressed in the HEK293 cells.

However, pERK was differentially expressed in the wild type compared to the mutant, after stimulation with NGF. As expected, NGF stimulation in wildtype TrkA transfected HEK293 cells resulted in a robust increase in pERK signaling at 1 and 5 minutes post NGF stimulation, which is representative of transient TrkA signaling. pERK then slowly begins to return to baseline pERK levels, where it appears to still persist at 60 minutes, albeit at far lower expression than the initial transient expression, indicating

the expected sustained signal response. In mutant TrkA transfect HEK293 cells, a robust transient signal occurs at 1 and 5 minutes post NGF stimulation, however the signal persists at a high expression level through 10 and 30 minutes post NGF stimulation. Though it appears to decrease at 60 minutes post NGF stimulation, expression still appears higher than in the wildtype cells. This overall change in expression over time is indicative of an increase in transient and sustained pERK signaling in the mutant TrkA transfected HEK293 cells.

Lastly, in order to capture a broader picture of the effect of E492K on NGF-TrkA signaling, RNA sequencing was performed on neural stem cells with and without the E492K mutation, both before and after stimulation with NGF for 3 hours. There were overall fewer differentially expressed genes in response to NGF stimulation in the wildtype NSCs (49 genes) in comparison to the mutant NSCs (273 genes). However, the lists of differentially expressed genes showed no overlap at all. No single differentially expressed gene provides a succinct picture for how NGF-TrkA signaling is impacted by the mutation. In fact, many of the genes are largely uncharacterized in the literature. However, the large number of differentially expressed genes in wildtype NSCs and mutant NSCs before any NGF stimulation consists of an unusually high portion of the total genome. This may suggest that the cell lines have developed at different rates, resulting in one or both cell lines consisting of subpopulations of neural progenitor cell line, as opposed to a purely neural stem cell population.

Gene set testing of the analysis revealed that genes differentially expressed in the wild type NSCs in response to NGF stimulation supported previous knowledge of NGF-TrkA signaling. The two gene sets passed the multiple comparisons threshold,

were gene sets for “neuron migration” and “neuron recognition”. Further exploration of the nominally significant gene sets revealed many more neuron-associated gene sets, as well as “transmembrane receptor protein kinase activity.” Alternatively many of the gene sets identified as differentially expressed in the mutant NSCs as a response to NGF appeared to involve ribosomal functions. Many of these gene sets encompass a large number of genes which likely play various roles throughout development and maintenance of cellular activity. One interesting link to neuronal function that may exist is the reported downregulation of ribosome biogenesis as the early forebrain develops.(89)

An additional point to note is that gene sets associated with acetylcholine response also appeared to downregulated at a nominally significant level in only mutant NSCs after stimulation to NGF. Lastly, evaluation of gene sets that are differentially expressed in mutant NSCs compared to wildtype NSCs in response to NGF stimulation did not result any significant sets that passed the multiple corrections threshold. Nonetheless several nominally significant gene sets still provide suggestive support for an overall altered neurotransmitter system due to the TrkA mutation. Of the top 50 nominally significant gene sets, “regulation of neurotransmitter receptor activity” and “negative regulation of neuron differentiation” are both upregulated.

5.2 Hypothesis regarding altered cholinergic neurotransmission

Taking into account the altered response to cholinergic stimulation in the mouse model, resulting in decreased pERK and increased depressive behavior, it is reasonable to hypothesize that the NTRK1 mutation may alter sensitivity to acetylcholine. Physostigmine stimulation results in an increase of acetylcholine within

the synaptic cleft. The depressive phenotypes observed in E495K mice and humans exposed to physostigmine might be explained by an increase in hypersensitivity to acetylcholine by target neurons, or an upregulation of acetylcholine receptors. Previous studies suggest that acetylcholine receptor number remains unchanged after physostigmine administration, suggesting the depressive phenotypes are more likely a result of cholinergic hypersensitivity.

In apparent contrast, NGF stimulation appears to downregulate genes that are associated with response to acetylcholine in the TrkA mutant NSCs. As described in Chapter 1, NGF-TrkA signaling has been shown to induce ACh release and TrkA may play a role in upregulation of cholinergic gene expression.(22,24) The mutation in TrkA appears to cause a hypersensitivity to acetylcholine in mice, which would presumably suggest an increase in expression of some genes that are associated with acetylcholine response. The tempting answer to explain this contradiction is a difference in cell type and age of the models. Neural stem cells, derived from induced pluripotent stem cells, derived from human lymphoblastoid cell lines are likely to exhibit different phenotypes and expression patterns when compared to mice or mouse embryonic hippocampal neurons.

Perhaps a more satisfying answer to explain this conflict can be found by evaluating the functions of genes associated with response to acetylcholine. The definition of GO gene set “response to acetylcholine” encompasses genes involved in “any process that results in a change in state or activity of a cell or an organism (in terms of movement, secretion, enzyme production, gene expression, etc.) as a result of an acetylcholine stimulus”. However many genes included in this set are muscarinic

receptors associated genes. Upon an increase of intracellular ACh, as can be caused by physostigmine, pre-synaptic muscarinic receptors are excessively stimulated, causing ACh release and presynaptic signaling to be reduced. Additionally, the dramatic increase in ACh in response to physostigmine could bind receptors that would not have been activated if not for the high concentrations of ACh produced by physostigmine. (21) In this context, a downregulation of acetylcholine response genes could then be explained by hypersensitivity to cholinergic stimulation.

It could be postulated that the enhanced ERK signaling observed due to the TrkA mutation could result in an increased basal level of acetylcholine, persisting over time. As suggested in Chapter 1, NGF has been shown to induce acetylcholine release via TrkA signaling. Acetylcholine within the CNS is considered to play more of a neuromodulatory role, as opposed to a direct neurotransmitter. Acetylcholine release is also suggested to be more diffuse, exerting its effects on neurotransmission over time.(20) Therefore a general increase in acetylcholine release over time in the mutant cells could lead to a sensitivity to cholinergic activity, causing cholinergic response genes to be downregulated in an effort to balance overall neurotransmitter activity. It is unclear what the precise effects are of high levels of ACh, however much of the neuronal circuitry works in feedback loops, so it is a reasonable hypothesis to make. This can be further supported by the upregulation of the gene set “regulation of neurotransmitter receptor activity” in mutant NSCs compared to wildtype NSCs.

To this end, a key future direction would be to determine whether the mutation directly effects endogenous ACh signaling. Given that ACh release has been found to be increased by NGF stimulation through TrkA, it is possible that the mutation may

result in an unusually high level of endogenous acetylcholine levels, overtime creating a general hypersensitivity to cholinergic activity in mAChRs, and downregulation ACh response related genes. This hypothesis could be tested by measuring endogenous ACh levels in the mice harboring the mutation, before and after NGF stimulation. Alternatively, this could be examined after differentiation of wildtype and mutant neural stem cells into a neuronal population capable of secreting ACh.

5.3 Hypothesis regarding neuronal differentiation

Another question posed by this study is the relationship between sustained MAPK signaling and neuronal differentiation. As previously described, sustained and transient MAPK signaling result in many similar actions, likely working synergistically to organize neuronal development and differentiation. However based on many factors, such as concentration of neurotrophins and localization of neurotrophin receptors, different downstream outcomes will result. Neuronal differentiation can include axonal growth, or less specifically, neurite growth, or patterning to guide neural stem cells into forming a specific neuronal subpopulation.

The studies presented here suggest an increase in pERK signaling is more robust in mutant NSCs. Similarly, in the mouse model, hippocampal neurons exhibit a higher level of basal pERK. However, mutant NSCs exhibit a decrease in neurite outgrowth and decrease in dendritic branching in mouse hippocampal neurons. Sustained MAPK signaling has been identified as a preferential method in axonal growth, and general differentiation, however neurite growth has also been induced via transient MAPK signaling. These downstream events could be considerably similar when observed visually. An increase in sustained signaling might result in increase in

axonal growth, which would appear contrary to the observed reduction in neurite growth.

Another perspective would be to consider the balance of sustained and transient MAPK signaling. Some studies have suggested that Shc and Frs-2 bind competitively at Y490. Frs-2 is required for sustained MAPK signaling, and thus the preferred method of neuronal differentiation. Neurite outgrowth observed in response to NGF via SHC signaling is commonly observed in PC12 cells, and appears to represent a less directed form of differentiation. Given the observed increase in sustained signaling it is possible that Frs-2 binds to Y490 more preferentially, and thus tips the balance towards sustained MAPK signaling, resulting in fewer neurite outgrowth and instead setting mutant NSCs towards a more directed differentiated NPC subtype, or vice versa where the wildtype cells have developed into more specific NPC populations and mutant TrkA NSC growth is delayed or altered in another way.

A change in neuronal developmental state in the mutants compared to the wildtype cells would also account for the abnormally high number of differentially expressed genes in the mutant cells compared to the wildtype cells. Neural stem cells in this study were stained for pluripotency and neural stem cell markers, Sox2 and Nestin, and there was no observed difference in either marker between wildtype and mutant NSCs. However they were not characterized by other NPC markers or following stimulation to NGF. A change in early neuronal development could easily go undetected if only based on morphology and staining with these markers. Additionally, given the pan-neural stem cell induction protocol used in this study, induced pluripotent stem cells

could be driven towards any number of NPC subtype populations, if left to differentiate without specific growth factor guidance.

This can be further supported by evaluating neurodevelopmental genes in the RNAseq analysis. Several developmental genes are significantly differentially expressed in the wildtype cells when compared to mutant cells. As shown in Figure 17, a key pluripotency gene, Nanog, largely observed in iPSCs, is still relatively upregulated in the mutant cells, when compared to the wildtype cells. Early developmental genes, such as Nestin and Pax6 are upregulated in mutant cells, as may be expected as the iPSCs are induced to neural stem cells. However, they are comparatively downregulated in the wildtype cells. Even further down the neural differentiation path, DCX, an intermediate neural progenitor marker, the reverse is seen and the mutant cells are comparatively downregulated compared to the wildtype cells. Combined, this suggests that mutant cells may be at an earlier stage of neural differentiation than the wildtype cells.

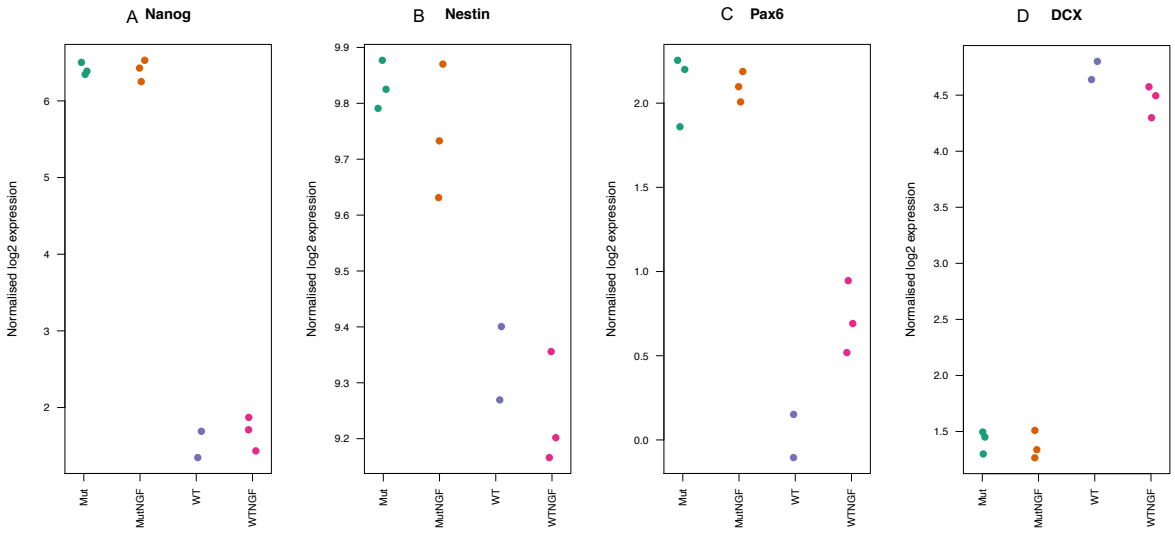

Figure 17: Expression of neurodevelopmental genes in wildtype and mutant neural cells. A) Nanog, B) Nestin C) Pax6 and D) DCX

This provides further support for a neurodevelopmental origin of bipolar disorder as well. There are many studies that have found defects at the neurodevelopmental level in bipolar patient samples. For example, genes related to neuron migration are differentially expressed and aberrant neuronal circuitry forms in brain tissue samples derived from bipolar patients.(91) In the wild type neural cells, the most significantly enriched gene set is “neuron migration”, indicating NGF plays a key role in inducing gene expression that promotes neuron migration. We also observed a decrease in gene expression in the mutant/bipolar cell lines of genes that have otherwise been found to be downregulated in bipolar samples. Reelin, a key factor in cell migration and development of GABAergic interneurons was found to be downregulated bipolar patients in a meta-analysis of 12 bipolar versus control studies.(92) Reelin is also found to be significantly down regulated in the mutant bipolar neural cell samples, when compared to the wildtype neural cells. (Appendix Figure 2a)

Another family study of bipolar disorder using iPSCs, NPCs and mature neurons, a similar neurodevelopmental phenotype was observed in terms of reduced proliferation.(93) However, this study differentiated iPSCs into a specific NPC subtype then performed an RNA seq analysis at each neuronal stage. At the NPC stage, the most downregulated gene in the bipolar samples was found to be Nkx6-1, which plays a key role in mediating the gene expression patterning during early neuronal development. Similarly, we find that the mutant bipolar samples in our RNAseq analysis are also significantly down regulated in Nkx6-1, when compared to the wildtype control samples. (Appendix Figure 2b)

Based on the combination of the mutant phenotypes and the RNAseq analysis, it is reasonable to conclude that the mutant and wildtype cells are at different stages of temporal development. This can likely be attributed to a change in early neuronal development in the mutant neural cells, as a result of the mutation in *NTRK1*, and likely other differentially expressed genes or mutations, which ultimately led to a differential response to the neural induction. A follow up to this hypothesis would be to further characterize the NSCs in order to determine whether there are NPC subtypes present that differ between mutant and wildtype cells.

Alternatively, this data could be compared to publicly available data on the neurodevelopmental transcriptome. The BrainSpan atlas has RNA Sequencing data available for numerous brain regions over the full course of human brain development. This data has been used to compare expression patterns during human brain development to gene expression during the neural differentiation of embryonic stem cells to neuronal cells.(94) A similar method could be applied to this data to determine whether mutant TrkA cells express transcriptome profiles similar to that of an earlier stage of brain development, compared to the wildtype TrkA cells and later developmental stage profiles.

Another method to verify a difference between sustained and transient pERK signaling would be to investigate endocytosis of the TrkA-NGF complex. Since endocytosis of the TrkA-NGF complex is required for sustained signaling, one might expect an increase in endocytosis in the mutant NSCs compared to the wildtype NSCs, if Frs-2 is binding Y490 more preferentially due to the mutation. This could be accomplished by labeling cell surface proteins with biotin before and after NGF

stimulation. After being stimulated with NGF, the TrkA-NGF complex will form a signaling endosome and be pulled from the cell surface. Biotin-labeled cell surface cells are then extracted and analyzed. NGF treated cells should have less cell surface TrkA proteins for biotin to label. Therefore a probe for TrkA in biotin labeled cell surface proteins would likely be reduced in NGF-treated samples, and hypothetically more so in mutant cells if sustained signaling is indeed enhanced. Alternatively, imaging could be used to visualize cell surface TrkA via the HaloTag® before and after NGF induced endocytosis.

Bipolar disorder has been thought to have developmental origins, as evidenced by many clinical, gene expression and cellular studies.(95) Many previous studies have identified specific genes involved in neural development and differentiation that are dysregulated in bipolar cells when compared to control.(96,97) While this hypothesis is continuously being investigated, much of the data found here supports those previous findings.

5.4 Concluding remarks, etc

The preceding studies have significantly contributed to the understanding of how TrkA impacts neuronal function. Beginning with the identification of a remarkable family with an incredibly rare genetic mutation, through mouse and multiple cellular models, the mutation has been thoroughly explored and characterized. On a behavioral level, the effect of E492K is a pronounced mood disorder, unfortunately affecting entire generations of a family to varying degrees. Recapitulation of this mood phenotype in a mouse model was a striking discovery made by our collaborators, increasingly strengthened by our subsequent supporting molecular and genetic evidence.

Future studies into this mutation and neuronal system may aspire to further understand the underpinning mechanisms of the findings found here. However more importantly, future studies should seek to improve the quality of life for the individuals that could be affected by dysregulation in this neuronal system. The mutation studied here is exceedingly rare, and is likely representative of but a small portion of heritable mood disorders, and an even smaller portion of our population. Yet in studying this mutation, it has become the epitome of how a single nucleotide mutation can be translated into changes concrete cellular effects that profoundly impacts on human behavior and quality of life. Pursuit of scientific knowledge should not be limited because of the perception that it may only impact a few individuals. The benefits of science should be meant for all of humankind, with no exception.

> "You cannot hope to build a better world without improving the individuals."
> -Marie Curie

Chapter 5 in part, is currently being prepared for submission for publication of the material. Miranda, Alannah; Kelsoe, John. The dissertation author was the primary investigator and author of this material.

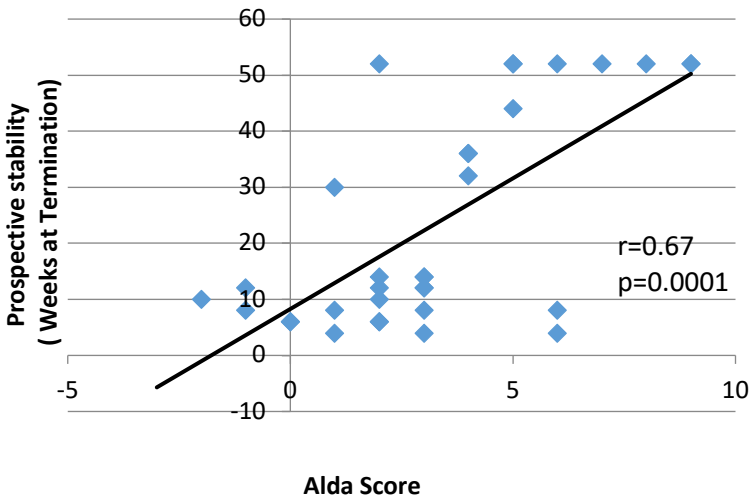

Appendix Figure 1: Alda Scale Validation
Alda Scale Validation in lithium responders and non-responders. The prospective study provided an ideal opportunity to conduct validation studies of the Alda scale in comparison with the "gold standard" prospective monotherapy trial. Prospective outcome data was available on 40 subjects, who had participated in the prospective arm of this study. After their participation in the prospective arm was complete, their records were blindly rated by two raters using the Alda scale. We examined the relationship between the scores in two ways. First, we compared the Alda scores for those who were successfully stabilized on lithium monotherapy vs. those that failed stabilization. Supplemental Table 1 illustrates a significantly higher mean Alda score in those that were stabilized. Similar support for the validity of the Alda scale is obtained when prospective response is measured as a quantitative variable of weeks to termination. In this analysis, weeks to termination was considered irrespective of the phase in which termination occurred. Appendix Figure 1 demonstrates a significant correlation between the Alda score rating of past lithium trials and the quantitative response in the prospective study. Together these data provide reasonable validation of the Alda scale.

Appendix Table 1: Alda Scores and Prospective Stabilization (n=40)

	Mean Alda score
Failed Stabilization	0.95 $\pm$ 2.2
Stabilized on Lithium	4.3 $\pm$ 2.6
P	0.0001

Appendix Table 2: Comorbidities and phenotype information for family 6807.

Subject	Psychiatric Diagnosis	Comorbidities	Age of Onset (psychiatric symptoms)	Age of Onset (ESRD)
1	Major Depression	ADTKD; alcoholism/substance dependency; panic disorder	19	34
2	Bipolar Type I	ADTKD; alcoholism/substance dependency; psychosis; rapid cycling, anorexia; panic disorder	7	18
3	Generalized Anxiety Disorder	Alcoholism	n/a	none
4	Bipolar Type I	ADTKD	n/a	n/a
5	Major Depression	n/a	n/a	none
6	Bipolar Type I	ADTKD; alcoholism/substance dependency; psychosis; rapid cycling,	12	24
7	Hyperthymia	ADTKD; short sleep periods	n/a	35
8	Bipolar Type I	ADTKD; psychosis; alcoholism/substance dependency		
9	Bipolar Type I	ADTKD; alcoholism/substance dependency; psychosis	28	~30
10	Major Depression	n/a	n/a	none
11	Bipolar Type I	ADTKD; substance abuse	n/a	n/a
12	Major Depression	ADTKD	n/a	n/a
13	Unknown	n/a	n/a	n/a
14	Psychiatrically healthy	n/a	none	none
15	Psychiatrically healthy	ADTKD; Gout	n/a	n/a
16	Unknown	n/a	n/a	none
17	Major Depression	ADTKD; Anxiety; sleep and memory complaints	n/a	24
18	Bipolar Type II	ADTKD; Anxiety; Sleep and memory complaints	n/a	22
19	Unknown	ADTKD	n/a	n/a

Appendix Table 3: List of significantly differentially expressed genes in wildtype NSCs after stimulation with NGF. (FDR $\leq$ 0.05)

Gene Ensembl ID	Gene Symbol /Name	Chromosome	Coef	t value	p-value	Direction
ENSG00000198774.5	RASSF9	12	-2.917338457	-4.746055243	0.000218004	Down
ENSG00000204428.12	LY6G5C	6	-0.954458712	-4.091205785	0.000848848	Down
ENSG00000204396.11	VWA7	6	-0.721445263	-4.046913996	0.000931635	Down
ENSG00000255284.2	Lnc-PANO1-1	11	-0.928790743	-4.043237405	0.000938863	Down
ENSG00000187650.4	VMAC	19	-0.871055455	-4.034108337	0.000957059	Down
ENSG00000276168.1	RN7SL1	14	0.847962059	3.95300214	0.001135219	Up
ENSG00000286502.1	AL645768.1	9	-1.662399671	-3.925503055	0.001202945	Down
ENSG00000214548.18	MEG3	14	-0.292943457	-3.85806509	0.001386805	Down
ENSG00000249406.3	LINC01969	17	-2.811634397	-3.807142747	0.001544188	Down
ENSG00000265735.2	RN7SL5P	9	0.962312028	3.797063227	0.00157741	Up
ENSG00000275410.5	HNF1B	17	-2.701547033	-3.7215425	0.001850295	Down
ENSG00000257894.2	Lnc-PAWR-1	12	-2.559422063	-3.690065404	0.001977593	Down
ENSG00000159267.15	HLCS	21	0.277240558	3.675274586	0.002040407	Up
ENSG00000256969.2	Lnc-CCND2-2	12	2.772516453	3.611888873	0.00233304	Up
ENSG00000185823.5	NPAP1	15	-2.588456581	-3.592690195	0.002429704	Down
ENSG00000155966.14	AFF2	X	0.244743587	3.52683261	0.002792742	Up
ENSG00000178171.11	AMER3	2	2.204653203	3.504337387	0.00292877	Up
ENSG00000260404.3	(GTF2I) Pseudogene	4	-0.330147185	-3.483038487	0.003063647	Down
ENSG00000262090.1	(PPP2R3B) pseudogene	16	-0.974518102	-3.440638002	0.003350849	Down
ENSG00000231943.9	PGM5P4-AS1	2	1.398310006	3.40521406	0.003611229	Up
ENSG00000254838.5	GVINP1	11	-1.923622488	-3.390717687	0.003723495	Down
ENSG00000152315.5	KCNK13	14	2.407322639	3.36744876	0.003910992	Up
ENSG00000182685.7	BRICD5	16	-0.597206262	-3.364039078	0.003939243	Down
ENSG00000197915.7	HRNR	1	0.984545446	3.319950559	0.004323297	Up
ENSG00000267365.1	KCNJ2-AS1	17	-1.017101845	-3.31923098	0.004329863	Down
ENSG00000229259.1	LRRC37A12P	1	-2.204853645	-3.306267876	0.004449867	Down
ENSG00000171130.18	ATP6V0E2	7	-0.291457552	-3.305587594	0.004456255	Down
ENSG00000275215.1	RNA5-8SN3	21	-0.578989512	-3.262632133	0.004878532	Down
ENSG00000173473.11	SMARCC1	3	0.163516262	3.258150273	0.00492481	Up
ENSG00000243836.5	WDR86-AS1	7	-1.829032277	-3.251240907	0.004997004	Down
ENSG00000278189.1	RNA5-8SN1	21	-0.578303998	-3.249356193	0.005016878	Down
ENSG00000242125.3	SNHG3	1	-0.350167431	-3.249121543	0.005019358	Down
ENSG00000242692.1	RPS27AP1	17	0.889246542	3.247322197	0.005038413	Up
ENSG00000248015.7	Lnc-GAMT-1	19	-1.522778371	-3.231689381	0.005207008	Down
ENSG00000198563.14	DDX39B	6	-0.220143765	-3.213675532	0.005408199	Down
ENSG00000254946.2	LINC02751	11	-2.117931899	-3.19895214	0.005578322	Down
ENSG00000286378.1	Lnc-C1orf21-1	1	-2.541111798	-3.186467596	0.005726704	Down
ENSG00000278233.1	RNA5-8SN2	21	-0.576513891	-3.185458994	0.00573886	Down
ENSG00000137033.11	IL33	9	1.78780076	3.183300415	0.005764962	Up
ENSG00000144230.16	GPR17	2	1.928104568	3.167508422	0.005959509	Up
ENSG00000147573.17	TRIM55	8	-0.882483462	-3.158174034	0.00607753	Down
ENSG00000280734.3	LINC01232	13	-0.938285353	-3.145497362	0.006241501	Down
ENSG00000288597.1	Lnc-RAB9B-2	X	2.263212361	3.144951614	0.006248657	Up
ENSG00000055609.19	KMT2C	7	0.202273415	3.144620518	0.006253003	Up
ENSG00000064393.16	HIPK2	7	0.174770859	3.133441026	0.006401485	Up
ENSG00000138621.12	PPCDC	15	-0.310773618	-3.119455662	0.006592124	Down
ENSG00000261628.1	(MPHOSPH10) Pseudogene	15	1.996008016	3.111265716	0.006706344	Up
ENSG00000222036.8	POTEM	14	0.925854549	3.108562494	0.006744469	Up
ENSG00000267452.3	LINC02073	17	-1.952661878	-3.08186482	0.007132624	Down

Appendix Table 4: List of significantly differentially expressed genes in mutant NSCs after stimulation with NGF. (FDR $\leq$ 0.05)

Gene Ensembl ID	Gene Symbol /Name	Chromosome	Coef	t value	p-value	Direction
ENSG00000101084.18	RAB5IF	20	-0.969485	-5.430629	5.51E-05	Down
ENSG00000213638.6	ADAT3	19	-1.487971	-4.978232	0.000136	Down
ENSG00000243449.6	C4orf48	4	-1.693117	-4.94782	0.000145	Down
ENSG00000168282.6	MGAT2	14	-1.833649	-4.913944	0.000155	Down
ENSG00000124942.14	AHNAK	11	0.365522	4.896248	0.00016	Up
ENSG00000103254.10	ANTKMT	16	-0.914848	-4.875944	0.000167	Down
ENSG00000188290.11	HES4	1	-1.07162	-4.842439	0.000179	Down
ENSG00000167996.16	FTH1	11	-0.74964	-4.608989	0.000289	Down
ENSG00000218891.5	ZNF579	19	-0.619904	-4.605271	0.000291	Down
ENSG00000099974.8	DDTL	22	-0.760103	-4.604108	0.000292	Down
ENSG00000178531.6	CTXN1	19	-0.71514	-4.586104	0.000303	Down
ENSG00000131188.12	PRR7	5	-1.123458	-4.558829	0.00032	Down
ENSG00000250479.9	CHCHD10	22	-0.527733	-4.537569	0.000335	Down
ENSG00000216866.5	RPS2P55	X	-1.065603	-4.447035	0.000404	Down
ENSG00000187140.6	FOXD3	1	-0.962947	-4.433368	0.000415	Down
ENSG00000196611.5	MMP1	11	0.564354	4.414324	0.000432	Up
ENSG00000175602.4	CCDC85B	11	-1.239748	-4.388953	0.000456	Down
ENSG00000224677.1	PDIA3P2	15	-2.17673	-4.373689	0.00047	Down
ENSG00000231686.1	ANKRD11P2	X	-0.758702	-4.361195	0.000483	Down
ENSG00000068137.15	PLEKHH3	17	-0.565045	-4.359701	0.000484	Down
ENSG00000006015.17	REX1BD	19	-0.703693	-4.352722	0.000491	Down
ENSG00000197102.12	DYNC1H1	14	0.239024	4.266524	0.000588	Up
ENSG00000204335.4	SP5	2	-0.465726	-4.246538	0.000613	Down
ENSG00000174021.11	GNG5	1	-0.392235	-4.216446	0.000653	Down
ENSG00000066735.14	KIF26A	14	-0.663852	-4.213334	0.000657	Down
ENSG00000038427.16	VCAN	5	0.207149	4.200021	0.000676	Up
ENSG00000188486.3	H2AX	11	-0.546334	-4.182757	0.000701	Down
ENSG00000213563.7	C8orf82	8	-0.404169	-4.175412	0.000711	Down
ENSG00000125901.6	MRPS26	20	-0.431721	-4.131516	0.00078	Down
ENSG00000160113.5	NR2F6	19	-0.401186	-4.117316	0.000804	Down
ENSG00000197582.5	GPX1P1	X	-0.740842	-4.083295	0.000863	Down
ENSG00000134250.20	NOTCH2	1	0.238623	4.076666	0.000875	Up
ENSG00000161179.14	YDJC	22	-0.53535	-4.070731	0.000886	Down
ENSG00000164736.6	SOX17	8	-0.494525	-4.067045	0.000893	Down
ENSG00000176788.9	BASP1	5	-0.296691	-4.066404	0.000894	Down
ENSG00000169228.14	RAB24	5	-0.849764	-4.06098	0.000904	Down
ENSG00000215808.4	LINC01139	1	0.442401	4.055626	0.000915	Up
ENSG00000100503.25	NIN	14	0.228454	4.026394	0.000973	Up
ENSG00000100075.10	SLC25A1	22	-0.267979	-4.017718	0.000991	Down
ENSG00000144036.16	EXOC6B	2	0.239132	4.01451	0.000997	Up
ENSG00000131116.12	ZNF428	19	-0.517281	-3.968584	0.001099	Down
ENSG00000099624.8	ATP5F1D	19	-0.529488	-3.967888	0.0011	Down
ENSG00000148450.13	MSRB2	10	-0.350067	-3.96057	0.001117	Down
ENSG00000261308.2	FIGNL2	12	-0.716734	-3.957271	0.001125	Down
ENSG00000108106.14	UBE2S	19	-0.308811	-3.947735	0.001148	Down
ENSG00000167642.13	SPINT2	19	-0.340018	-3.923548	0.001208	Down
ENSG00000172780.17	RAB43	3	-0.689051	-3.922454	0.001211	Down
ENSG00000177732.8	SOX12	20	-0.300289	-3.917888	0.001222	Down
ENSG00000129968.16	ABHD17A	19	-0.561316	-3.916327	0.001226	Down
ENSG00000140406.4	TLNRD1	15	-0.473118	-3.916158	0.001227	Down
ENSG00000167962.14	ZNF598	16	-0.446038	-3.882006	0.001318	Down
ENSG00000179271.3	GADD45GIP1	19	-0.325746	-3.858985	0.001384	Down
ENSG00000123144.11	TRIR	19	-0.347444	-3.852746	0.001402	Down
ENSG00000227582.2	ADGRF5P1	9	-2.457894	-3.846838	0.00142	Down
ENSG00000187514.16	PTMA	2	-0.161472	-3.845771	0.001423	Down
ENSG00000130748.7	TMEM160	19	-0.81484	-3.84157	0.001436	Down
ENSG00000127481.15	UBR4	1	0.190045	3.82187	0.001497	Up
ENSG00000253276.4	CCDC71L	7	-0.353053	-3.806825	0.001545	Down
ENSG00000244486.9	SCARF2	22	-0.506815	-3.804381	0.001553	Down
ENSG00000182768.9	NGRN	15	-0.382715	-3.799631	0.001569	Down
ENSG00000272667.1	LINC00863	2	-0.751482	-3.794857	0.001585	Down
ENSG00000181588.16	MEX3D	19	-0.52905	-3.793974	0.001588	Down
ENSG00000167641.11	PPP1R14A	19	-0.69393	-3.793163	0.00159	Down
ENSG00000010818.10	HIVEP2	6	0.249812	3.790556	0.001599	Up
ENSG00000138944.8	SHISAL1	22	0.435463	3.7879	0.001608	Up
ENSG00000162733.19	DDR2	1	0.259684	3.787356	0.00161	Up
ENSG00000261150.3	EPPK1	8	-0.709773	-3.786415	0.001613	Down
ENSG00000136068.15	FLNB	3	0.220263	3.784811	0.001619	Up
ENSG00000095951.17	HIVEP1	6	0.278668	3.756188	0.00172	Up
ENSG00000177283.7	FZD8	10	-0.486801	-3.737302	0.00179	Down
ENSG00000165804.16	ZNF219	14	-0.599044	-3.732096	0.001809	Down
ENSG00000007376.8	RPUSD1	16	-0.433941	-3.725551	0.001835	Down
ENSG00000130770.18	ATP5IF1	1	-0.297281	-3.715748	0.001873	Down
ENSG00000124074.12	ENKD1	16	-0.452901	-3.71247	0.001886	Down
ENSG00000105204.14	DYRK1B	19	-0.357962	-3.698094	0.001944	Down
ENSG00000122705.17	CLTA	9	-0.197771	-3.696013	0.001953	Down
ENSG00000104825.17	NFKBIB	19	-0.455775	-3.6859	0.001995	Down
ENSG00000130182.8	ZSCAN10	16	-0.423404	-3.684133	0.002003	Down
ENSG00000177383.5	MAGEF1	3	-0.259825	-3.681048	0.002016	Down
ENSG00000245275.8	SAP30L-AS1	5	0.689895	3.680968	0.002016	Up
ENSG00000083857.14	FAT1	4	0.277197	3.680221	0.002019	Up
ENSG00000241860.7	Lnc-OR4F29-3	1	0.356484	3.666642	0.002078	Up
ENSG00000224094.1	RPS24P8	3	-0.529912	-3.665219	0.002084	Down
ENSG00000169683.8	LRRC45	17	-0.486966	-3.651794	0.002144	Down
ENSG00000234009.1	RPL5P34	22	-0.492235	-3.648669	0.002158	Down
ENSG00000230897.1	RPS18P12	17	-0.653905	-3.643763	0.002181	Down
ENSG00000069011.16	PITX1	5	-0.587024	-3.628669	0.002252	Down
ENSG00000229107.2	ABHD17AP4	22	-1.36304	-3.622297	0.002282	Down
ENSG00000112667.13	DNPH1	6	-0.553415	-3.617894	0.002304	Down
ENSG00000161677.12	JOSD2	19	-0.707127	-3.615612	0.002315	Down

Appendix Table 4: List of significantly differentially expressed genes in mutant NSCs after stimulation with NGF, Continued

Gene Ensembl ID	Gene Symbol /Name	Chromosome	Coef	t value	p-value	Direction
ENSG00000126934.14	MAP2K2	19	-0.293087	-3.280274	0.004701	Down
ENSG00000287245.1	Lnc-ZC3H12C-1	11	2.046545	3.279838	0.004705	Up
ENSG00000128309.16	MPST	22	-0.311912	-3.278643	0.004717	Down
ENSG00000099849.15	RASSF7	11	-0.321997	-3.268614	0.004817	Down
ENSG00000100836.10	PABPN1	14	-0.232127	-3.256796	0.004939	Down
ENSG00000279692.1	AC110285.6	17	-0.919724	-3.255275	0.004955	Down
ENSG00000125492.10	BARHL1	9	-1.456473	-3.253818	0.00497	Down
ENSG00000064961.19	HMG20B	19	-0.268638	-3.25222	0.004987	Down
ENSG00000115268.10	RPS15	19	-0.362558	-3.243569	0.005078	Down
ENSG00000165655.17	ZNF503	10	-0.773316	-3.239023	0.005127	Down
ENSG00000086504.17	MRPL28	16	-0.184034	-3.23834	0.005135	Down
ENSG00000099804.9	CDC34	19	-0.317309	-3.232441	0.005199	Down
ENSG00000185507.21	IRF7	11	-0.371727	-3.23215	0.005202	Down
ENSG00000173077.16	DELEC1	9	0.544435	3.231057	0.005214	Up
ENSG00000130203.10	APOE	19	-0.431366	-3.230995	0.005215	Down
ENSG00000272933.1	Lnc-ARL3-1	10	-0.700132	-3.230965	0.005215	Down
ENSG00000145908.12	ZNF300	5	0.540465	3.229447	0.005232	Up
ENSG00000169564.7	PCBP1	2	-0.320569	-3.228625	0.005241	Down
ENSG00000158715.6	SLC45A3	1	-0.35697	-3.227635	0.005252	Down
ENSG00000200913.1	SNORD46	1	1.242531	3.225223	0.005278	Up
ENSG00000243678.12	NME2	17	-0.703276	-3.223421	0.005298	Down
ENSG00000165506.15	DNAAF2	14	-0.258395	-3.223329	0.005299	Down
ENSG00000051523.11	CYBA	16	-0.37791	-3.219975	0.005337	Down
ENSG00000127445.14	PIN1	19	-0.277135	-3.215128	0.005392	Down
ENSG00000133275.16	CSNK1G2	19	-0.336197	-3.214465	0.005399	Down
ENSG00000180767.10	CHST13	3	-1.369569	-3.213401	0.005411	Down
ENSG00000285976.2	AL135905.2	6	-0.661906	-3.211205	0.005436	Down
ENSG00000153487.13	ING1	13	-0.240645	-3.208601	0.005466	Down
ENSG00000122386.11	ZNF205	16	-0.492591	-3.208108	0.005472	Down
ENSG00000171365.17	CLCN5	X	0.240314	3.207194	0.005482	Up
ENSG00000230383.1	Ribosomal Protein L6 (RPL6) Pseudoger	7	-0.319713	-3.199549	0.005571	Down
ENSG00000155657.27	TTN	2	0.277455	3.199521	0.005572	Up
ENSG00000179085.8	DPM3	1	-0.39219	-3.197306	0.005598	Down
ENSG00000234498.3	RPL13AP20	12	-0.514557	-3.196754	0.005604	Down
ENSG00000183458.14	PKD1P3	16	-0.731036	-3.191785	0.005663	Down
ENSG00000279744.1	AC132938.6	17	1.363366	3.191468	0.005667	Up
ENSG00000149761.9	NUDT22	11	-0.316593	-3.186301	0.005729	Down
ENSG00000261221.3	ZNF865	19	-0.549237	-3.184992	0.005744	Down
ENSG00000198517.10	MAFK	7	-0.375795	-3.180879	0.005794	Down
ENSG00000087085.15	ACHE	7	-0.386409	-3.180203	0.005803	Down
ENSG00000126709.15	IFI6	1	-0.400571	-3.179223	0.005815	Down
ENSG00000138326.21	RPS24	10	-0.14763	-3.179195	0.005815	Down
ENSG00000173020.11	GRK2	11	-0.224345	-3.179174	0.005815	Down
ENSG00000183691.6	NOG	17	-0.426336	-3.176064	0.005853	Down
ENSG00000086758.16	HUWE1	X	0.172723	3.17598	0.005854	Up
ENSG00000227827.3	PKD1P2	16	-0.552237	-3.175378	0.005862	Down
ENSG00000136213.10	CHST12	7	-0.319651	-3.170219	0.005926	Down
ENSG00000133169.6	BEX1	X	-0.254667	-3.169039	0.00594	Down
ENSG00000184990.13	SIVA1	14	-0.319521	-3.16832	0.005949	Down
ENSG00000141965.5	FEM1A	19	-0.736094	-3.167345	0.005962	Down
ENSG00000101182.15	PSMA7	20	-0.15751	-3.166281	0.005975	Down
ENSG00000196460.14	RFX8	2	0.887316	3.156431	0.0061	Up
ENSG00000234287.1	Ribosomal Protein S27 (RPS27) Pseudo	3	-0.483172	-3.150588	0.006175	Down
ENSG00000168061.17	SAC3D1	11	-0.373526	-3.148179	0.006206	Down
ENSG00000135940.7	COX5B	2	-0.324735	-3.146899	0.006223	Down
ENSG00000197989.14	SNHG12	1	-0.247784	-3.146817	0.006224	Down
ENSG00000160867.15	FGFR4	5	-0.273811	-3.146304	0.006231	Down
ENSG00000110492.15	MDK	11	-0.288388	-3.144615	0.006253	Down
ENSG00000185049.16	NELFA	4	-0.317818	-3.143071	0.006273	Down
ENSG00000167526.14	RPL13	16	-0.266679	-3.141137	0.006299	Down
ENSG00000226981.2	ABHD17AP6	17	-0.822927	-3.139828	0.006316	Down
ENSG00000127564.17	PKMYT1	16	-0.401724	-3.139805	0.006317	Down
ENSG00000205100.2	HSP90AA4P	4	-0.858724	-3.13946	0.006321	Down
ENSG00000232346.1	Ribosomal Protein S17 (RPS17) Pseudo	22	-0.672328	-3.137615	0.006346	Down
ENSG00000130299.17	GTPBP3	19	-0.299219	-3.137427	0.006348	Down
ENSG00000071564.17	TCF3	19	-0.303738	-3.136879	0.006355	Down
ENSG00000140993.11	TIGD7	16	-0.702856	-3.136172	0.006365	Down
ENSG00000180730.5	SHISA2	13	-0.273188	-3.136073	0.006366	Down
ENSG00000214761.3	HNRNPA1P15	9	-1.342885	-3.133842	0.006396	Down
ENSG00000166165.13	CKB	14	-0.371117	-3.132364	0.006416	Down
ENSG00000099901.17	RANBP1	22	-0.16929	-3.131294	0.00643	Down
ENSG00000157927.17	RADIL	7	-0.521441	-3.130809	0.006437	Down
ENSG00000225093.1	RPL3P7	6	-0.766917	-3.130266	0.006444	Down
ENSG00000140443.15	IGF1R	15	0.140734	3.12619	0.0065	Up
ENSG00000260428.3	SCX	8	-1.187702	-3.12397	0.00653	Down
ENSG00000162783.11	IER5	1	-0.259984	-3.122777	0.006546	Down
ENSG00000065268.11	WDR18	19	-0.413848	-3.121253	0.006567	Down
ENSG00000182871.16	COL18A1	21	-0.448437	-3.118254	0.006609	Down
ENSG00000063245.15	EPN1	19	-0.369184	-3.114678	0.006659	Down
ENSG00000181449.4	SOX2	3	-0.267185	-3.114249	0.006665	Down
ENSG00000137076.21	TLN1	9	0.136126	3.11129	0.006706	Up
ENSG00000153443.13	UBALD1	16	-0.303406	-3.105389	0.006789	Down
ENSG00000183048.12	SLC25A10	17	-0.490357	-3.099962	0.006867	Down
ENSG00000165782.11	PIP4P1	14	-0.206481	-3.099027	0.006881	Down
ENSG00000143793.13	C1orf35	1	-0.327012	-3.096064	0.006924	Down
ENSG00000170296.10	GABARAP	17	0.375912	3.094833	0.006941	Up
ENSG00000256001.2	Lnc-SLC15A4-14	12	-2.022354	-3.093544	0.00696	Down
ENSG00000130511.16	SSBP4	19	-0.60154	-3.093004	0.006968	Down
ENSG00000236801.1	RPL24P8	9	-0.680785	-3.092258	0.006979	Down
ENSG00000233276.6	GPX1	3	-0.268593	-3.091803	0.006986	Down

Appendix Table 4: List of significantly differentially expressed genes in mutant NSCs after stimulation with NGF, Continued

Gene Ensembl ID	Gene Symbol /Name	Chromosome	Coef	t value	p-value	Direction
ENSG00000253899.1	AC067904.2	8	-0.849151	-3.610905	0.002338	Down
ENSG00000179588.9	ZFPM1	16	-0.768201	-3.60496	0.002367	Down
ENSG00000148291.10	SURF2	9	-0.271219	-3.599035	0.002397	Down
ENSG00000125534.10	PPDPF	20	-0.591074	-3.598888	0.002398	Down
ENSG00000160972.9	PPP1R16A	8	-0.760504	-3.591339	0.002437	Down
ENSG00000130669.17	PAK4	19	-0.372176	-3.586278	0.002463	Down
ENSG00000227008.2	Ribosomal Protein S24 (RPS24) Pseudo	X	-0.418023	-3.583822	0.002476	Down
ENSG00000165716.11	DIPK1B	9	-0.38863	-3.576967	0.002512	Down
ENSG00000198113.3	TOR4A	9	-0.549603	-3.574182	0.002527	Down
ENSG00000280071.4	GATD3B	21	-0.739847	-3.569596	0.002551	Down
ENSG00000285722.1	AC207130.1	22	-1.100393	-3.566556	0.002568	Down
ENSG00000125656.11	CLPP	19	-0.280238	-3.562962	0.002587	Down
ENSG00000142544.7	CTU1	19	-0.793315	-3.561067	0.002598	Down
ENSG00000143768.13	LEFTY2	1	-0.382493	-3.553244	0.002641	Down
ENSG00000167968.13	DNASE1L2	16	-1.25576	-3.543251	0.002697	Down
ENSG00000167543.16	TP53I13	17	-0.363771	-3.538794	0.002723	Down
ENSG00000172216.6	CEBPB	20	-0.437524	-3.53605	0.002739	Down
ENSG00000283475.1	MIR1244-4	12	-1.410713	-3.534726	0.002747	Down
ENSG00000174482.10	LINGO2	9	0.770293	3.534629	0.002747	Up
ENSG00000129038.16	LOXL1	15	-0.332231	-3.534194	0.00275	Down
ENSG00000138759.19	FRAS1	4	0.204312	3.533503	0.002754	Up
ENSG00000276368.2	H2AC14	6	-1.43471	-3.527831	0.002787	Down
ENSG00000130522.6	JUND	19	-0.570102	-3.523182	0.002814	Down
ENSG00000141933.9	TPGS1	19	-1.180961	-3.518638	0.002842	Down
ENSG00000185453.13	ZSWIM9	19	-0.39783	-3.517035	0.002851	Down
ENSG00000092758.18	COL9A3	20	-0.600368	-3.514104	0.002869	Down
ENSG00000099364.17	FBXL19	16	-0.350399	-3.508185	0.002905	Down
ENSG00000124486.13	USP9X	X	0.20328	3.502973	0.002937	Up
ENSG00000130731.16	METTL26	16	-0.324287	-3.500513	0.002953	Down
ENSG00000129932.10	DOHH	19	-0.487372	-3.495699	0.002983	Down
ENSG00000286279.1	Lnc-SLC16A7-4	12	1.383583	3.491435	0.00301	Up
ENSG00000174197.16	MGA	15	0.262107	3.484672	0.003053	Up
ENSG00000182154.8	MRPL41	9	-0.439243	-3.484219	0.003056	Down
ENSG00000091129.21	NRCAM	7	0.244594	3.467806	0.003164	Up
ENSG00000177106.16	EPS8L2	11	-0.340114	-3.463974	0.00319	Down
ENSG00000072364.13	AFF4	5	0.201183	3.46069	0.003212	Up
ENSG00000226085.3	UQCRFS1P1	22	-0.514416	-3.45915	0.003222	Down
ENSG00000261609.8	GAN	16	0.247316	3.4587	0.003225	Up
ENSG00000163814.8	CDCP1	3	0.296047	3.454954	0.003251	Up
ENSG00000184160.8	ADRA2C	4	-0.625317	-3.452647	0.003267	Down
ENSG00000188483.8	IER5L	9	-0.795923	-3.448474	0.003296	Down
ENSG00000182752.10	PAPPA	9	0.268765	3.44762	0.003302	Up
ENSG00000152818.18	UTRN	6	0.211654	3.447127	0.003305	Up
ENSG00000099783.12	HNRNPM	19	-0.159081	-3.446492	0.00331	Down
ENSG00000137834.15	SMAD6	15	-0.424533	-3.438344	0.003367	Down
ENSG00000011132.12	APBA3	19	-0.336179	-3.435433	0.003388	Down
ENSG00000159884.12	CCDC107	9	-0.854168	-3.433251	0.003404	Down
ENSG00000156381.9	ANKRD9	14	-0.376203	-3.431531	0.003416	Down
ENSG00000132967.9	HMGB1P5	3	-0.173809	-3.430721	0.003422	Down
ENSG00000125652.8	ALKBH7	19	-0.597197	-3.429715	0.003429	Down
ENSG00000198832.10	SELENOM	22	-0.57263	-3.428607	0.003437	Down
ENSG00000071051.14	NCK2	2	-0.319727	-3.426162	0.003455	Down
ENSG00000259781.1	HMGB1P6	15	-0.172351	-3.418874	0.003509	Down
ENSG00000171222.10	SCAND1	20	-0.532363	-3.415764	0.003532	Down
ENSG00000161016.17	RPL8	8	-0.249218	-3.415486	0.003534	Down
ENSG00000107872.12	FBXL15	10	-1.01794	-3.408322	0.003588	Down
ENSG00000250471.2	GMPSP1	4	0.805601	3.408066	0.00359	Up
ENSG00000147065.17	MSN	X	0.131511	3.401174	0.003642	Up
ENSG00000071626.17	DAZAP1	19	-0.238036	-3.397217	0.003673	Down
ENSG00000162585.17	FAAP20	1	-0.493926	-3.393521	0.003702	Down
ENSG00000147526.20	TACC1	8	0.197238	3.388666	0.00374	Up
ENSG00000164442.10	CITED2	6	-0.304503	-3.386703	0.003755	Down
ENSG00000122641.11	INHBA	7	0.220986	3.384381	0.003774	Up
ENSG00000004779.10	NDUFAB1	16	-0.238475	-3.384179	0.003775	Down
ENSG00000103024.7	NME3	16	-0.547613	-3.376792	0.003835	Down
ENSG00000197483.10	ZNF628	19	-0.56117	-3.37588	0.003842	Down
ENSG00000148296.7	SURF6	9	-0.184565	-3.369638	0.003893	Down
ENSG00000107290.14	SETX	9	0.203843	3.365784	0.003925	Up
ENSG00000176945.17	MUC20	3	1.758547	3.362689	0.00395	Up
ENSG00000249685.1	Lnc-KLHL5-1	4	-1.313535	-3.361046	0.003964	Down
ENSG00000130312.6	MRPL34	19	-0.475736	-3.358545	0.003985	Down
ENSG00000063241.8	ISOC2	19	-0.331982	-3.357987	0.00399	Down
ENSG00000216285.5	Phosphoglycerate Mutase 1 (Brain) (PGA	12	-0.332996	-3.356741	0.004	Down
ENSG00000103266.11	STUB1	16	-0.334106	-3.349326	0.004063	Down
ENSG00000262814.8	MRPL12	17	-0.921591	-3.341613	0.00413	Down
ENSG00000130520.11	LSM4	19	-0.207332	-3.339784	0.004146	Down
ENSG00000287021.1	Lnc-MFSD8-2	4	-2.34009	-3.338967	0.004153	Down
ENSG00000166704.11	ZNF606	19	0.360225	3.327396	0.004256	Up
ENSG00000212907.2	MT-ND4L	MT	0.206534	3.325814	0.00427	Up
ENSG00000175756.13	AURKAIP1	1	-0.330948	-3.32084	0.004315	Down
ENSG00000187244.12	BCAM	19	-0.325069	-3.312355	0.004393	Down
ENSG00000167674.15	HDGFL2	19	-0.273019	-3.309244	0.004422	Down
ENSG00000075618.18	FSCN1	7	-0.292189	-3.307999	0.004434	Down
ENSG00000181649.8	PHLDA2	11	-0.614345	-3.304326	0.004468	Down
ENSG00000104852.15	SNRNP70	19	-0.277443	-3.297758	0.00453	Down
ENSG00000102763.18	VWA8	13	0.244714	3.296868	0.004539	Up
ENSG00000130513.6	GDF15	19	-0.417854	-3.295568	0.004551	Down
ENSG00000286482.1	AL117344.2	6	-1.770189	-3.289475	0.00461	Down
ENSG00000124097.7	HMGB1P1	20	-0.716864	-3.287403	0.00463	Down
ENSG00000241697.5	TMEFF1	9	-1.239721	-3.283483	0.004669	Down
ENSG00000158716.9	DUSP23	1	-0.443121	-3.090984	0.006998	Down
ENSG00000105127.9	AKAP8	19	-0.18706	-3.089742	0.007016	Down
ENSG00000273706.5	LHX1	17	-0.368246	-3.086381	0.007065	Down

Appendix Table 5: List of top 50 significantly differentially expressed genes in wildtype NSCs compared to mutant NSCs (FDR $\leq$ 0.05)

Gene Ensemble ID	Gene Symbol/Name	Chromosome	Coef	t-value	p-value	Direction
ENSG00000187498.	COL4A1	13	-3.194522	-60.44524	2.89E-16	Down
ENSG00000170421.	KRT8	12	-4.046404	-59.68316	2.89E-16	Down
ENSG00000113140.	SPARC	5	-2.925201	-58.40548	2.89E-16	Down
ENSG00000111057.	KRT18	12	-3.77122	-52.65252	1.13E-15	Down
ENSG00000135074.	ADAM19	5	-3.787742	-49.92316	1.99E-15	Down
ENSG00000149591.	TAGLN	11	-3.720445	-49.54724	1.99E-15	Down
ENSG00000101134.	DOK5	20	3.706631	46.26354	5.08E-15	Up
ENSG00000183117.	CSMD1	8	7.457095	44.68424	7.73E-15	Up
ENSG00000189056.	RELN	7	4.894969	44.34761	7.75E-15	Up
ENSG00000164742.	ADCY1	7	3.190049	43.50723	8.91E-15	Up
ENSG00000100285.	NEFH	22	3.50295	43.2673	8.91E-15	Up
ENSG00000163191.	S100A11	1	-3.010012	-43.17267	8.91E-15	Down
ENSG00000168824.	NSG1	4	3.85059	42.60262	1.01E-14	Up
ENSG00000101335.	MYL9	20	-2.053409	-41.90754	1.01E-14	Down
ENSG00000107438.	PDLIM1	10	-3.93296	-41.57751	1.01E-14	Down
ENSG00000140416.	TPM1	15	Down.9553	-41.55069	1.01E-14	Down
ENSG00000157227.	MMP14	14	-3.265846	-41.54389	1.01E-14	Down
ENSG00000128573.	FOXP2	7	3.927639	41.53721	1.01E-14	Up
ENSG00000091656.	ZFHX4	8	4.083702	41.42159	1.01E-14	Up
ENSG00000008196.	TFAP2B	6	7.365511	41.38647	1.01E-14	Up
ENSG00000096696.	DSP	6	-3.99138	-41.36083	1.01E-14	Down
ENSG00000198825.	INPP5F	10	2.572581	41.20536	1.02E-14	Up
ENSG00000119681.	LTBP2	14	-5.50589	-40.91086	1.09E-14	Down
ENSG00000143369.	ECM1	1	-4.060422	-40.3198	1.27E-14	Down
ENSG00000173281.	PPP1R3B	8	-3.987702	-40.3161	1.27E-14	Down
ENSG00000103257.	SLC7A5	16	-3.083972	-40.08049	1.34E-14	Down
ENSG00000177519.	RPRM	2	4.367855	39.80237	1.44E-14	Up
ENSG00000183049.	CAMK1D	10	3.511983	39.54058	1.54E-14	Up
ENSG00000185885.	IFITM1	11	-4.167057	-38.84961	1.97E-14	Down
ENSG00000134871.	COL4A2	13	-2.414844	-38.51441	2.19E-14	Down
ENSG00000150687.	PRSS23	11	-3.57578	-38.41917	2.20E-14	Down
ENSG00000185008.	ROBO2	3	4.827736	37.73301	2.84E-14	Up
ENSG00000116285.	ERRFI1	1	-2.460035	-37.44142	2.99E-14	Down
ENSG00000044524.	EPHA3	3	4.960059	37.42201	2.99E-14	Up
ENSG00000152377.	SPOCK1	5	2.771051	37.3533	2.99E-14	Up
ENSG00000005884.	ITGA3	17	-3.887521	-37.32885	2.99E-14	Down
ENSG00000152578.	GRIA4	11	4.66226	37.24731	2.99E-14	Up
ENSG00000184226.	PCDH9	13	4.092356	37.20543	2.99E-14	Up
ENSG00000115414.	FN1	2	-3.186162	-36.71564	3.59E-14	Down
ENSG00000104722.	NEFM	8	3.58454	36.33076	4.14E-14	Up
ENSG00000198959.	TGM2	20	-7.283487	-36.18451	4.31E-14	Down
ENSG00000087245.	MMP2	16	-2.505794	-35.91055	4.74E-14	Down
ENSG00000139209.	SLC38A4	12	6.034382	35.76103	4.95E-14	Up
ENSG00000268606.	MAGEA2	X	5.173366	35.46221	5.44E-14	Up
ENSG00000183305.	MAGEA2B	X	5.169852	35.44528	5.44E-14	Up
ENSG00000108001.	EBF3	10	4.059958	35.17999	5.99E-14	Up
ENSG00000112378.	PERP	6	-2.942367	-35.10526	6.02E-14	Down
ENSG00000245526.	LINC00461	5	4.507755	35.07611	6.02E-14	Up
ENSG00000122778.	KIAA1549	7	2.893756	34.96611	6.20E-14	Up
ENSG00000197747.	S100A10	1	-3.480339	-34.89778	6.27E-14	Down

Appendix Table 6: List of significantly differentially expressed genes in mutant NSCs compared to wildtype NSCs after stimulation with NGF. (FDR $\leq$ 0.05)

Gene Ensembl ID	Gene Symbol /Name	Chromosome	Coef	t value	p-value	Direction
ENSG00000286966.1	RASSF9	12	-2.7649023	-4.3661282	0.0004777	Down
ENSG00000286502.1	AL645768.1	9	-2.0725255	-4.2181533	0.00065053	Down
ENSG00000286340.1	RN7SL5P	9	1.48482999	4.05909526	0.00090808	Up
ENSG00000285722.1	MALAT1	11	-0.5269354	-4.0328716	0.00095955	Down
ENSG00000283475.1	RN7SL1	14	1.13871908	3.77903256	0.00163864	Up
ENSG00000280734.3	AMER3	2	2.57283283	3.73706073	0.0017906	Up
ENSG00000279716.1	CTF1	16	-1.0620764	-3.6862853	0.00199346	Down
ENSG00000276168.1	AC006128.1	19	-1.368393	-3.6613154	0.00210152	Down
ENSG00000275410.5	HNF1B	17	-2.6725949	-3.6451907	0.00217441	Down
ENSG00000274561.1	RPL39P15	2	1.52198476	3.64026494	0.00219717	Up
ENSG00000272084.1	LINC02073	17	-2.4764914	-3.5687393	0.00255593	Down
ENSG00000267452.3	MEG3	14	-0.3807606	-3.5295312	0.00277685	Down
ENSG00000265735.2	LINC01232	13	-1.2325951	-3.5279109	0.00278638	Down
ENSG00000257894.2	Lnc-CCND2-2	12	2.75744794	3.51728105	0.00284971	Up
ENSG00000256969.2	NPAP1	15	-2.5714008	-3.4536039	0.00326029	Down
ENSG00000254838.5	Lnc-PAWR-1	12	-2.6618456	-3.4531795	0.00326321	Down
ENSG00000251562.8	MIR1244-4	12	1.71482002	3.41132717	0.0035649	Up
ENSG00000249685.1	LRRC37A12P	1	-2.5157773	-3.3987819	0.00366062	Down
ENSG00000249406.3	AL627309.5	1	-0.5294849	-3.391815	0.00371488	Down
ENSG00000243449.6	C4orf48	4	1.85870822	3.38718853	0.00375135	Up
ENSG00000242125.3	LINC01969	17	-2.6356901	-3.3755231	0.00384489	Down
ENSG00000241923.2	Lnc-KPNA2-6	17	1.74330743	3.33887789	0.00415407	Up
ENSG00000241860.7	SNHG3	1	-0.4855885	-3.3150968	0.00436778	Down
ENSG00000239797.1	POTEM	14	1.38053609	3.30936878	0.00442086	Up
ENSG00000239467.6	PTMA	2	0.20108334	3.29553194	0.00455174	Up
ENSG00000236056.1	Lnc-ERICH2-1	2	1.6109252	3.28358722	0.0046678	Up
ENSG00000234009.1	AL137800.1	1	2.24955251	3.27724508	0.00473061	Up
ENSG00000233885.7	MT-ND4L	MT	-0.2981394	-3.2700207	0.00480318	Down
ENSG00000233393.1	AC207130.1	22	2.0502547	3.26012752	0.00490434	Up
ENSG00000232710.1	RPS24P8	3	0.74047318	3.2514737	0.00499455	Up
ENSG00000232082.1	GABARAP	17	-0.5737191	-3.24729	0.00503875	Down
ENSG00000231414.1	GAPDHP14	21	2.74140741	3.24677878	0.00504418	Up
ENSG00000230383.1	RPL14P3	4	2.06605415	3.24651485	0.00504699	Up
ENSG00000229259.1	RPL21P39	3	0.53887118	3.24239394	0.00509097	Up
ENSG00000224094.1	RPS6KA2-IT1	6	-2.0184421	-3.238995	0.00512754	Down
ENSG00000222036.8	GVINP1	11	-2.1397508	-3.23836	0.0051344	Down
ENSG00000214548.18	ALPK2	18	-0.2647884	-3.2358821	0.00516125	Down
ENSG00000212907.2	Lnc-KLHL5-1	4	1.85674869	3.21558327	0.00538653	Up
ENSG00000198796.7	Lnc-IRAK1BP1-3	6	1.06925878	3.21199132	0.0054274	Up
ENSG00000198774.5	RPL6P19	7	0.49089578	3.21164554	0.00543135	Up
ENSG00000197915.7	RPL5P34	22	0.59195516	3.18777182	0.00571102	Up
ENSG00000187514.16	HMGB1P1	20	0.95667145	3.17990639	0.00580624	Up
ENSG00000185823.5	C8G	9	-2.3740156	-3.1689128	0.00594195	Down
ENSG00000178171.11	HRNR	1	1.65314928	3.16098889	0.0060417	Up
ENSG00000176919.13	Lnc-CYP2D6-1	22	-1.8811762	-3.1345988	0.00638595	Down
ENSG00000170296.10	Lnc-UBR4-1	1	-1.4098735	-3.1250435	0.00651529	Down
ENSG00000150281.7	YEATS2-AS1	3	-1.25944	-3.1188695	0.00660023	Down
ENSG00000145908.12	ZNF300	5	-0.5860099	-3.1047494	0.00679861	Down
ENSG00000124097.7	LHX4	1	-0.9086078	-3.0994716	0.00687425	Down

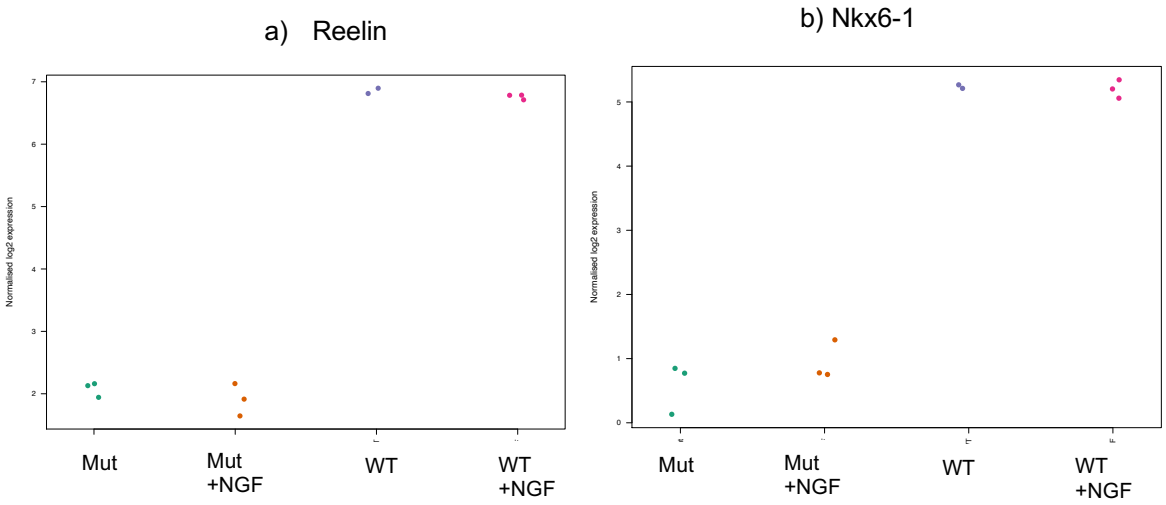

Appendix Figure 2: Differential gene expression for a) Reelin and b)Nkx6-1 in wildtype and mutant neural cells.

Bibliography

1. Vieta E, Berk M, Schulze TG, Carvalho AF, Suppes T, Calabrese JR, et al. Bipolar disorders. Nat Rev Dis Prim [Internet]. 2018 Jun 8 [cited 2020 Apr 27];4(1):18008. Available from: http://www.nature.com/articles/nrdp20188

2. Cloutier M, Greene M, Guerin A, Touya M, Wu E. The economic burden of bipolar I disorder in the United States in 2015. J Affect Disord [Internet]. 2018 Jan 15 [cited 2020 Jun 3];226:45–51. Available from: https://www.sciencedirect.com/science/article/pii/S0165032717315100

3. Hirschfeld RMA, Lewis L, Vornik LA. Perceptions and Impact of Bipolar Disorder. J Clin Psychiatry [Internet]. 2003 Feb 15 [cited 2020 Jun 3];64(2):161–74. Available from: http://article.psychiatrist.com/?ContentType=START&ID=10000180

4. Gordovez FJA, McMahon FJ. The genetics of bipolar disorder [Internet]. Vol. 25, Molecular Psychiatry. Springer Nature; 2020 [cited 2021 Jan 18]. p. 544–59. Available from: https://doi.org/10.1038/s41380-019-0634-7

5. Identification of risk loci with shared effects on five major psychiatric disorders: a genome-wide analysis. Lancet [Internet]. 2013 Apr 20 [cited 2020 Apr 27];381(9875):1371–9. Available from: https://www.sciencedirect.com/science/article/pii/S0140673612621291

6. Dulawa SC, Janowsky DS. Cholinergic regulation of mood: from basic and clinical studies to emerging therapeutics. Mol Psychiatry [Internet]. 2019 May 17 [cited 2019 Sep 16];24(5):694–709. Available from: http://www.nature.com/articles/s41380-018-0219-x

7. Janowsky D, Davis J, El-Yousef MK, Sekerke HJ. A CHOLINERGIC-ADRENERGIC HYPOTHESIS OF MANIA AND DEPRESSION. Lancet [Internet]. 1972 Sep 23 [cited 2020 Jun 9];300(7778):632–5. Available from: https://www.sciencedirect.com/science/article/pii/S0140673672930218

8. Janowsky DS, Risch SC, Kennedy B, Ziegler M, Huey L. Central muscarinic effects of physostigmine on mood, cardiovascular function, pituitary and adrenal neuroendocrine release. Psychopharmacology (Berl). 1986;89:150–4.

9. Janowsky DS, Risch SC. Cholinomimetic and anticholinergic drugs used to investigate an acetylcholine hypothesis of affective disorders and stress. Drug Dev Res [Internet]. 1984 [cited 2015 Oct 5];4(2):125–42. Available from: http://doi.wiley.com/10.1002/ddr.430040202

10. van Enkhuizen J, Janowsky DS, Olivier B, Minassian A, Perry W, Young JW, et al. The catecholaminergic–cholinergic balance hypothesis of bipolar disorder

revisited. Eur J Pharmacol [Internet]. 2015;753:114–26. Available from: http://linkinghub.elsevier.com/retrieve/pii/S0014299914005858

11. Risch SC, Cohen RM, Janowsky DS, Kalin NH, Sitaram N, Christian Gillin J, et al. Physostigmine induction of depressive symptomatology in normal human subjects. Psychiatry Res [Internet]. 1981 Feb 1 [cited 2020 Jun 9];4(1):89–94. Available from: https://www.sciencedirect.com/science/article/pii/0165178181900123?via%3Dihub

12. Nurnberger JI, Jimerson DC, Simmons-Alling S, Tamminga C, Nadi NS, Lawrence D, et al. Behavioral, physiological, and neuroendocrine responses to arecoline in normal twins and “well state” bipolar patients. Psychiatry Res [Internet]. 1983 Jul 1 [cited 2020 Jun 9];9(3):191–200. Available from: https://www.sciencedirect.com/science/article/pii/0165178183900434

13. Gillin JC, Sutton L, Ruiz C, Kelsoe J, Dupont RM, Darko D, et al. The Cholinergic Rapid Eye Movement Induction Test With Arecoline in Depression. Arch Gen Psychiatry [Internet]. 1991 Mar 1 [cited 2019 Nov 19];48(3):264. Available from: http://www.ncbi.nlm.nih.gov/pubmed/1996921

14. Cannon DM, Carson RE, Nugent AC, Eckelman WC, Kiesewetter DO, Williams J, et al. Reduced Muscarinic Type 2 Receptor Binding in Subjects With Bipolar Disorder. Arch Gen Psychiatry [Internet]. 2006 Jul 1 [cited 2018 Apr 10];63(7):741. Available from: http://archpsyc.jamanetwork.com/article.aspx?doi=10.1001/archpsyc.63.7.741

15. Zavitsanou K, Katsifis A, Yu Y, Huang XF. M2/M4 muscarinic receptor binding in the anterior cingulate cortex in schizophrenia and mood disorders. Brain Res Bull [Internet]. 2005 May 15 [cited 2018 Apr 10];65(5):397–403. Available from: https://www.sciencedirect.com/science/article/pii/S0361923005000432

16. West RJ, Hajek P, Belcher M. Severity of withdrawal symptoms as a predictor of outcome of an attempt to quit smoking. Psychol Med [Internet]. 1989 Nov [cited 2020 Jun 9];19(4):981–5. Available from: http://www.ncbi.nlm.nih.gov/pubmed/2594893

17. Major depression following smoking cessation. Am J Psychiatry [Internet]. 1997 Feb 1 [cited 2020 Jun 9];154(2):263–5. Available from: http://psychiatryonline.org/doi/abs/10.1176/ajp.154.2.263

18. Hannestad JO, Cosgrove KP, DellaGioia NF, Perkins E, Bois F, Bhagwagar Z, et al. Changes in the cholinergic system between bipolar depression and euthymia as measured with [123I]5IA single photon emission computed tomography. Biol Psychiatry [Internet]. 2013 Nov 15 [cited 2015 Sep 19];74(10):768–76. Available from:

http://www.pubmedcentral.nih.gov/articlerender.fcgi?artid=3805761&tool=pmcentrez&rendertype=abstract

19. Saricicek A, Esterlis I, Maloney KH, Mineur YS, Ruf BM, Muralidharan A, et al. Persistent β2*-nicotinic acetylcholinergic receptor dysfunction in major depressive disorder. Am J Psychiatry [Internet]. 2012 Aug 1 [cited 2015 Sep 21];169(8):851–9. Available from: http://ajp.psychiatryonline.org/doi/full/10.1176/appi.ajp.2012.11101546

20. Colangelo C, Shichkova P, Keller D, Markram H, Ramaswamy S. Cellular, Synaptic and Network Effects of Acetylcholine in the Neocortex. Front Neural Circuits [Internet]. 2019 Apr 12 [cited 2020 Jul 22];13:24. Available from: https://www.frontiersin.org/article/10.3389/fncir.2019.00024/full

21. Hasselmo ME, Sarter M. Modes and Models of Forebrain Cholinergic Neuromodulation of Cognition. Neuropsychopharmacology [Internet]. 2011 Jan 28 [cited 2020 Aug 4];36(1):52–73. Available from: http://www.nature.com/articles/npp2010104

22. Auld DS, Ëoise Mennicken F, Day JC, Âmi Quirion R. Neurotrophins differentially enhance acetylcholine release, acetylcholine content and choline acetyltransferase activity in basal forebrain neurons. Int Soc Neurochem J Neurochem 253±262 J Neurochem. 2001;77(77):253–62.

23. Sanchez-Ortiz E, Yui D, Song D, Li Y, Rubenstein JL, Reichardt LF, et al. TrkA Gene Ablation in Basal Forebrain Results in Dysfunction of the Cholinergic Circuitry. J Neurosci [Internet]. 2012;32(12):4065–79. Available from: http://www.jneurosci.org/cgi/doi/10.1523/JNEUROSCI.6314-11.2012

24. López-Coviella I, Berse B, Krauss R, Thies RS, Blusztajn JK. Induction and maintenance of the neuronal cholinergic phenotype in the central nervous system by BMP-9. Science. 2000;289(5477):313–6.

25. Nguyen N, Lee SB, Lee YS, Lee K-H, Ahn J-Y. Neuroprotection by NGF and BDNF Against Neurotoxin-Exerted Apoptotic Death in Neural Stem Cells Are Mediated Through Trk Receptors, Activating PI3-Kinase and MAPK Pathways. Neurochem Res [Internet]. 2009 May 10 [cited 2019 Nov 21];34(5):942–51. Available from: http://link.springer.com/10.1007/s11064-008-9848-9

26. Reichardt LF. Neurotrophin-regulated signalling pathways. Philos Trans R Soc B Biol Sci [Internet]. 2006 Sep 29 [cited 2019 Dec 6];361(1473):1545–64. Available from: https://royalsocietypublishing.org/doi/10.1098/rstb.2006.1894

27. Scola G, Andreazza AC. The role of neurotrophins in bipolar disorder. Prog Neuropsychopharmacol Biol Psychiatry [Internet]. 2014;56C:122–8. Available from: http://www.ncbi.nlm.nih.gov/pubmed/25193130

28. Marshall C. Specificity of receptor tyrosine kinase signaling: Transient versus sustained extracellular signal-regulated kinase activation. Cell [Internet]. 1995 Jan [cited 2019 Dec 2];80(2):179–85. Available from: https://linkinghub.elsevier.com/retrieve/pii/0092867495904018

29. Hondermarck H, Demont Y, Bradshaw RA. The TrK Receptor Family. In: Receptor Tyrosine Kinases: Family and Subfamilies [Internet]. Cham: Springer International Publishing; 2015 [cited 2020 Apr 6]. p. 777–820. Available from: http://link.springer.com/10.1007/978-3-319-11888-8_17

30. Madziar B, Lopez-Coviella I, Zemelko V, Berse B. Regulation of cholinergic gene expression by nerve growth factor depends on the phosphatidylinositol-3'-kinase pathway. J Neurochem [Internet]. 2005 Feb 1 [cited 2020 Apr 22];92(4):767–79. Available from: http://doi.wiley.com/10.1111/j.1471-4159.2004.02908.x

31. Tomioka T, Shimazaki T, Yamauchi T, Oki T, Ohgoh M, Okano H. LIM Homeobox 8 (Lhx8) Is a Key Regulator of the Cholinergic Neuronal Function via a Tropomyosin Receptor Kinase A (TrkA)-mediated Positive Feedback Loop. J Biol Chem [Internet]. 2014;289(2):1000–10. Available from: http://www.jbc.org/cgi/doi/10.1074/jbc.M113.494385

32. Marlin MC, Li G. Biogenesis and function of the NGF/TrkA signaling endosome. Int Rev Cell Mol Biol [Internet]. 2015 [cited 2019 Dec 2];314:239–57. Available from: http://www.ncbi.nlm.nih.gov/pubmed/25619719

33. Meakin SO, MacDonald JI, Gryz EA, Kubu CJ, Verdi JM. The signaling adapter FRS-2 competes with Shc for binding to the nerve growth factor receptor TrkA. A model for discriminating proliferation and differentiation. J Biol Chem [Internet]. 1999 Apr 2 [cited 2019 Dec 2];274(14):9861–70. Available from: http://www.ncbi.nlm.nih.gov/pubmed/10092678

34. Arévalo JC, Wu SH. Neurotrophin signaling: many exciting surprises! Cell Mol Life Sci [Internet]. 2006 Jul 15 [cited 2020 Apr 6];63(13):1523–37. Available from: http://link.springer.com/10.1007/s00018-006-6010-1

35. Lonze BE, Ginty DD. Function and Regulation of CREB Family Transcription Factors in the Nervous System. Neuron [Internet]. 2002 Aug 15 [cited 2019 Nov 5];35(4):605–23. Available from: https://www.sciencedirect.com/science/article/pii/S0896627302008280

36. Chen W-T, Huang T-L, Tsai M-C. Bcl-2 associated with severity of manic symptoms in bipolar patients in a manic phase. Psychiatry Res [Internet]. 2015 Feb 28 [cited 2020 Sep 4];225(3):305–8. Available from: https://www.sciencedirect.com/science/article/pii/S0165178114010130?via%3Dihub

37. Lowthert L, Leffert J, Lin A, Umlauf S, Maloney K, Muralidharan A, et al. Increased ratio of anti-apoptotic to pro-apoptotic Bcl2 gene-family members in lithium-responders one month after treatment initiation. Biol Mood Anxiety Disord [Internet]. 2012 Sep 12 [cited 2018 Dec 11];2(1):15. Available from: http://biolmoodanxietydisord.biomedcentral.com/articles/10.1186/2045-5380-2-15

38. Watson FL, Heerssen HM, Bhattacharyya A, Klesse L, Lin MZ, Segal RA. Neurotrophins use the Erk5 pathway to mediate a retrograde survival response. Nat Neurosci [Internet]. 2001 Oct 4 [cited 2020 Apr 22];4(10):981–8. Available from: http://www.nature.com/articles/nn720

39. Inagaki N, Thoenen H, Lindholm D. TrkA Tyrosine Residues Involved in NGF-induced Neurite Outgrowth of PC12 Cells. Eur J Neurosci [Internet]. 1995 Jun 1 [cited 2020 Apr 22];7(6):1125–33. Available from: http://doi.wiley.com/10.1111/j.1460-9568.1995.tb01102.x

40. Ehlers MD, Kaplan DR, Price DL, Koliatsos VE. NGF-stimulated retrograde transport of trkA in the mammalian nervous system. J Cell Biol [Internet]. 1995 Jul 1 [cited 2020 Apr 27];130(1):149–56. Available from: https://rupress.org/jcb/article/130/1/149/56350/NGFstimulated-retrograde-transport-of-trkA-in-the

41. Bronfman FC, Escudero CA, Weis J, Kruttgen A. Endosomal transport of neurotrophins: Roles in signaling and neurodegenerative diseases. Dev Neurobiol [Internet]. 2007 Aug 1 [cited 2019 Nov 26];67(9):1183–203. Available from: http://doi.wiley.com/10.1002/dneu.20513

42. Da Silva JS, Hasegawa T, Miyagi T, Dotti CG, Abad-Rodriguez J. Asymmetric membrane ganglioside sialidase activity specifies axonal fate. Nat Neurosci [Internet]. 2005 May 17 [cited 2019 Nov 21];8(5):606–15. Available from: http://www.nature.com/articles/nn1442

43. Psychiatric GWAS Consortium Bipolar Disorder Working Group. Large-scale genome-wide association analysis of bipolar disorder identifies a new susceptibility locus near ODZ4. Nat Genet [Internet]. 2011 Oct 18 [cited 2014 Jul 11];43(10):977–83. Available from: http://www.nature.com/ng/journal/v43/n10/full/ng.943.html#supplementary-information

44. Stahl EA, Breen G, Forstner AJ, McQuillin A, Ripke S, Trubetskoy V, et al. Genome-wide association study identifies 30 Loci Associated with Bipolar Disorder. bioRxiv [Internet]. 2018 Jan 24 [cited 2019 Nov 19];173062. Available from: https://www.biorxiv.org/content/10.1101/173062v4

45. Nurnberger JI, Blehar MC, Kaufmann CA, York-Cooler C, Simpson SG, Harkavy-

Friedman J, et al. Diagnostic interview for genetic studies. Rationale, unique features, and training. NIMH Genetics Initiative. Arch Gen Psychiatry [Internet]. 1994 Nov [cited 2018 Apr 10];51(11):849–59; discussion 863-4. Available from: http://www.ncbi.nlm.nih.gov/pubmed/7944874

46. Nissen S, Liang S, Shehktman T, Kelsoe JR, Bipolar Genome Study (BiGS), Greenwood TA, et al. Evidence for association of bipolar disorder to haplotypes in the 22q12.3 region near the genes stargazin, ift27 and parvalbumin. Am J Med Genet Part B Neuropsychiatr Genet [Internet]. 2012 Dec [cited 2018 Apr 10];159B(8):941–50. Available from: http://www.ncbi.nlm.nih.gov/pubmed/23038240

47. Silberberg G, Levit A, Collier D, St. Clair D, Munro J, Kerwin RW, et al. Stargazin involvement with bipolar disorder and response to lithium treatment. Pharmacogenet Genomics [Internet]. 2008 May [cited 2018 Apr 10];18(5):403–12. Available from: https://insights.ovid.com/crossref?an=01213011-200805000-00004

48. Willer CJ, Li Y, Abecasis GR. METAL: fast and efficient meta-analysis of genomewide association scans. Bioinforma Appl NOTE [Internet]. 2010 [cited 2018 Apr 12];26(17):2190–219110. Available from: http://

49. Need AC, Keefe RSE, Ge D, Grossman I, Dickson S, McEvoy JP, et al. Pharmacogenetics of antipsychotic response in the CATIE trial: a candidate gene analysis. Eur J Hum Genet [Internet]. 2009 Jul [cited 2018 Oct 22];17(7):946–57. Available from: http://www.ncbi.nlm.nih.gov/pubmed/19156168

50. Kelsoe JR, Spence MA, Loetscher E, Foguet M, Sadovnick AD, Remick RA, et al. A genome survey indicates a possible susceptibility locus for bipolar disorder on chromosome 22. Proc Natl Acad Sci [Internet]. 2001 Jan 16 [cited 2018 Apr 10];98(2):585–90. Available from: http://www.pnas.org/cgi/doi/10.1073/pnas.98.2.585

51. Kimmel RJ, Kovacs I, Vrabel C, Wood B, Schalling M, Kelsoe JR. Cosegregation of bipolar disorder and autosomal-dominant medullary cystic kidney disease in a large family. Am J Psychiatry [Internet]. 2005;162(10):1972–4. Available from: http://www.ncbi.nlm.nih.gov/pubmed/16199849

52. Kirby A, Gnirke A, Jaffe DB, Barešová V, Pochet N, Blumenstiel B, et al. Mutations causing medullary cystic kidney disease type 1 lie in a large VNTR in MUC1 missed by massively parallel sequencing. Nat Genet [Internet]. 2013 Mar 10 [cited 2019 Jun 14];45(3):299–303. Available from: http://www.nature.com/articles/ng.2543

53. Greenwood TA, Nievergelt CM, Sadovnick AD, Remick RA, Keck PE, McElroy SL, et al. Further evidence for linkage of bipolar disorder to chromosomes 6 and

17 in a new independent pedigree series. Bipolar Disord [Internet]. 2012 Feb 1 [cited 2019 Sep 16];14(1):71–9. Available from: http://doi.wiley.com/10.1111/j.1399-5618.2011.00970.x

54. Marshall CR, Howrigan DP, Merico D, Thiruvahindrapuram B, Wu W, Greer DS, et al. Contribution of copy number variants to schizophrenia from a genome-wide study of 41,321 subjects. Nat Genet [Internet]. 2017 [cited 2020 Aug 19];49(1):27–35. Available from: http://www.ncbi.nlm.nih.gov/pubmed/27869829

55. Mellerup E, Andreassen OA, Bennike B, Dam H, Djurovic S, Jorgensen MB, et al. Combinations of genetic variants associated with bipolar disorder. PLoS One [Internet]. 2017 [cited 2020 Aug 19];12(12):e0189739. Available from: http://www.ncbi.nlm.nih.gov/pubmed/29267373

56. Whalley HC, Pickard BS, McIntosh AM, Zuliani R, Johnstone EC, Blackwood DHR, et al. A GRIK4 variant conferring protection against bipolar disorder modulates hippocampal function. Mol Psychiatry [Internet]. 2009 May 22 [cited 2020 Aug 19];14(5):467–8. Available from: http://www.nature.com/articles/mp20097

57. Debnath M, Busson M, Jamain S, Etain B, Hamdani N, Oliveira J, et al. The HLA-G low expressor genotype is associated with protection against bipolar disorder. Hum Immunol [Internet]. 2013 May 1 [cited 2020 Aug 19];74(5):593–7. Available from: https://www.sciencedirect.com/science/article/pii/S0198885912006581

58. Davidson GL, Murphy SM, Polke JM, Laura M, Salih MAM, Muntoni F, et al. Frequency of mutations in the genes associated with hereditary sensory and autonomic neuropathy in a UK cohort. J Neurol [Internet]. 2012 Aug 1 [cited 2019 Nov 19];259(8):1673–85. Available from: http://link.springer.com/10.1007/s00415-011-6397-y

59. Li N, Guo S, Wang Q, Duan G, Sun J, Liu Y, et al. Heterogeneity of clinical features and mutation analysis of NTRK1 in Han Chinese patients with congenital insensitivity to pain with anhidrosis. J Pain Res [Internet]. 2019 Jan 22 [cited 2019 Sep 17];Volume 12:453–65. Available from: https://www.dovepress.com/heterogeneity-of-clinical-features-and-mutation-analysis-of-ntrk1-in-h-peer-reviewed-article-JPR

60. Verhoeven K, Timmerman V, Mauko B, Pieber TR, De Jonghe P, Auer-Grumbach M. Recent advances in hereditary sensory and autonomic neuropathies. Curr Opin Neurol [Internet]. 2006 Oct [cited 2019 Sep 17];19(5):474–80. Available from: http://www.ncbi.nlm.nih.gov/pubmed/16969157

61. Brennand KJ, Simone A, Jou J, Gelboin-Burkhart C, Tran N, Sangar S, et al. Modelling schizophrenia using human induced pluripotent stem cells. Nature [Internet]. 2011;473(7346):221–5. Available from:

http://www.nature.com/doifinder/10.1038/nature09915

62. Nilbratt M, Porras O, Marutle A, Hovatta O, Nordberg A. Neurotrophic factors promote cholinergic differentiation in human embryonic stem cell-derived neurons. J Cell Mol Med [Internet]. 2009;14(6b):1476–84. Available from: http://doi.wiley.com/10.1111/j.1582-4934.2009.00916.x

63. Bissonnette CJ, Lyass L, Bhattacharyya BJ, Belmadani A, Miller RJ, Kessler J a. The Controlled Generation of Functional Basal Forebrain Cholinergic Neurons from Human Embryonic Stem Cells. Stem Cells [Internet]. 2011;29(5):802–11. Available from: http://doi.wiley.com/10.1002/stem.626

64. Crompton L a., Byrne ML, Taylor H, Kerrigan TL, Bru-Mercier G, Badger JL, et al. Stepwise, non-adherent differentiation of human pluripotent stem cells to generate basal forebrain cholinergic neurons via hedgehog signaling. Stem Cell Res [Internet]. 2013;11(3):1206–21. Available from: http://linkinghub.elsevier.com/retrieve/pii/S187350611300113X

65. Sassa T, Gomi H, Itohara S. Postnatal expression of Cdkl2 in mouse brain revealed by LacZ inserted into the Cdkl2 locus. Cell Tissue Res [Internet]. 2004 Feb 1 [cited 2019 Nov 19];315(2):147–56. Available from: http://www.ncbi.nlm.nih.gov/pubmed/14605869

66. Sakai K, Miyazaki J. A Transgenic Mouse Line That Retains Cre Recombinase Activity in Mature Oocytes Irrespective of thecreTransgene Transmission. Biochem Biophys Res Commun [Internet]. 1997 Aug 18 [cited 2019 Nov 25];237(2):318–24. Available from: http://www.ncbi.nlm.nih.gov/pubmed/9268708

67. Nakajima K, Kazuno A, Kelsoe J, Nakanishi M, Takumi T, Kato T. Exome sequencing in the knockin mice generated using the CRISPR/Cas system. Sci Rep [Internet]. 2016 Dec 4 [cited 2019 Nov 25];6(1):34703. Available from: http://www.ncbi.nlm.nih.gov/pubmed/27698470

68. Yamanishi K, Doe N, Sumida M, Watanabe Y, Yoshida M, Yamamoto H, et al. Hepatocyte Nuclear Factor 4 Alpha Is a Key Factor Related to Depression and Physiological Homeostasis in the Mouse Brain. Shimizu E, editor. PLoS One [Internet]. 2015 Mar 16 [cited 2019 Nov 19];10(3):e0119021. Available from: https://dx.plos.org/10.1371/journal.pone.0119021

69. Kasahara T, Takata A, Kato TM, Kubota-Sakashita M, Sawada T, Kakita A, et al. Depression-like episodes in mice harboring mtDNA deletions in paraventricular thalamus. Mol Psychiatry [Internet]. 2016 Jan 20 [cited 2019 Nov 19];21(1):39–48. Available from: http://www.ncbi.nlm.nih.gov/pubmed/26481320

70. Kaech S, Banker G. Culturing hippocampal neurons. Nat Protoc [Internet]. 2006 Dec 11 [cited 2019 Nov 19];1(5):2406–15. Available from:

http://www.ncbi.nlm.nih.gov/pubmed/17406484

71. Castrén E, Rantamäki T. The role of BDNF and its receptors in depression and antidepressant drug action: Reactivation of developmental plasticity. Dev Neurobiol [Internet]. 2010 Apr 1 [cited 2019 Aug 19];70(5):289–97. Available from: http://doi.wiley.com/10.1002/dneu.20758

72. Kumamaru E, Numakawa T, Adachi N, Yagasaki Y, Izumi A, Niyaz M, et al. Glucocorticoid Prevents Brain-Derived Neurotrophic Factor-Mediated Maturation of Synaptic Function in Developing Hippocampal Neurons through Reduction in the Activity of Mitogen-Activated Protein Kinase. Mol Endocrinol [Internet]. 2008 Mar 1 [cited 2019 Aug 19];22(3):546–58. Available from: https://academic.oup.com/mend/article-lookup/doi/10.1210/me.2007-0264

73. Acsády L, Pascual M, Rocamora N, Soriano E, Freund TF. Nerve growth factor but not neurotrophin-3 is synthesized by hippocampal GABAergic neurons that project to the medial septum. Neuroscience [Internet]. 2000 Jun 1 [cited 2019 Jul 17];98(1):23–31. Available from: https://www.sciencedirect.com/science/article/pii/S0306452200000919#BIB59

74. Chin BWW. A Novel Construct to Study the Functional Effects of SNPs on TrkA Protein Interactions and Localization. Unpublished Thesis. 2015.

75. Liao Y, Smyth GK, Shi W. FeatureCounts: An efficient general purpose program for assigning sequence reads to genomic features. Bioinformatics [Internet]. 2014 Apr 1 [cited 2020 Dec 15];30(7):923–30. Available from: https://pubmed.ncbi.nlm.nih.gov/24227677/

76. Law CW, Chen Y, Shi W, Smyth GK. Voom: Precision weights unlock linear model analysis tools for RNA-seq read counts. Genome Biol [Internet]. 2014 Feb 3 [cited 2020 Dec 15];15(2):R29. Available from: http://genomebiology.biomedcentral.com/articles/10.1186/gb-2014-15-2-r29

77. Robinson MD, Oshlack A. A scaling normalization method for differential expression analysis of RNA-seq data. Genome Biol [Internet]. 2010 Mar 2 [cited 2020 Dec 15];11(3):R25. Available from: http://genomebiology.biomedcentral.com/articles/10.1186/gb-2010-11-3-r25

78. Phipson B, Lee S, Majewski IJ, Alexander WS, Smyth GK. Robust hyperparameter estimation protects against hypervariable genes and improves power to detect differential expression. Ann Appl Stat [Internet]. 2016 Jun 1 [cited 2020 Dec 15];10(2):946–63. Available from: https://projecteuclid.org/euclid.aoas/1469199900

79. Durinck S, Spellman PT, Birney E, Huber W. Mapping identifiers for the integration of genomic datasets with the R/ Bioconductor package biomaRt. Nat

Protoc [Internet]. 2009 [cited 2020 Dec 15];4(8):1184–91. Available from: https://pubmed.ncbi.nlm.nih.gov/19617889/

80. Wu D, Smyth GK. Camera: A competitive gene set test accounting for inter-gene correlation. Nucleic Acids Res [Internet]. 2012 Sep [cited 2020 Dec 15];40(17):e133. Available from: /pmc/articles/PMC3458527/?report=abstract

81. Subramanian A, Tamayo P, Mootha VK, Mukherjee S, Ebert BL, Gillette MA, et al. Gene set enrichment analysis: A knowledge-based approach for interpreting genome-wide expression profiles. Proc Natl Acad Sci U S A [Internet]. 2005 Oct 25 [cited 2020 Dec 15];102(43):15545–50. Available from: www.pnas.orgcgidoi10.1073pnas.0506580102

82. Liberzon A, Birger C, Thorvaldsdóttir H, Ghandi M, Mesirov JP, Tamayo P. The Molecular Signatures Database Hallmark Gene Set Collection. Cell Syst [Internet]. 2015 Dec 23 [cited 2020 Dec 15];1(6):417–25. Available from: /pmc/articles/PMC4707969/?report=abstract

83. Ashburner M, Ball CA, Blake JA, Botstein D, Butler H, Cherry JM, et al. Gene ontology: Tool for the unification of biology [Internet]. Vol. 25, Nature Genetics. Nat Genet; 2000 [cited 2020 Dec 15]. p. 25–9. Available from: https://pubmed.ncbi.nlm.nih.gov/10802651/

84. Carbon S, Douglass E, Dunn N, Good B, Harris NL, Lewis SE, et al. The Gene Ontology Resource: 20 years and still GOing strong. Nucleic Acids Res [Internet]. 2019 Jan 8 [cited 2020 Dec 15];47(D1):D330–8. Available from: https://pubmed.ncbi.nlm.nih.gov/30395331/

85. Choi D-Y, Toledo-Aral JJ, Segal R, Halegoua S. Sustained Signaling by Phospholipase C-γ Mediates Nerve Growth Factor-Triggered Gene Expression. Mol Cell Biol [Internet]. 2001 Apr 15 [cited 2020 Dec 15];21(8):2695–705. Available from: http://mcb.asm.org/

86. Alder J, Thakker-Varia S, Bangasser DA, Kuroiwa M, Plummer MR, Shors TJ, et al. Brain-Derived Neurotrophic Factor-Induced Gene Expression Reveals Novel Actions of VGF in Hippocampal Synaptic Plasticity. J Neurosci [Internet]. 2003 Nov 26 [cited 2020 Dec 15];23(34):10800–8. Available from: https://www.jneurosci.org/content/23/34/10800

87. Freeman RS, Burch RL, Crowder RJ, Lomb DJ, Schoell MC, Straub JA, et al. NGF deprivation-induced gene expression: after ten years, where do we stand? Prog Brain Res [Internet]. 2004 Jan 1 [cited 2019 Nov 21];146:111–26. Available from: https://www.sciencedirect.com/science/article/pii/S0079612303460081

88. Angelastro JM, Klimaschewski L, Tang S, Vitolo O V., Weissman TA, Donlin LT, et al. Identification of diverse nerve growth factor-regulated genes by serial

analysis of gene expression (SAGE) profiling. Proc Natl Acad Sci U S A [Internet]. 2000 Sep 12 [cited 2020 Dec 15];97(19):10424–9. Available from: www.ncbi.nlm.nih.gov

89. Chau KF, Shannon ML, Fame RM, Fonseca E, Mullan H, Johnson MB, et al. Downregulation of ribosome biogenesis during early forebrain development. Elife [Internet]. 2018 May 10 [cited 2020 Dec 15];7. Available from: /pmc/articles/PMC5984036/?report=abstract

90. Dmitrzak-Weglarz M, Rybakowski JK, Suwalska A, Skibinska M, Leszczynska-Rodziewicz A, Szczepankiewicz A, et al. Association studies of the *BDNF* and the *NTRK2* gene polymorphisms with prophylactic lithium response in bipolar patients. Pharmacogenomics [Internet]. 2008 Nov 20 [cited 2018 Dec 3];9(11):1595–603. Available from: https://www.futuremedicine.com/doi/10.2217/14622416.9.11.1595

91. Uribe E, Wix R. Migración neuronal, apoptosis y trastorno bipolar [Internet]. Rev Psiquiatr Salud Ment (Barc.). 2012 [cited 2021 Jan 20]. p. 127–33. Available from: https://www.elsevier.es/en-revista-revista-psiquiatria-salud-mental-486-pdf-S2173505012000386

92. Elashoff M, Higgs BW, Yolken RH, Knable MB, Weis S, Webster MJ, et al. Meta-Analysis of 12 Genomic Studies in Bipolar Disorder. [cited 2018 Dec 11]; Available from: https://link.springer.com/content/pdf/10.1385%2FJMN%3A31%3A03%3A221.pdf

93. Madison JM, Zhou F, Nigam a, Hussain a, Barker DD, Nehme R, et al. Characterization of bipolar disorder patient-specific induced pluripotent stem cells from a family reveals neurodevelopmental and mRNA expression abnormalities. Mol Psychiatry [Internet]. 2015;20(6):703–17. Available from: http://www.nature.com/doifinder/10.1038/mp.2015.7

94. Li Y, Wang R, Qiao N, Peng G, Zhang K, Tang K, et al. Transcriptome analysis reveals determinant stages controlling human embryonic stem cell commitment to neuronal cells. J Biol Chem [Internet]. 2017 Dec 1 [cited 2020 Dec 22];292(48):19590–604. Available from: http://www.jbc.org/

95. O'Shea KS, McInnis MG. Neurodevelopmental origins of bipolar disorder: IPSC models. Vol. 73, Molecular and Cellular Neuroscience. Academic Press Inc.; 2016. p. 63–83.

96. Nurnberger JI, Koller DL, Jung J, Edenberg HJ, Foroud T, Guella I, et al. Identification of pathways for bipolar disorder: A meta-analysis. JAMA Psychiatry [Internet]. 2014 Jun 1 [cited 2020 Dec 28];71(6):657–64. Available from: https://jamanetwork.com/

97. O'dushlaine C, Rossin L, Lee PH, Duncan L, Parikshak NN, Newhouse S, et al. Psychiatric genome-wide association study analyses implicate neuronal, immune and histone pathways. Nat Neurosci [Internet]. 2015 Feb 17 [cited 2020 Dec 28];18(2):199–209. Available from: https://pubmed.ncbi.nlm.nih.gov/25599223/